Molecular Mechanisms Of HIV-1 Maturation And Host Factor Utilization

By

Jordan Anderson-Daniels

Dissertation

Submitted to the Faculty of the

Graduate School of Vanderbilt University in

partial fulfillment of the requirements for the

degree of

DOCTOR OF PHILOSOPHY

in

Microbiology and Immunology

October 31, 2019

Nashville, Tennessee

Approved:

Mark Denison, M.D.

Christopher Aiken, Ph.D.

Andrew Link, Ph.D.

David Bader, Ph.D.

DEDICATION

To anyone with self-doubt: you are better than you think. To anyone walking through darkness: just keep walking.

ACKNOWLEDGEMENTS

A great way to become humble is to learn something you didn't think you needed to. When I started this program, I didn't realize how much I had to learn to become a scientist. Fortunately, I had great educators that sacrificed their time and energy so that I could learn. My mentor, Chris, is a great model scientist. Time and again he emphasized the importance of the question, the hypothesis, and the expected outcomes, all while instilling the value of owning one's own project. I am extremely grateful for the opportunity to study with him and for his mentorship. My committee members, Mark Denison, Andy Link, David Bader, and former members, Earl Ruley and Terry Dermody, taught me the importance of staying focused and always demanded that I be better. Thank you for those demands, your patience, and the chance to start over. I hope that my efforts in stoicism were not mistaken as apathy.

I also had the opportunity to learn from great peers and collogues. The Aiken Lab is and has been home to an exceedingly generous, friendly, and diverse group of people. Thank you for the uplifting laughs, lessons, and friendships. Our friends across town at Meharry Medical College, CV Dash and Muthu Balasubramaniam, were not only a source of a much-needed reagent, but also a great source of encouragement and advice.

A special thanks goes to Alan Engelman and his lab members, Parmit Singh, Greg Sowd, and Wen Li, at the Dana Farber Cancer Institute for a great collaboration on my MA-CA project. Their efforts were a fantastic addition to the story.

My scientific journey started at Augustana College, where Mike Wanous asked if I wanted to join his lab for the summer after my freshman year. The following two summers, I worked in Mark Larson's lab, spending summers in South Dakota and in Boston. It was fantastic. Later, I worked in Casey Wright's lab at Sanford Research, where I learned what it took to do research independently and full-time. To all, I say thank you for the introduction and continued encouragement to pursue science.

Of course, my family has been the strongest source of support. I was always encouraged to be anything I wanted and to pursue it with excellence and passion. I was always given the opportunities, encouragement, and means to be successful, the gift of which I can only hope to some day repay. My mom is the strongest, most incredible person I know, and much of my success has been achieved while doing my best to emulate her. Finally, unmeasurable support has come from my wife. She followed me to Nashville where she quickly started her own impressive career. She could write her own dissertation on what it means to support someone through a Ph.D. To all my friends and family who have seen me through this, thank you, and I love you.

TABLE OF CONTENTS

LIST OF TABLES

LIST OF FIGURES

LIST OF ABBREVIATIONS

AIDS	acquired immune deficiency syndrome
ALU	arbitrary light units
AMD	AMD3100, fusion inhibitor
AMLV	amphotropic murine leukemia virus
ATP	adenosine triphosphate
BME	2-mercaptoethanol
CA	capsid protein, p24
CCR5	CC chemokine receptor 5
CD4+	protein marker on surface of HIV-1 target cells
Crix	crixivan
CTD	carboxy-terminal end
CypA	Cyclophilin A
CXCR4	CX chemokine receptor 4
DMEM	Dulbecco's modified eagle's medium
DMSO	dimethyl sulfoxide
dNTP	deoxynucleotide
DNA	deoxyribonucleic acid
DPC	N-dodecylphosphocholine
DS	dextran sulfate
EF1A	elongation factor 1 A
ELISA	enzyme-linked immunosorbent assay

EM	electron microscopy
Env	envelope glycoprotein
FBS	fetal bovine serum
Gag	group specific antigen
GALT	gut associated lymphoid tissue
GFP	green fluorescent protein
gp120	envelope glycoprotein
HAART	highly active antiretroviral therapy
HIV-1	human immunodeficiency virus type 1
IN	integrase
Kb	kilobases
LTR	long terminal repeat
MA	matrix protein, p17
MLV	murine leukemia virus
MuDPIT	multidimensional protein identification technology
MXB	myxovirus resistance protein B
NaCl	sodium chloride
NC	nucleocapsid protein, p7
Nef	negative factor
Nup	nucleoporin
NTD	amino-terminal end
OMK	Owl Monkey kidney
PAGE	polyacrylamide gel electroporesis

PBS	phosphate-buffered saline
PCR	polymerase chain reaction
PEI	polyethylenimine
PIC	preintegration complex
qPCR	quantitative PCR
RIC	random integration control
RNA	ribonucleic acid
RNAi	RNA interference
RT	reverse transcriptase
RTC	reverse transcription complex
SDS	sodium dodecyl sulfate
shRNA	short hairpin RNA
siRNA	small interfering RNA
Tat	HIV transactivator of transcription
TCA	trichloroacetic acid
TRIM	tripartite motif
TRIMCyp	tripartite motif fused with cyclophilin A
Vif	viral infectivity factor
vRNP	viral ribonucleoprotein complex
VSV	vesicular stomatitis virus
VSV-G	vesicular stomatitis V glycoprotein

Chapter 1

Background And Research Goals

Viruses are pathogens that infect every domain of life, from bacteria and single-celled eukaryotes, to insects, animals, and plants. While their inclusion into the category of life is debated, they outnumber all forms of life by orders of magnitude, with an estimated 10^{31} bacteriophages on the planet (1). Given the approximately 200 nm length of a bacteriophage, when lined up end-to-end these viruses would extend 200 million light years across the universe. While many illnesses can be traced to viral origins, even healthy individuals are fundamentally impacted by viruses, as an estimated 8% of the human genome is retroviral in origin (2). As obligate intracellular parasites, virus replication requires exploitation of their host cell machinery and resources while evading mechanisms hosts have evolved to counteract them. Thus, to study viruses is to study life. In an effort to study a small corner of life, I have spent my graduate studies working to understand the basic functions of the Human Immunodeficiency Virus Type 1 (HIV-1).

HIV & AIDS

The pandemic pathogen HIV-1 is the major etiologic agent of acquired immune deficiency syndrome (AIDS) (3, 4). HIV-1 was isolated from an AIDS patient and subsequently identified as the causative agent of the disease in 1983. Two years later the term “AIDS” was first used to describe patients suffering from depleted $CD4^+$ T cell

blood counts. HIV-1 education and surveillance has improved globally since the virus was identified in the early 1980s. However, despite these improvements, HIV-1 transmission has grown to pandemic status. In 2017 the World Health Organization (WHO) reported that approximately 36.9 million people were infected with HIV-1 and estimated that 77.3 million people had become infected since the start of the pandemic (5). HIV infection rates rose steadily through the 1990s, peaking in 1995 with an estimated 3.4 million cases (6). Despite a steady decline in transmission since then, 1.8 million people became infected in 2017 (6). AIDS-related deaths also rose throughout the 1990s, peaking in 2005 at 1.9 million (6). As of 2017, cumulative AIDS-related deaths were estimated to be over 35 million since the start of the pandemic. Thus, HIV-1 has been and continues to be a scourge of human health.

HIV-1 Pathogenesis

HIV-1 transmission occurs after exposure to mucous membranes during sex or ingestion of breast milk, during birth, or direct exposure to the blood stream via intravenous needle use (7). The primary cellular target for HIV-1 is $CD4^+$ T lymphocytes (8). The epithelial cells lining the gut and reproductive tissues are exposed to the virus upon transmission, and mucosal transit is facilitated by local inflammation and/or ulcerations or by contact with dendritic cells: the viral Env protein can interact with the surface-expressed DC-SIGN protein on dendritic cells (9). Dendritic cells can then act as a shuttle and present the virus directly to $CD4^+$ T cells in lymphatic tissues, where replicating virus quickly disseminates throughout the body.

Disease progression varies between individuals and circumstances; however, most infections result in a three-phase clinical course. First, an acute phase of viremia lasts two to six weeks, where many infected individuals experience flu-like symptoms (10). Viral replication expands rapidly with a loss of $CD4^+$ T cells, specifically in the gut associated lymphoid tissue (GALT) (10). The initial viremia is eventually controlled by the immune system; however, the GALT is not restored, thus compromising the immune protection and homeostasis of the gut in infected individuals. When acute infection resolves, patients enter into clinical latency (11). During this time, circulating viral titers remain low; however, persistent $CD4^+$ T cell infection gradually depletes the host's immune system, eventually to a point at which the virus cannot be controlled (12-14). The subsequent $CD4^+$ T cell decline results in a failure of the host immune system to control infections and cancer, resulting in AIDS, see Figure 1-1. AIDS-related deaths are not directly caused by HIV-1 replication, rather are commonly the result of other opportunistic pathogen infections (viral and/or bacterial) that the host would otherwise typically be able to defend against (10).

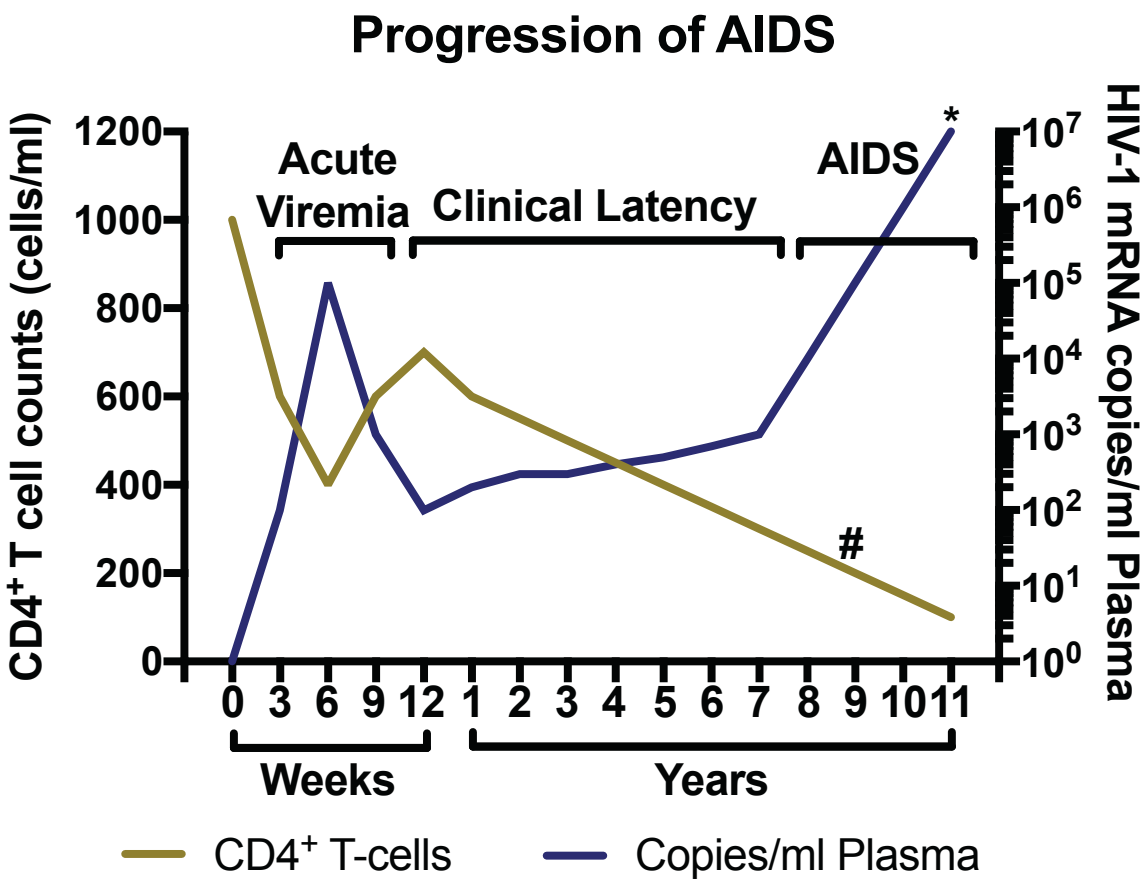

Figure 1-1: HIV-1 Disease Progression Towards AIDS. The disease progression towards AIDS can be segmented into three phases. Acute viremia lasts for a few weeks when viremia spikes with an accompanying loss in $CD4^+$ T cells. When the initial viremia is controlled and T cell counts rebound, a period of clinical latency starts, which can last for several years. Eventually, HIV-1 replication exceeds control, and $CD4^+$ T cell counts fall below 200 cells/ml (#). Patients become highly susceptible to opportunistic pathogens during AIDS and eventually die (*) from opportunistic infections and/or cancers. Adapted from Fauci *et al. Ann. Int. Med.* (1996) (11).

The course of clinical latency can vary between individuals. Rapid progressors develop AIDS within two to three years after infection, while slow progressors (the vast majority of infected individuals) may remain healthy for ten or more years (15). A small percentage of patients never develop AIDS (15). These long-term non-progressors do not lose $CD4^+$ T cells despite viral infection. Differences in disease progression can depend on the strain of virus exposed to, initial viral titer during the exposure, as well as the nature of the immune response. For example, broad epitope recognition results in a better chance of clearing viremia faster and for a longer time than a narrow recognition window.

Disease progression is also affected by treatment, the goal of which is to reduce virus replication to undetectable levels. Current therapeutics successfully target the viral enzymes: reverse transcriptase, integrase, and protease (16). The combined administration of three drugs, referred to as highly active antiretroviral therapy (HAART), is a successful treatment for delaying the disease progression towards AIDS (17-19). However, once started, treatment must continue for the lifespan of patients, as a lapse in treatment can stimulate replication of drug-resistant virions and accelerated AIDS progression (16).

There is currently no vaccine or cure for HIV-1 infection. While current therapeutics effectively block viral replication, no therapy currently targets or eliminates the reservoir of cells with integrated provirus. This population of cells has been infected and is capable of spreading virus, which means infected patients will always have a source of viral replication. However, to date, at least one individual has effectively been cured of his HIV-1 infection (20, 21). The so-called “Berlin Patient” underwent

chemotherapy and irradiation to ablate his immune system in an attempt to cure his acute myeloid leukemia. He then received a bone marrow transplant from an individual naturally immune to HIV-1 infection due to a mutation in the CCR5 HIV-1 co-receptor, which is necessary for viral fusion with the target cell membrane. After the transplant, the patient stopped HAART, and years later, remains HIV-1 free. In 2019, a second HIV-1 infected patient underwent the same procedure and currently has undetectable levels of the virus (22). While this approach has resulted in at least one cure for HIV-1 infection, irradiation and donor-matched transplantation do not represent a viable option for the millions of, mostly impoverished, infected individuals. Thus, a different approach is necessary to cure the millions of infected people around the globe. In this dissertation, I describe efforts aimed at understanding HIV-1 host-factor interactions as well as maturation determinants critical for generating infectious virions. This information may help guide novel therapeutic design.

HIV-1 Structure

HIV-1 is a member of the *Lentivirus* genus of the larger *Retroviridae* family (23). It is an enveloped virus that contains two identical, positive-sense strands of RNA (see Figure 1-2). The major structural proteins of the virus are derived from the Gag polyprotein, which is composed of the matrix (MA), capsid (CA), and nucleocapsid (NC) polypeptides. In addition to the three main structural proteins of Gag, there are two small spacer peptides, SP1 and SP2, as well as the C-terminal peptide p6. Associated with the membrane of the virion are the receptor-binding Env protein gp120 and the fusion protein gp41, also termed surface (SU) and transmembrane (TM) proteins,

respectively. Env is a trimer of heterodimers of the gp120 and gp41 proteins, and approximately fourteen trimers are present on the surface of a single virion (24). In addition to the Gag structural proteins and Env proteins, an HIV-1 particle also contains the enzymatic proteins necessary for replication: reverse transcriptase (RT), integrase (IN), and protease (PR). Finally, HIV-1 particles also contain an accessory protein, Vpr, which is reported to enhance infection in macrophages (25) and primary T cells (26, 27).

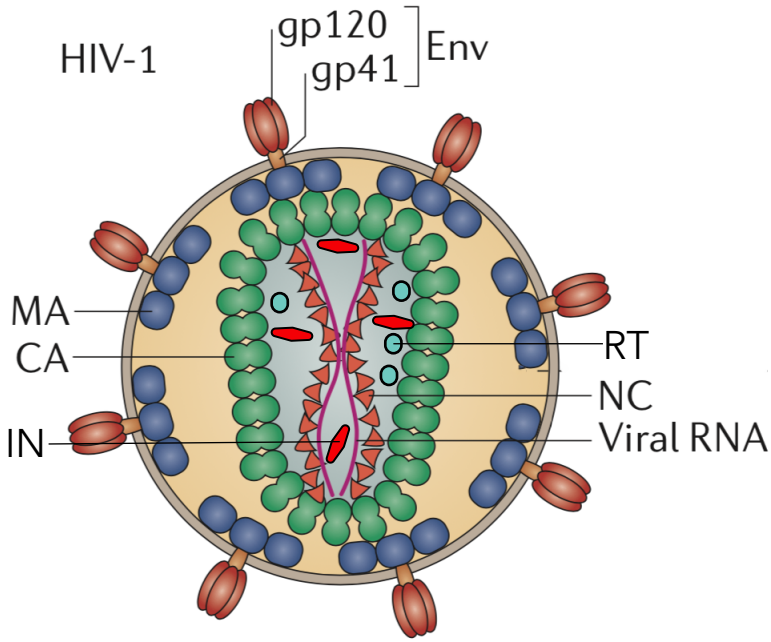

Figure 1-2: Structure Of A Mature HIV-1 Virion. HIV-1 is an enveloped, single-stranded RNA virus. It contains two copies of its genome within a conical capsid which includes the viral enzymes reverse transcriptase and integrase. The nucleocapsid protein coats the RNA. Viral envelope proteins span the viral lipid membrane and exist as a trimer of heterodimers of gp120 and gp41 proteins. A single virion is approximately 120 nm in diameter. Adapted and modified from Campbell and Hope, *Nature Reviews* (2015) (28).

HIV-1 transitions between two distinct structures: immature particles and mature virions. Immature particles are compositionally identical to mature virions; however, the two are structurally distinct. Gag polyproteins are present as an incomplete, spherical lattice in immature particles, which are non-infectious (29). Activation of the viral protease results in cleavage of Gag polyproteins at each junction. Cleaved CA molecules then assemble into a cone-shaped, hexameric lattice referred to as the capsid, (see Figure 1-4 B). The capsid surrounds the RNA genome and cleaved NC, IN, and RT proteins. Collectively, the capsid and its contents comprise the viral core. The conversion of an immature particle to a mature virion is required for infection, and is termed maturation, as discussed below (29).

The ≈9-kb genome of HIV-1 also encodes several accessory proteins that perform various functions during replication. These include Tat and Rev, which upregulate viral protein expression by promoting HIV-1 transcription and subsequent RNA transport to the cytosol (30). Additionally, viral proteins Vif, Vpu, and Nef function to augment infectivity and pathogenesis by counteracting cellular defense factors. Expression of the structural and non-structural viral proteins from the provirus is achieved by RNA splicing (31). Full-length RNA transcripts are used to generate the Gag and Gag-Pol polyproteins. A medium-length 4-kb single splice variant is required for Env, Vpr, Vif, and Vpu expression. The 2-kb multiply-spliced RNAs are required for Tat, Rev, and Nef expression.

HIV-1 Replication Cycle

HIV-1 replication begins with attachment of a mature, infectious virion to the host cell via Env interactions (32). Entry into host cells begins with gp120 contact with surface-exposed CD4, followed by interaction with either CCR5 or CXCR4 co-receptors (33). Co-receptor engagement triggers a conformational change in gp41, which extends from the viral membrane into the host cell membrane (32). Unfolding of gp41 and its interaction with the target cell membrane bridges viral and cell membranes and initiates fusion of the virus to the host cell. The viral core then enters the cell and begins five processes: uncoating, reverse transcription, trafficking to the nucleus, entry into the nucleus, and integration into host chromatin, (see Figure 1-3).

Several different models account for these early replication events; however, most models depict the first four events occurring in concert (28, 34, 35). Viral cores begin to traffic to the nucleus via engagement of the cytoskeletal network (36-40). During transport, CA dissociates from the capsid in a process termed uncoating (34, 41). The rate of uncoating appears to be a regulated event: uncoating that proceeds too quickly or too slowly results in poor infection (42-46). Reverse transcription occurs during trafficking and uncoating (47-50) and is the conversion of the positive-sense, single stranded RNA genome to double stranded DNA via RT (51). During reverse transcription, the uncoating, trafficking core is referred to as the “reverse transcription complex” (RTC). Once a sufficient amount of uncoating has occurred and the viral genome reverse is transcribed, a complex of the remaining core elements, termed the “pre-integration complex” (PIC), traverses the nuclear envelope via CA interactions with

the nuclear pore (NUP) proteins (52-58). IN and host DNA repair elements then direct the integration of the viral genome into gene-dense areas of the host chromatin (59).

Host cell factors activate the transcription of viral RNA and translation of viral proteins, beginning with Tat and Rev, which facilitate further transcription and export of viral RNA for translation. Env proteins, initially translated as the gp160 polyprotein, are glycosylated and proteolytically cleaved before transport to the cellular membrane (60). Gag polyproteins are directed to the membrane and Env via N-terminal myristoylation and basic residues of the MA subunit (61-63). Gag and Gag-Pol proteins coassemble at the membrane via interactions between the CA regions of associated Gag molecules, followed by recruitment of the viral RNA genome and accessory proteins. Immature Gag assemblies begin to bud from the surface of the host cell while PR begins the maturation process, resulting in a mature virus (64).

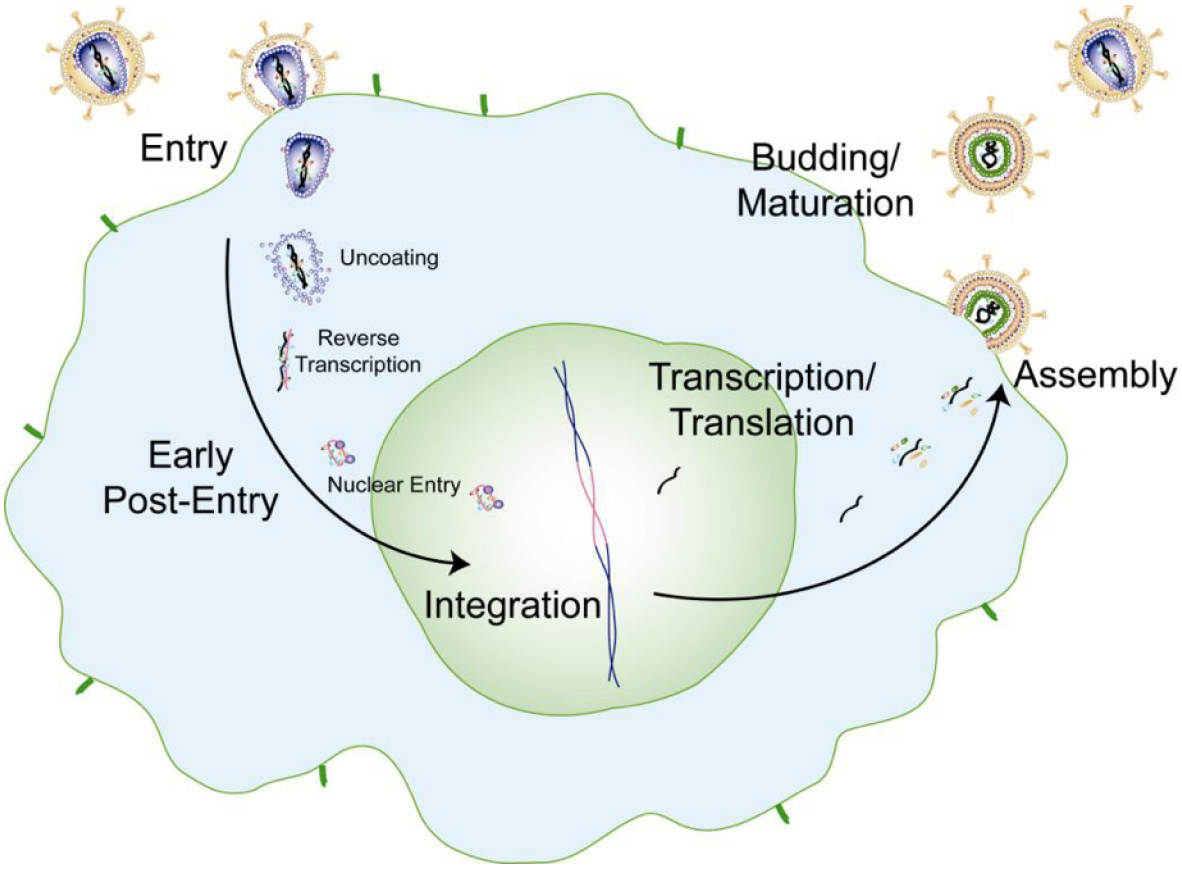

Figure 1-3: The Replication Cycle Of HIV-1. HIV-1 replication begins with attachment to CD4 at the cellular membrane and entry via membrane fusion. The core enters the cell and is transported to the nucleus. Uncoating, reverse transcription, and nuclear penetration follow. Once the PIC has entered the nucleus, the reverse transcribed viral DNA is integrated into the host chromatin. Viral proteins are synthesized by the host and assemble at the cellular membrane. Non-infectious, immature particles are released from the cell. Proteolytic cleavage of the gag polyprotein results in a mature virion capable of repeating the cycle. Drawing was prepared by David Dismuke.

HIV-1 Maturation

As mentioned above, maturation results in the conversion of a non-infectious immature particle to an infectious, mature virion via proteolytic cleavage of the Gag polyprotein, (see Figure 1-4 A). Maturation begins by the auto-activation of the viral protease (PR) which cleaves itself from the Gag-Pol polyprotein. PR then cleaves the Gag subunits at varying rates (65). Cleavage between SP1 and NC occurs most rapidly, followed by cleavage between MA and CA. Two cleavage events then occur between NC and p6 at both ends of SP2. The slowest cleavage product occurs between CA and SP1. PR cleavage results in a dramatic conformational change in HIV-1 from an incomplete spherical, radially-arranged lattice of Gag polyproteins, to a closed, conical assembly of CA hexamers, see Figure 1-4 B. While the structures of the immature Gag lattice (66-68) and mature CA lattice (67, 69-73) are well characterized, the exact mechanism of maturation has yet to be determined. Two competing models of maturation have emerged from an abundance of structural studies: disassembly/reassembly and displacive. The disassembly/reassembly model predicts that cleaved, soluble CA assembles into the capsid lattice *de novo* (66, 74-80), while the displacive model of HIV-1 capsid maturation predicts that the CA-CA interactions of the immature lattice transform following PR cleavage from Gag, resulting in the mature capsid without CA disassembly (81, 82). Recently, evidence in support of a third model has been proposed to combine elements of both disassembly/reassembly and displacive models (83).

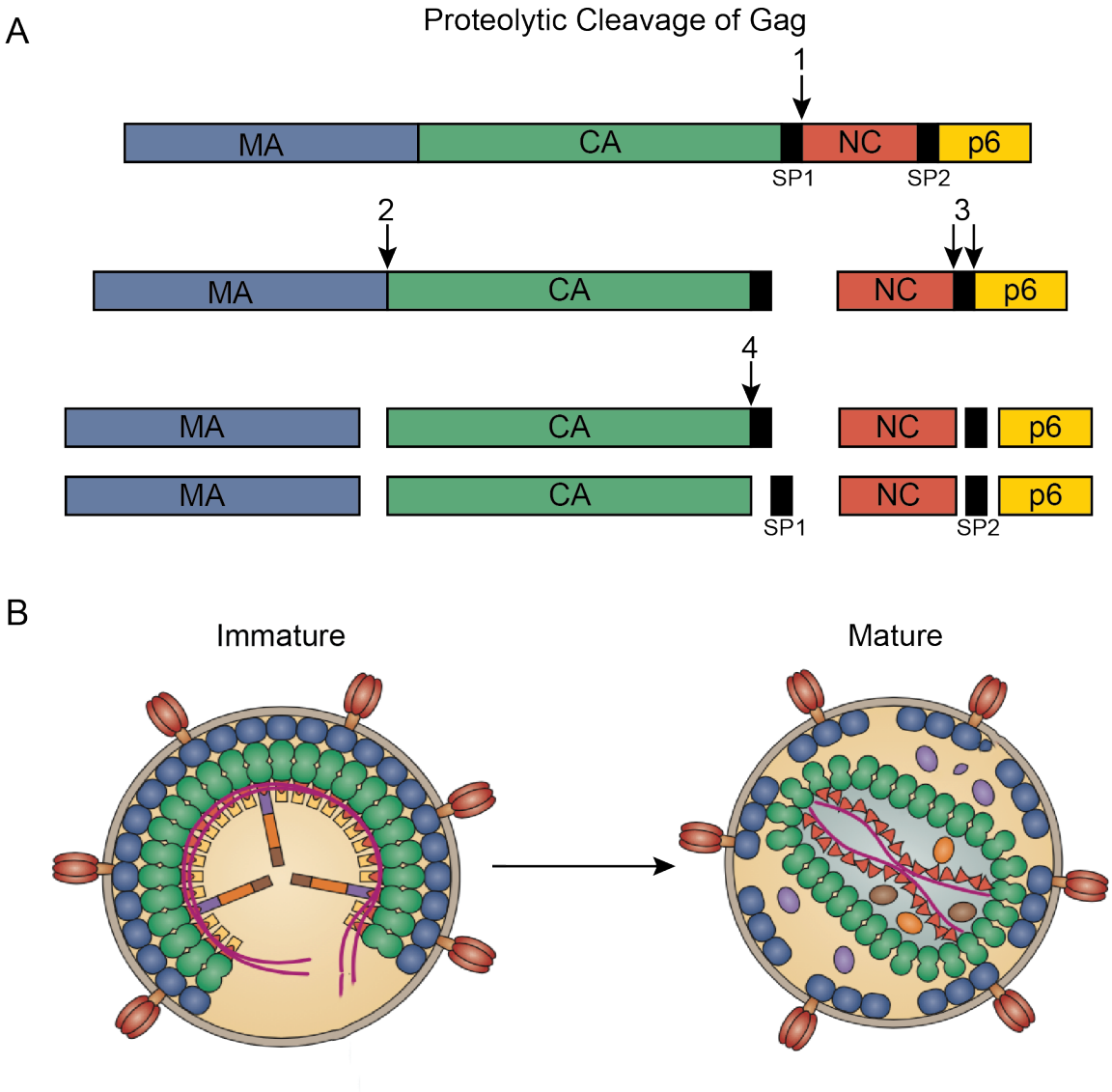

Figure 1-4: HIV-1 Maturation. A. HIV-1 maturation requires proteolytic cleavage of the gag polyprotein at each subunit site. Subunit cleavage proceeds at different rates. The numbers indicate rate of subunit release: SP1-NC cleavage occurs most rapidly, and CA-SP1 cleavage occurs least rapidly. B. Schematic representation of immature HIV-1 particles and mature HIV-1 virions before and after proteolytic gag processing. Adapted and modified from Freed *Nature Reviews* (2015) (29).

HIV-1 CA-CA Interactions

The cleaved CA protein of HIV-1 is 231 amino acids long, and it is the major structural protein of the mature virion. CA consists of two, independently-folded domains: the N-terminal domain (NTD), amino acids 1-145, is joined to the C-terminal domain (CTD), amino acids 152-231, by a flexible linker (84). Both domains are largely helical, with the NTD consisting of seven alpha helices and two beta hairpins, and the CTD consisting of four alpha helices and a 3-10 helix (84, 85). Regardless of the exact mechanism of maturation, cleaved CA assembles into the capsid via CA-CA interactions at three interfaces (Figure 1-5).

Hexamer assemblies of CA subunits form via interactions between neighboring NTDs at the NTD-NTD interface (71, 72, 85-87). The interaction forms an 18-helix bundle that consists of the first three helices of each CA NTD. CA hexamers also involve interactions between the NTD and CTDs of neighboring subunits (NTD-CTD interface) (72, 88, 89). A lattice of hexamers is supported via CA CTD-CTD interactions at the two-fold and three-fold axes (84-86, 90).

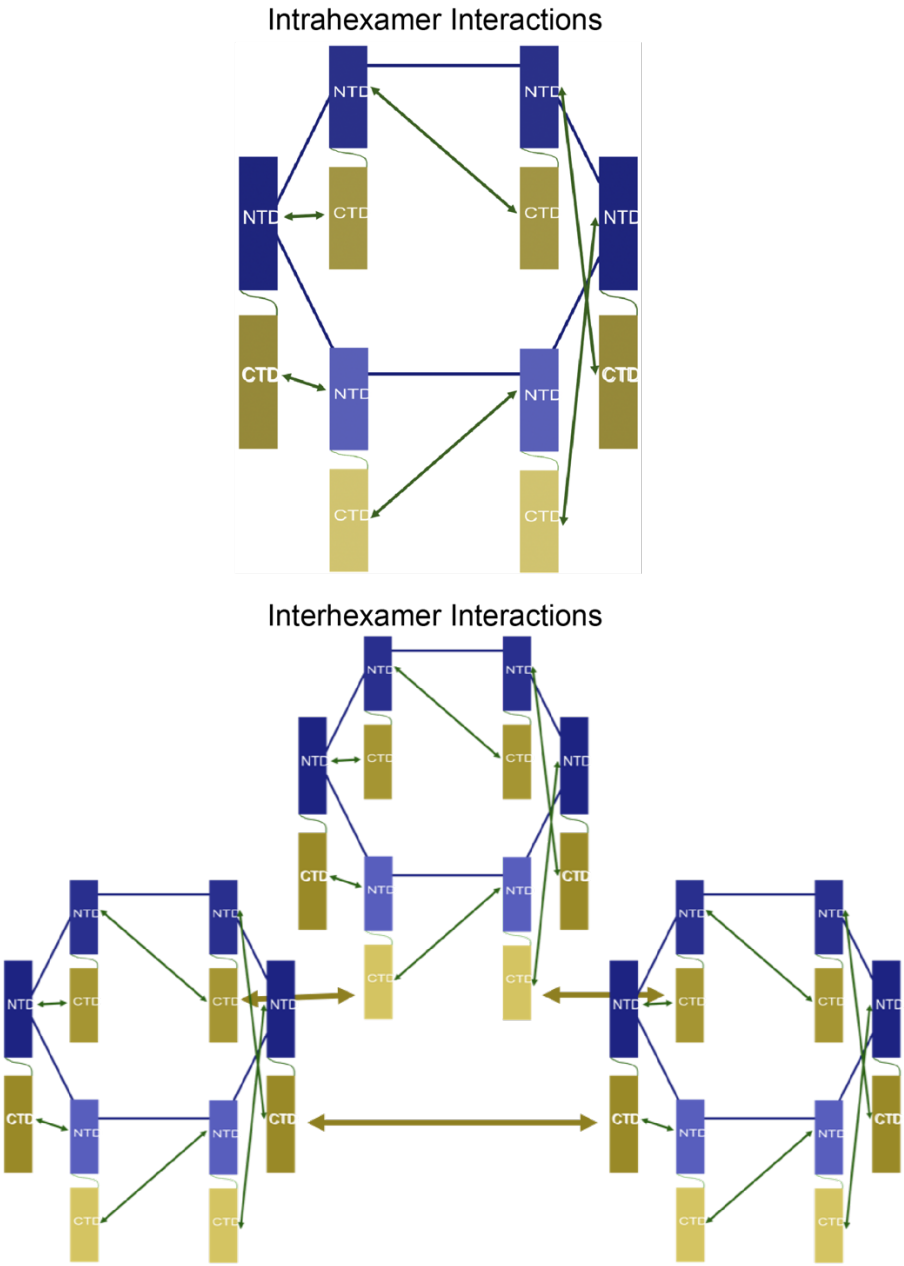

Figure 1-5: CA-CA Interactions At The Capsid Intermolecular Interfaces. CA forms hexamers via intermolecular interactions between neighboring NTDs (blue boxes and blue arrows) and through interactions between NTDs and CTDS (gold boxes and green arrows). CA hexamers form a lattice of hexamers via intermolecular interactions at the CTD three-fold interface between neighboring CTDs (gold arrows).

The assembled HIV-1 capsid consists of ≈250 CA hexamers that adopt a fullerene cone shape (67, 69-73). This geometry is promoted, in part, by the addition of 12 CA pentamers with an asymmetric distribution on the two ends: 12 pentamers are located at the wide end of the capsid, while 7 pentamers are located at the narrow end (70). The formation of the CA pentamer occurs less efficiently than the hexamer, likely due to electrostatic repulsion forces via the internal arginine residue at position 18. The hexamer arrangement mitigates this repulsion more efficiently than the pentamer arrangement, and mutagenesis studies at this position have resulted in particles with more curved, spherical capsids hypothesized to result from more efficient pentamer formation (85, 91). The mechanisms of CA pentamer formation and asymmetric arrangement are presently unknown.

HIV-1 CA-Host Factor Interactions

As a hallmark of viral replication, HIV-1 usurps host proteins and processes for its own benefit. Passive examples of host factor utilization are DNA and RNA replication machinery, ribosome use, and Golgi secretory pathways required for protein production, as well as the use of deoxynucleotide triphosphates (dNTPs) during reverse transcription. However, HIV-1 also uses more direct approaches of host factor utilization during replication. Often, these require interactions between the host protein and a viral protein. During early replication events, the HIV-1 capsid and core elements interact with numerous host proteins (28). Most of these interactions are required for efficient replication; however, the capsid is also a target for antiviral defenses.

Upon entry into the cell, one of the first interactions between the capsid and the host occurs at the microtubule network. Work in our lab and others has shown that the core traffics to the nucleus and may undergo uncoating while on the microtubule network via interactions with the capsid and dynein and kinesin motor proteins and adaptor proteins (36-40, 92-96). One report also suggests a model in which the act of trafficking facilitates the uncoating process through multiple motor protein engagements to the capsid that exert opposing forces, overcoming the structural integrity of the lattice (94).

HIV-1 and other members of the *Lentivirus* genera are unusual among retroviruses with respect to their efficient ability to infect non-dividing cells (97-99). Other retroviruses require cell division which renders the host chromatin accessible for integration (97). The ability of lentiviruses to infect non-dividing cells has been genetically mapped to CA (100-102). While various uncoating models disagree as to the nature of the capsid that arrives at the nucleus, that is, whether the capsid has uncoated or not and to what extent, there is currently no model that accounts for nuclear penetration that is not facilitated by the nuclear pore complex (NPC). The NPC consists of several different proteins, nucleoporins (Nup), that act to actively transport large proteins and complexes in and out of the nucleus. The nucleoporins Nup153 and Nup358 have been implicated with PIC nuclear entry via CA interactions (55-57, 103-106). Additionally, nuclear import and integration are also facilitated via CA interactions with transportin 3 (TNPO3) (107-110) and cleavage and polyadenylation specificity factor 6 (CPSF6) (107, 111-113). While the mechanisms by which these proteins facilitate HIV-1 nuclear entry are unknown, their requirements have been documented in

mutagenesis and depletion studies. Additionally, CPSF6 has been shown to affect where HIV-1 DNA integrates into the host chromatin by targeting integration into gene-dense areas, away from the perinuclear space (114, 115).

Perhaps the most studied CA interaction within cells is that between CA and cyclophilin A (CypA). CypA is an abundant, peptidyl-prolyl isomerase host protein that binds to CA at an unstructured loop between helices 4 and 5 at positions G89 and P90 (116-120). CA binds to the active sites of CypA, which results in *cis* to *trans* isomerization at P90 (116); however, it is unknown if this isomerization is mechanistically involved in how CypA influences HIV-1 replication. The CA-CypA interaction promotes infection, and has been implicated in reverse transcription, uncoating, and nuclear entry (57, 104, 108, 121-124). However, the requirement for CypA is strain specific (125) as well as cell type-dependent (126, 127), and CypA can even inhibit HIV-1 in certain cell types (128, 129).

Recently, our lab and others have identified the host protein elongation factor 1 A (EF1A) to be necessary for HIV-1 infection. EF1A was identified as an HIV-1 Gag binding protein at both MA and NC sites, which was initially speculated to promote viral RNA incorporation into virions (130). Later, EF1A was reported to specifically interact with HIV-1 RT and IN (131). This report demonstrated the necessity of EF1A for late reverse transcription and implicated EF1A in stabilizing the reverse transcription complex. At the same time as this report, work in our lab identified EF1A from cell extracts that promoted uncoating of purified cores *in vitro*. Uncoating was then observed again with the use of recombinant EF1A (David Hout, unpublished data). EF1A has since been demonstrated to directly bind RT, an interaction that can be

blocked by the small molecule didemnin B (132-134). I spent the early work of my thesis project studying the requirement of EF1A for HIV-1 infection, which is detailed in Chapter 3 of my dissertation.

While CA and the viral capsid mediate host factor interactions that promote infection, the capsid is also the target of cellular restriction factors (35, 135). The two most studied capsid-binding restriction factors are tripartite motif protein 5 alpha (TRIM5α) and myxovirus resistance protein B (MxB). TRIM5α is unique among the TRIM family of proteins in that, in addition to its three canonical domains: ring, B-box, and coiled-coil, it contains the capsid-binding SPRY domain (135). TRIM5α binds to the capsid lattice and forms a large cage around it. The capsid is then prematurely disassembled via ubiquitin recruitment and proteasomal degradation, resulting in reverse transcription impairment (136-139). Interestingly, proteasome inhibition does not rescue HIV-1 replication in TRIM5α expressing cells: reverse transcription is no longer impaired, but nuclear entry is (140, 141). The homologous protein TRIMCyp also restricts HIV-1 replication; however, the capsid recognition occurs via a CypA domain in place of the SPRY domain of TRIM5α (142, 143). The interferon-induced protein MxB also binds to the capsid and restricts HIV-1 replication before and after nuclear import (144-149).

Goals Of My Thesis Work

My thesis work has focused on two different aspects of HIV-1 replication: 1) host factor interactions and 2) maturation. During my early thesis work, I used an *in vitro* binding assay and Multidimensional Protein Identification Technology (MuDPIT)

proteomics in an attempt to identify novel capsid-binding host proteins. From my screen, I identified EF1A as a candidate CA-binding host protein. I then proceeded to simultaneously validate EF1A as a CA-binding host protein, as well as a functional protein required for HIV-1 infection. While I determined that EF1A had a low, substoichiometric interaction with CA, I also determined that EF1A was required for efficient infection, and that this requirement varied with the Env protein. HIV-1 particles bearing native Env depend on EF1A during infection of $CD4^+$ HeLa and T cells; however, EF1A was dispensable for HIV-1 infection of particles pseudotyped with VSV-G protein. I also determined that EF1A depletion results in down-regulation of surface-exposed CD4. While most of the literature regarding HIV-1 and EF1A was focused on the RT-EF1A interaction, my finding, that EF1A is an Env-dependent host factor, is novel. This work is described in Chapter 3.

The second part of my thesis project focused on determining the antiviral mechanism of a single mutation at the cleavage site between MA and CA in Gag. The single Y132I substitution had previously been shown to be transdominant when used in a phenotypic mixing experiment (150). The authors of that study reported that particles resulting from cotransfections between wild type and Y132I proviral plasmids had morphologically aberrant cores, and they were impaired for reverse transcription; however, the exact mechanism remained undetermined. My goal was to determine the antiviral mechanism of the uncleaved MA-CA protein. I found that the uncleaved MA-CA protein coassembles with CA in particles without affecting the hexameric assembly of CA and that the MA-CA-containing cores are stable. In contrast to what had previously been reported, I observed no impairment at reverse transcription; rather,

nuclear entry was impaired, and integration targeting was altered. Finally, by performing a mutational analysis, I determined that the membrane-binding elements of MA are required for the antiviral potency of MA-CA. I proposed a model that uncleaved MA-CA protein coassembles into the capsid and tethers the core to the cellular membrane of the infected cell, thus impeding trafficking to the nucleus. My work has resulted in several novel findings, including the coassembly of uncleaved and cleaved Gag subunits, which suggest that CA must be cleaved during maturation in order to avoid improper assembly and impaired infection. This work was published in Journal of Virology (151), and it is described in Chapter 2.

Chapter 2

Dominant Negative MA-CA Fusion Protein Is Incorporated Into HIV-1 Cores And Inhibits Nuclear Entry Of Viral Preintegration Complexes

Introduction

As described in Chapter 1, particle maturation occurs late in the HIV-1 replication cycle and is required for producing an infectious virus. Immature HIV-1 particles are composed of Gag polyproteins containing segments corresponding to the matrix (MA), capsid (CA), spacer peptide 1 (SP1), nucleocapsid (NC), spacer peptide 2 (SP2), and p6 proteins. In cells, Gag is myristoylated at its amino terminus; this modification, together with a nearby highly conserved stretch of positively charged residues in the MA region, promotes its association with the plasma membrane during particle assembly. As the assembling particle begins to bud from the cell membrane, the viral protease is activated and cleaves Gag into its individual protein components. The cleavage sites are processed at different rates, with SP1-NC cleaved most rapidly, followed by MA-CA, NC-SP2, SP2-p6, and finally CA-SP1 (Figure 1-4) (65, 152-154). The first cleavage releases NC, resulting in formation of the condensed viral ribonucleoprotein complex (vRNP) and the stable genomic RNA dimer. Subsequently, cleavage at the MA-CA junction releases CA-SP1, leaving MA attached to the inner face of the viral membrane. CA-SP1 then assembles and is slowly cleaved, resulting in formation of the hexameric capsid lattice. Maturation results in the conversion of immature particles, which contain a spherical lattice of Gag and Gag-Pol polyproteins, into mature particles harboring a

conical metastable capsid. The capsid, a closed conical assembly of CA polymers, encases the nucleic acid and protein components necessary for viral replication: two copies of viral genomic RNA and cognate tRNA, reverse transcriptase (RT), integrase (IN), and nucleocapsid (NC), which collectively comprise the vRNP. The capsid and its contents comprise the viral core (recently reviewed in (35)).

While the starting and ending products of maturation are hexameric lattices, the structural organizations of the immature and mature lattices are distinct. Each lattice involves contacts between the two independently folded domains of CA: the amino-terminal and carboxy-terminal domains (NTD and CTD, respectively). The immature lattice is an incomplete sphere of radially arranged 8 nm Gag hexamers formed by neighboring CA NTD-NTD interactions and stabilized by CA CTD-CTD dimer interactions (66-68). In contrast, the mature lattice adopts a fullerene cone shape consisting of ~250 hexamers and 12 pentamers, which are arranged asymmetrically with 7 on one end and 5 on the other (67, 69-73). Once cleaved from MA, the N-terminal 51 residues of CA fold into a beta-hairpin structure (155). The mature CA lattice is composed of hexamers assembled via CA NTD-NTD (71, 72, 85-87) and NTD-CTD (72, 88, 89) interactions, and adjacent hexamers are stabilized via CTD-CTD interactions at the three-fold interface (84-86, 90).

Maturation is a critical step in HIV-1 replication, making it attractive for antiviral inhibitor development. Protease inhibitors are a highly successful strategy for limiting viral replication (156), as perturbations or interruptions in Gag cleavage result in abortive infection (157). A separate class of maturation inhibitors (MIs), typified by bevirimat, bind to the assembled Gag lattice and inhibit cleavage at the CA-SP1 junction

(78, 158-160). Another class, allosteric IN inhibitors (ALLINIs), bind IN and decouple the incorporation of the vRNP into the viral capsid shell during maturation (161-168). Although both MIs and ALLINIs potently inhibit HIV-1 replication, none of these compounds is yet clinically approved.

The effects of inhibiting cleavage at each site in Gag have been studied in both murine leukemia virus (MLV) (169, 170) and HIV-1 (150, 171-173). Using phenotypic mixing strategies to produce viruses harboring ratios of cleavable and non-cleavable Gag proteins, both Lee et al. (150) and Muller et al. (172) reported that incorporation of uncleaved MA-CA protein markedly inhibited HIV-1 infectivity, while Checkley and coworkers reported a similar phenotype when the CA-SP1 junction was blocked (171). Ruli et al. reported that uncleaved p12-CA in MLV was transdominant due to the absence of an N-terminal proline residue on CA. Lee et al., by contrast, demonstrated that substituting the N-terminal proline of HIV-1 CA to either Lys or Phe did not result in potent inhibition of infection, suggesting that uncleaved MA-CA HIV-1 protein impairs infectivity through a different mechanism than that by p12-CA in MLV. Notwithstanding these differences, these studies highlight the importance of proper Gag processing for retroviral replication, since relatively small amounts of uncleaved Gag can dramatically inhibit infection. Lee and coworkers reported that HIV-1 particles containing uncleaved MA-CA protein are impaired for reverse transcription and harbored morphologically aberrant and eccentrically located cores, suggestive of a maturation defect (150). However, the effects of the uncleaved protein on maturation were not analyzed in detail.

In my studies, I sought to further define the mechanism by which uncleaved MA-CA reduces HIV-1 infectivity. Based on previously-reported results (150), I

hypothesized that coassembly of uncleaved MA-CA and cleaved CA proteins within particles perturbs the intermolecular interfaces in the capsid and that the resulting capsids are intrinsically unstable. I observed evidence for coassembly between uncleaved MA-CA and cleaved CA proteins in virus particles but without detectable perturbation of the CA-CA intermolecular interfaces. Additionally, I observed that the particles contained stable cores and were proficient for reverse transcription. However, nuclear entry was predominantly inhibited, and integration targeting was also altered. Finally, the results of genetic analysis suggest that the membrane-binding ability of Gag contributes to the antiviral potency of uncleaved MA-CA.

Results

Confirming The Transdominant Phenotype Of Uncleaved MA-CA

Lee et al. (2009) reported that incorporation of a Gag protein containing a substitution preventing cleavage of the MA-CA junction (MA Y132I) profoundly reduced HIV-1 infectivity and yielded morphologically eccentric particles. To confirm these results, I transfected HEK293T cells with a wild type HIV-1 proviral plasmid together with various quantities of the mutant, MA Y132I (MA-CA) proviral plasmid. The resulting particles, normalized for CA content by p24 ELISA, were assayed for infectivity in Hela TZM-bl cells by quantifying the expression of the luciferase reporter gene that is transactivated in the cells upon expression of the HIV-1 Tat protein from integrated proviruses. Consistent with the previous study (150), I observed potent inhibition of HIV-1 infectivity by MA-CA, with 5% of the plasmid resulting in a 70% loss of infectivity and 20% of MA-CA essentially abolishing infectivity (Fig. 2-1A). The cotransfection

approach resulted in particles containing both CA and uncleaved MA-CA proteins (Fig. 2-1B). I refer to particles generated from WT and MA-CA cotransfections as MA-CA mixed particles.

I then collaborated with Alan Engelman's group to visualize mixed particles. MA-CA mixed particle morphologies were characterized by thin-section EM based on the following classifications: mature, with centrally located electron density oftentimes in association with a conical core; immature, with partial of full toroidal electron density beneath the viral membrane; eccentric, with blob-like electron density in association with the viral membrane, most often separated from translucent core-like structures; and empty, which predominantly lacked clear electron density signal (Fig. 2-1C). Based on cryogenic electron tomography (cryo-ET) bubblegram imaging of wild-type HIV-1 and morphologically eccentric class II IN mutant particles as well as eccentric particles produced in the presence of ALLINIs, the electron density is coincident with NC protein and thus maps the position of the vRNP within viral particles (164). Similar to the prior study (150), preparations of MA-CA mixed particles harbored populations of virions with eccentrically located electron density (Fig. 2-1D). The percentage of particles with eccentric particle morphology was proportional to the percentage of MA-CA plasmid in the cotransfections ($R^2 = 0.90$).

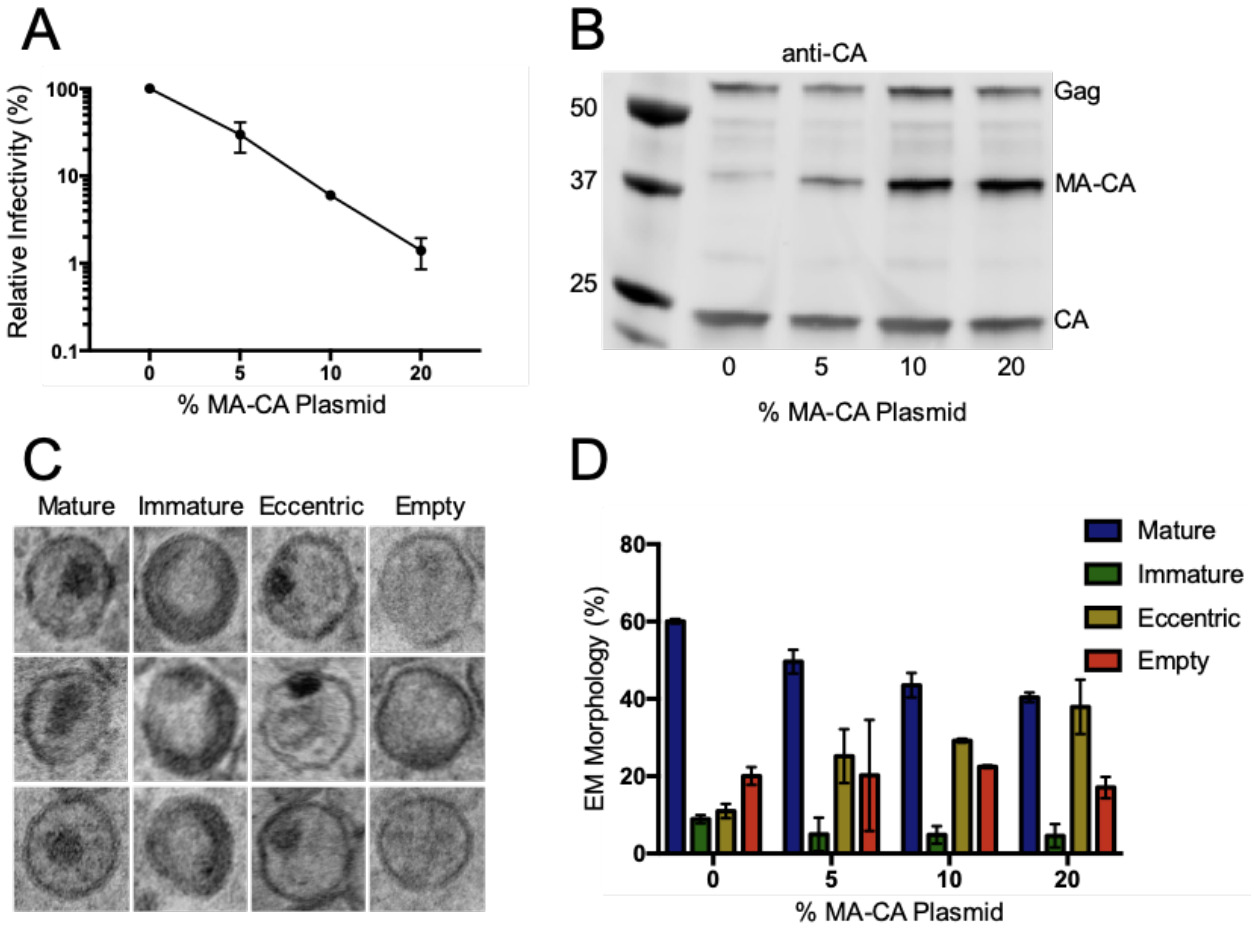

Figure 2-1. Virological Properties Of HIV-1 Containing Uncleaved MA-CA. (A) Infectivity of HIV-1 particles produced by transfection of 293T cells with a wild type HIV-1 plasmid together with the indicated fractions of the MA-CA plasmid encoding the Y132I substitution in Gag that prevents cleavage of the MA-CA junction. Shown are the mean values from 5 independent experiments. Error bars represent standard deviations. (B) Immunoblotting analysis of the pelleted particles, probed with antiserum specific for CA. Shown are representative results from one of three independent experiments which exhibited similar outcomes. (C) Particles from MA-CA cotransfections analyzed by thin-section EM. Representative images of mature, immature, eccentric, and empty particle morphologies. (D) Quantitative analysis from thin-section EM. Results are percentages normalized for the different morphologies from counting at least 100 particles per experiment; error bars show standard deviations from two independent experiments. (C and D) Images were curated and analyzed by Wen Li in Alan Engelman's lab.

Assembly Properties Of MA-CA Mixed Particles

The observed effects of uncleaved MA-CA protein on the morphology of the viral core suggested that the inhibitory effect occurs through disruption of capsid assembly. Therefore, I sought to determine whether uncleaved MA-CA and cleaved CA proteins coassemble in particles, and if so, what effect this has on formation of the various intermolecular contacts necessary for capsid assembly. I employed an approach involving engineered disulfide crosslinking between CA subunits. It has previously been shown that the NTD-NTD intermolecular interface critical for CA hexamer assembly can be covalently stabilized by engineering disulfide crosslinks between CA positions A14 and E45, resulting in CA hexamers that can be detected by SDS-PAGE (174). To determine whether the uncleaved MA-CA protein coassembles with CA in virions, I cotransfected a plasmid harboring the A14C substitution with the MA-CA plasmid harboring the E45C substitution (Fig. 2-2A and 2-2B). The predicted molecular weight of the MA-CA/CA heterodimer resulting from disulfide crosslinking is approximately 67 kDa. Under non-reducing conditions, I observed an approximately 70 kDa protein, the intensity of which correlated to the ratios of the two constructs used in the cotransfection. This species was detected by both anti-CA and anti-MA antibodies but was not observed under reducing conditions, indicating that it resulted from disulfide crosslinking and contains the MA-CA protein. I confirmed the results by performing the reciprocal analysis by cotransfecting a plasmid harboring the E45C substitution together with the MA-CA plasmid harboring the A14C substitution. Similar to the original result, I observed the same 70 kDa species under non-reducing conditions (Fig. 2-2C and 2-

2D). These results indicate that uncleaved MA-CA is capable of associating with CA in particles.

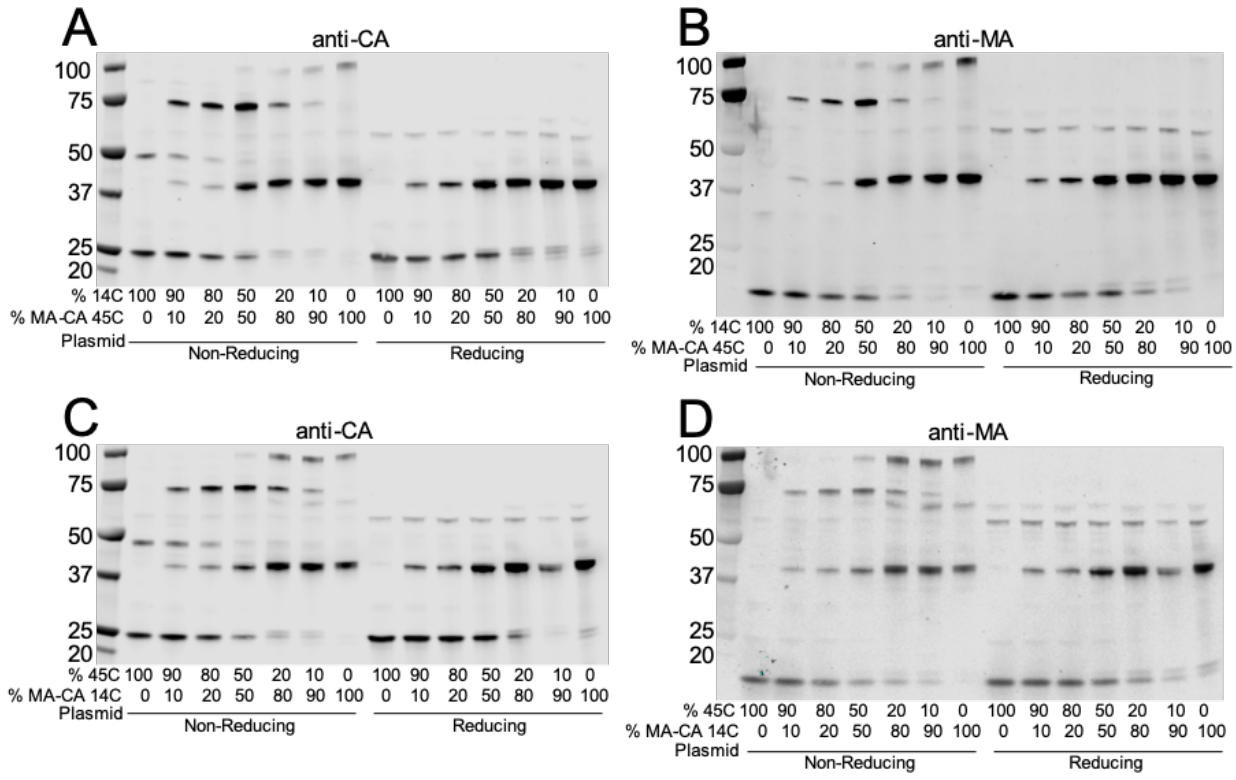

Figure 2-2. Association Of Uncleaved MA-CA Protein With CA In HIV-1 Particles. An HIV-1 plasmid encoding the A14C substitution in CA was cotransfected with the MA-CA plasmid encoding the E45C substitution in CA at the indicated percentages. Particles were pelleted, and proteins were separated by SDS-PAGE under reducing and non-reducing conditions and immunoblotted with antiserum specific for CA (panel A) and MA (panel B). Panels C and D show the results of the same analysis with plasmids encoding the reciprocal Cys substitutions (E45C, and MA-CA/CA A14C). Shown are representative results from one of two independent experiments that produced similar outcomes.

I next asked whether CA and MA-CA proteins can coassemble *in vitro* using purified recombinant 14C/45C CA and MA-CA proteins and immunoprecipitation. Because tubular assemblies of recombinant CA pellet at low speeds, I employed immunoprecipitation by magnetic beads to avoid centrifugation and consequent pelleting of independently assembled CA tubes. I assembled CA and MA-CA proteins in the presence of 1 M NaCl, either separately or together, pelleted them to remove the unassembled proteins, and added the assemblies to beads coated with antiserum directed against HIV-1 MA protein. I observed coimmunoprecipitation of CA with MA-CA when the proteins were first coassembled in the same assembly reaction (Fig. 2-3A lane 4). However, when separately assembled CA and MA-CA proteins were added to the same immunoprecipitation reaction, the quantity of CA in the immunoprecipitate was approximately 20% of that observed with coassembled proteins (Fig. 2-3A, compare lanes 4 and 5). These observations indicated that CA and MA-CA can coassemble *in vitro*. I also analyzed the assembled proteins by negative-stain EM. Recombinant 14C/45C CA protein forms long, hollow nanotubes when assembled under high salt conditions (Fig. 2-3B, left panel). Interestingly, when recombinant CA and MA-CA proteins were coassembled, I did not observe ordered nanotube structures. Rather, I observed densely-packed protein aggregates (Fig. 2-3B, right panel). Non-reducing SDS-PAGE and Coomassie staining revealed that MA-CA alone did not yield higher-order structures, and that CA efficiently formed hexamers in the presence of MA-CA (Fig. 2-3C). Thus, consistent with my characterizations of virus particles, recombinant MA-CA protein induced a capsid assembly defect without preventing CA hexamer formation.

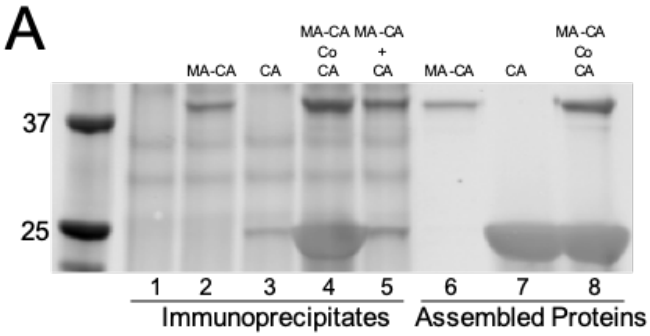
A
MA-CA
CA
MA-CA Co CA
MA-CA + CA
MA-CA
CA
MA-CA Co CA
37
25
1 2 3 4 5 6 7 8
Immunoprecipitates
Assembled Proteins

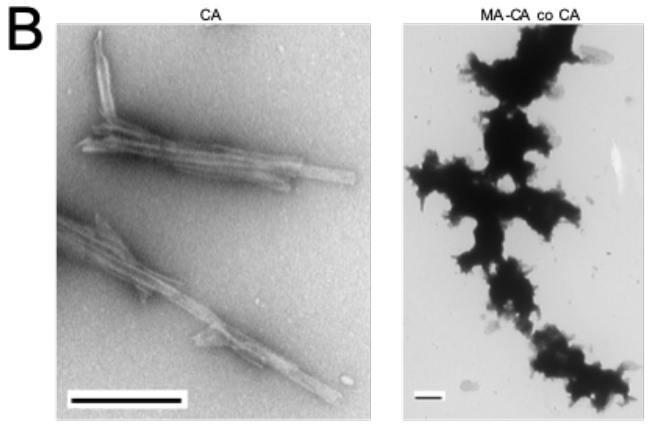
B
CA
MA-CA co CA

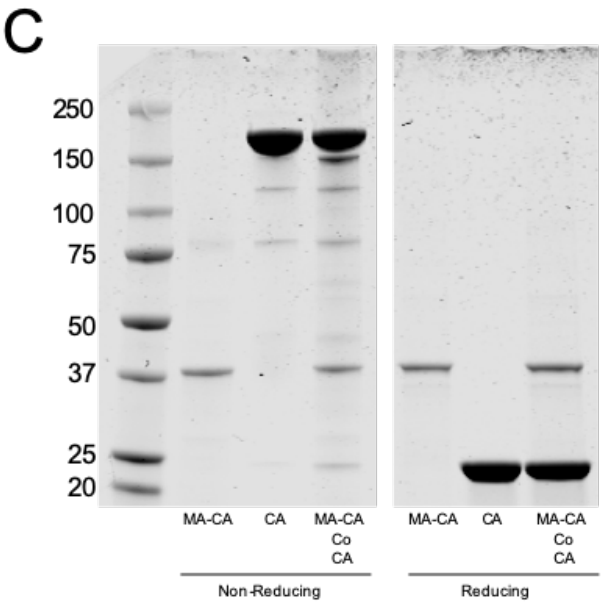
C
250
150
100
75
50
37
25
20
MA-CA
CA
MA-CA Co CA
MA-CA
CA
MA-CA Co CA
Non-Reducing
Reducing

Figure 2-3. *in vitro* Assembly Of Recombinant CA And MA-CA Proteins. (A) Immunoprecipitation of MA-CA with anti-MA antibody coated protein A/G magnetic beads. Purified recombinant HIV-1 CA and MA-CA proteins were assembled separately or coassembled at 0.8 mg/ml each and pelleted. The assembled proteins were resuspended and captured with magnetic beads coated with MA-specific polyclonal antibody. Immunoprecipitated proteins were separated by SDS-PAGE under reducing conditions and immunoblotted with CA-specific antiserum. Lanes 6-8 contain equivalent quantities of the assembled proteins that were added to the beads, analyzed for reference. Shown are representative results from one of three independent experiments which exhibited similar outcomes. (B) Representative negative-stain EM images of recombinant CA (left panel) and CA coassembled with recombinant MA-CA (right panel) from one of two independent experiments with similar outcomes. Each scale bar represents 500 nm. (C) Assembly reactions from (B) separated by non-reducing and reducing SDS-PAGE followed by Coomassie staining. Shown is a representative result from one of two independent experiments with similar outcomes.

My results indicate that uncleaved MA-CA protein induces assembly defects both in particles and *in vitro* without prohibiting CA hexamer assembly. I next asked whether uncleaved MA-CA perturbs the CA-CA intermolecular interfaces necessary for proper capsid assembly. It has previously been shown that engineered cysteine substitution pairs at the three CA-CA intermolecular interfaces in the viral capsid can yield disulfide crosslinks, resulting in CA oligomers that can be detected by SDS-PAGE. To test the effects of incorporation of uncleaved MA-CA protein on CA-CA crosslinking at each interface, I cotransfected MA-CA proviral plasmid with proviral plasmids encoding for appropriate Cys-substituted proteins and analyzed the mixed particles by non-reducing SDS-PAGE and immunoblotting. As previously demonstrated, substitution of Cys for codons A14 and E45 results in spontaneous disulfide crosslinks at the NTD-NTD intrahexameric interface, resulting in a ladder of disulfide-stabilized CA oligomers up to hexamers (174). I observed efficient formation of these CA forms in particles containing various quantities of uncleaved MA-CA protein (Fig. 2-4A, lanes 1-5). Uncleaved MA-CA inclusion quantitatively reduced the crosslinking to an extent that paralleled what was observed upon cotransfection of the A14C/E45C construct with wild type plasmid, consistent with a dilution effect (Fig. 2-4A, lanes 8-12). I attributed the approximately 41 kDa band observed in lane 8 in Fig. 2-4A to spillover of sample from lane 7 during loading. In replicates of this experiment, that band was not observed in this sample.

Similar to the NTD-NTD intrahexameric crosslinks formed by Cys substitutions at CA codons 14 and 45, substitutions of Cys for M68 and E212 result in intrahexameric crosslinks at the NTD-CTD interface (89), also resulting in a ladder of CA oligomers up to hexamer. As observed for NTD-NTD crosslinking, the pattern was not detectably

altered by uncleaved MA-CA incorporation into particles (Fig. 2-4B, compare lanes 1-4 with 8-11). These data suggest that uncleaved MA-CA protein does not prohibit CA-CA contact at the intrahexameric interfaces in virions.

In the HIV-1 capsid, hexamers interact to form a three-fold interface stabilized by specific amino acid side chains in the C-terminal domains of CA subunits. I probed the formation of the three-fold interface by two types of engineered disulfide bonds. First, I analyzed crosslinking resulting from a single Cys substitution at position A204 (175), which results in formation of a CA-CA dimer. As observed in Fig. 2-4C, formation of the dimer was not detectably affected by incorporation of uncleaved MA-CA. Secondly, I observed that crosslinked CA dimer and trimer species resulting from Cys substitutions at CA positions 207 and 216 (86) were not detectably altered in particles containing uncleaved MA-CA (Fig. 2-4D, lanes 1-3 vs. 6-8). Collectively, the crosslinking results suggest that MA-CA does not detectably perturb CA-CA intersubunit interfaces during capsid assembly, and that the capsids in MA-CA mixed particles, despite their morphologically altered phenotype, assemble into a hexameric lattice.

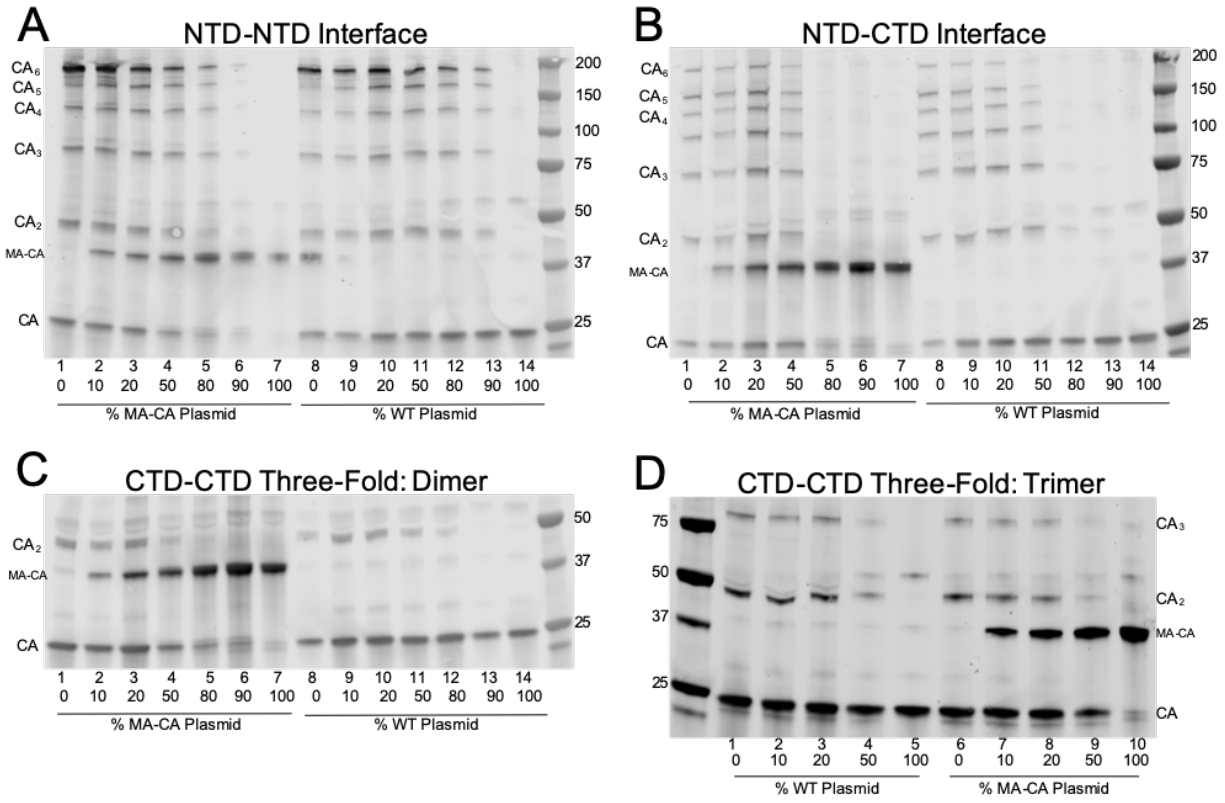

Figure 2-4. Incorporation Of Uncleaved MA-CA Protein Does Not Interfere With CA Hexamer Assembly In Virions. HIV-1 plasmids encoding mutations in CA were cotransfected with MA-CA plasmid or wild type R9 plasmid DNA. Particles were pelleted, and 200 ng p24 of each viral lysate was analyzed by SDS-PAGE, under non-reducing conditions, and immunoblotted with antiserum specific for CA. (A) A14C/E45C, (B) M68C/E212C, (C) A204C, (D) P207C/T216C. Shown are the results of one of three independent experiments, all of which produced similar outcomes.

Uncleaved MA-CA Protein Associates With Stable HIV-1 Cores

Mutations in CA that stabilize or destabilize the viral capsid often result in poorly infectious particles (46, 86, 175, 176). Lee et al. previously reported that particles containing uncleaved MA-CA protein are impaired for reverse transcription in target cells. Because mutations that destabilize the HIV-1 capsid often result in impaired reverse transcription in target cells, I hypothesized that uncleaved MA-CA destabilizes the viral capsid. To test this, I isolated and analyzed cores from particles containing uncleaved MA-CA. Following centrifugation of concentrated particles through a layer of nonionic detergent, density gradient fractions were collected, and HIV-1 proteins and viral RNA were analyzed (177). ELISA quantification of the CA in each fraction revealed elevated levels of core-associated CA in MA-CA mixed particles vs. the wild type (Fig. 2-5A). However, the p24 ELISA can detect both CA and MA-CA proteins, thus the CA detected in mixed particles may represent the sum quantities of these two proteins. To determine if uncleaved MA-CA incorporation specifically alters the level of core-associated CA, I concentrated the proteins in the gradient fractions by precipitation with TCA, separated the proteins by SDS-PAGE, and detected individual viral proteins CA, MA, IN, RT, NC, and, where appropriate, MA-CA by immunoblotting (Fig. 2-5B). Additionally, I quantified viral RNA by RT-qPCR (Fig. 2-5C). I also quantified the levels of CA species in each fraction of the gradients with a Li-COR Odyssey imager and calculated the amount of core-associated CA as a percentage of the entire gradient. The core-containing fractions were identified based on the presence of the known core-associated proteins IN, NC, and RT as well as viral RNA. While there was a small trend toward an elevated level of core-associated CA in MA-CA mixed particles vs. the wild

type, the difference was not statistically significant (Fig. 2-5D). Because mutant particles with unstable capsids display a distinct reduction in core-associated CA (176), my data suggest that uncleaved MA-CA incorporation does not reduce the intrinsic stability of the capsid. Particles bearing only uncleaved MA-CA exhibited high levels of MA-CA cosedimentation following detergent treatment (Fig. 2-5B, lower right blot, and D), consistent with a previous report (178), which suggests that the fully MA-CA core is hyperstable. I also observed that uncleaved MA-CA cosedimented with other core-associated components: CA, NC, RT, IN, and viral RNA (Fig. 2-5B and C), further indicating that MA-CA coassembles with CA in particles. Additionally, I observed a small but statistically significant shift in peak CA density in MA-CA mixed particles, with the peak of cores from particles produced with 20% MA-CA plasmid at a density of 1.19 g/ml, which was lower than the density of the control wild type cores (1.22 g/ml) (Fig. 2-5E). The density shift was not associated with an obvious change in protein composition or RNA levels (Fig. 2-5B, C).

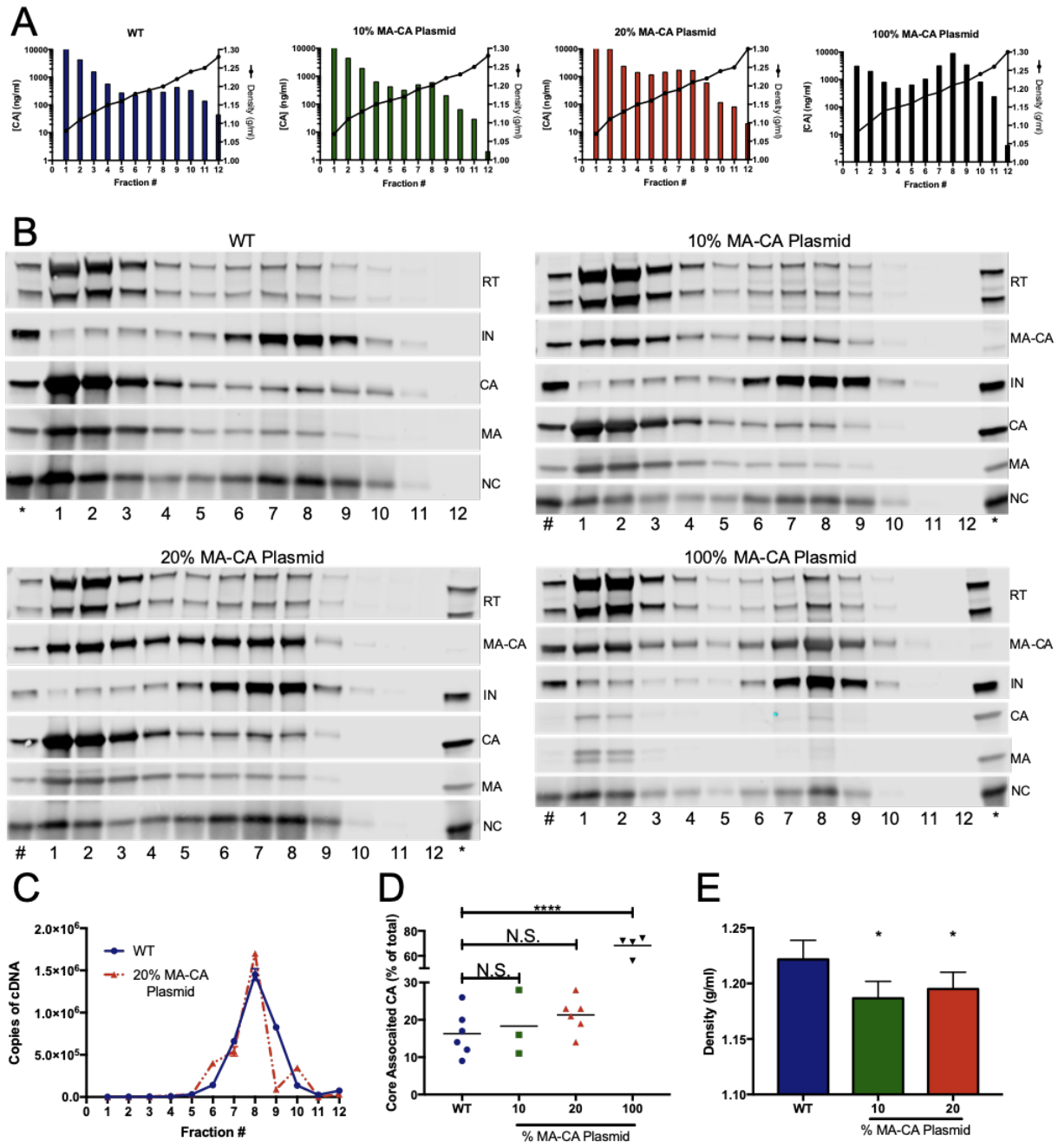
A
WT
10% MA-CA Plasmid
20% MA-CA Plasmid
100% MA-CA Plasmid
[CA] (ng/ml)
Density (g/ml)
Fraction #
B
WT
10% MA-CA Plasmid
20% MA-CA Plasmid
100% MA-CA Plasmid
RT
IN
CA
MA
NC
MA-CA
C
Copies of cDNA
WT
20% MA-CA Plasmid
Fraction #
D
Core Associated CA (% of total)
****
N.S.
N.S.
WT
10
20
100
% MA-CA Plasmid
E
Density (g/ml)
*
*
WT
10
20
% MA-CA Plasmid

Figure 2-5. Uncleaved MA-CA Protein Associates With Stable Cores. Wild type control and MA-CA protein containing particles were concentrated, and the cores were isolated by sedimentation through a layer of Triton X-100 into a sucrose gradient. Fractions were collected from the top of the gradient (Fraction 1) and assayed for CA concentration by p24 ELISA (Panel A). The refractive index for each fraction was used to determine the solution density. The results shown are representative of six independent experiments. (B) Immunoblotting analysis of fractions from wild type and MA-CA mixed particles. The proteins present in each fraction were concentrated and analyzed by SDS-PAGE, immunoblotted with antisera specific for CA, IN, NC, RT, and MA. As a reference, samples (500 ng p24) of the corresponding pelleted virions were analyzed: * WT viral lysate; # MA-CA-containing particles from each corresponding transfection. The numbering corresponds to the sequential fractions as shown in panel A. The immunoblots shown are representative of three to six independent experiments. (C) Quantification of HIV-1 RNA in the corresponding fractions. RNA was extracted and quantified by RT-qPCR, and quantification performed using HIV-1 plasmid DNA as standards. Shown are the mean values of duplicate measurements from one of two independent experiments, with error bars representing one standard deviation. (D) Immunoblot quantification of core-associated CA. Bars represent mean values from 3 to 6 independent experiments. Significance as analyzed by unpaired t-test: N.S., not significant; ****, $p<0.0001$. (E) Mean density of the peak core-associated CA gradient fraction. The fraction containing the peak core-associated CA was identified from CA band quantification as in (D). Shown are mean values from 3 to 6 independent determinations, with error bars representing one standard deviation. *: $p<0.05$ by unpaired t-test.

Although the biochemical analyses suggested that incorporation of uncleaved MA-CA does not destabilize the viral capsid, I also sought to determine whether the particles undergo premature uncoating in target cells. To do this, I exploited the well-known property of the host restriction factor TRIMCyp. TRIMCyp, expressed in cells of some nonhuman primate species, inhibits infection at early post-entry stages by binding to the viral capsid (179, 180). Restriction can be saturated by high virus doses (181-184) and can be abrogated by co-inoculation with noninfectious particles *in trans,* so long as the particles are competent for cell entry and contain stable capsids that can be recognized by the restriction factor. Therefore, the ability of a mutant virus to abrogate restriction by TRIMCyp *in trans* provides a useful assay for capsid stability in target cells (182, 185). To determine if HIV-1 particles containing uncleaved MA-CA protein can abrogate TRIMCyp restriction, I inoculated OMK cells with titrations of VSV-G pseudotyped, mixed viruses together with a fixed, subsaturating quantity of an HIV-GFP reporter virus and monitored infectivity by analyzing GFP expression by flow cytometry. Although particles composed of 100% MA-CA were unable to overcome restriction, consistent with a previous report (182), I observed that particles containing lower amounts of uncleaved MA-CA efficiently promoted infection by the reporter virus (Fig. 2-6A). I did observe a slight reduction in abrogation activity at the highest doses of the inocula, suggestive of a saturation effect. Collectively, the results from my biochemical and TRIMCyp abrogation assays indicate that HIV-1 particles containing uncleaved MA-CA contain stable capsids. Because TRIMCyp recognizes a hexameric lattice (182, 185), these results further indicate that uncleaved MA-CA does not inhibit hexamer

lattice assembly, consistent with my intersubunit crosslinking data (Fig. 2-4) and *in vitro* assembly data (Fig. 2-3C).

Because VSV-G pseudotyping changes particle entry from fusion to endocytosis (186), I also performed a control experiment to determine if pseudotyping by VSV-G alters the antiviral potency of uncleaved MA-CA incorporation. I observed that uncleaved MA-CA reduced the infectivity of the pseudotyped particles; however, at low MA-CA plasmid doses, the inhibition was approximately 50% less potent than exhibited by non-pseudotyped HIV-1 particles (Fig. 2-6B). Immunoblotting of the particles showed comparable levels of MA-CA protein in pseudotyped and control particles, suggesting that the difference in antiviral susceptibility is not a consequence of altered MA-CA incorporation (Fig. 2-6C). Importantly, the pseudotyped particles produced from 20% MA-CA plasmid cotransfection remained markedly inhibited for infectivity (Fig. 2-6B).

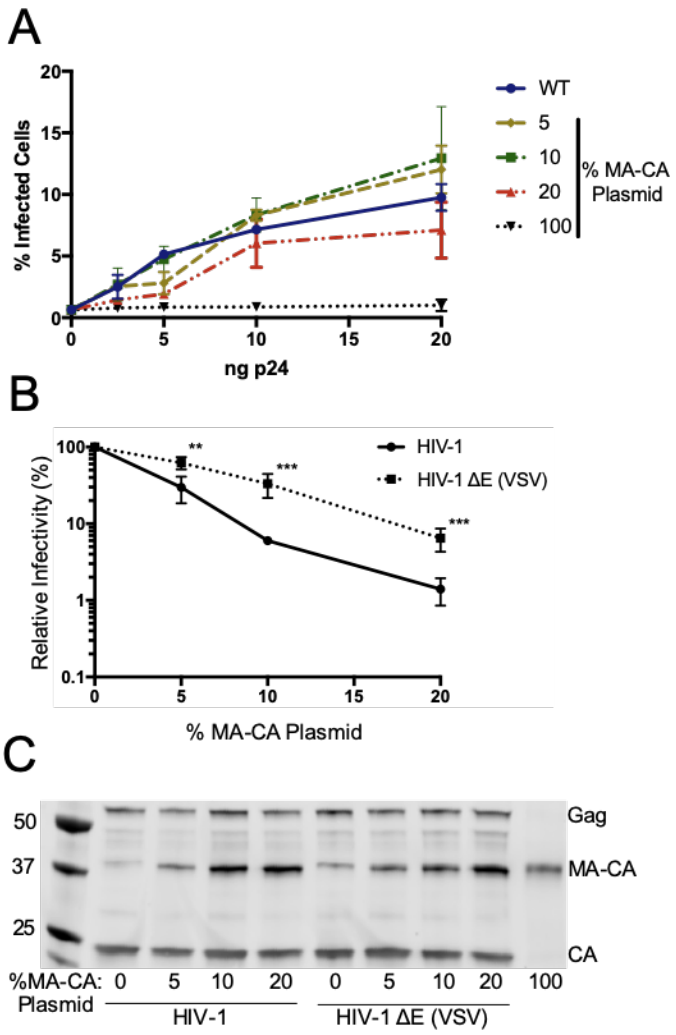

Figure 2-6. Incorporation Of Uncleaved MA-CA Protein Does Not Inhibit The Ability Of HIV-1 Particles To Abrogate Restriction By TRIMCyp In Target Cells. (A) Wild type (pNL4-3 ΔE (VSV)) and MA-CA mixed particles were coinfected with the reporter virus HIV-GFP (VSV) (2 ng of p24) in Owl Monkey Kidney cells. WT and mixed particles were titrated at the amounts shown. Single-cycle infection was monitored by GFP expression, analyzed by flow cytometry. Shown is a representative of four independent experiments with similar outcomes. Error bars represent standard deviations of technical triplicates. (B) Relative infectivity values of the pseudotyped viruses shown in panel A assayed in parallel with nonpseudotyped HIV-1 particles containing the same proportions of uncleaved MA-CA protein. Shown are the mean values from 5 independent experiments. Error bars represent standard deviations. Significance as analyzed by unpaired t-test: **, $p<0.01$; ***, $p<0.001$. (C) Immunoblotting analysis of pelleted particles, probed with antiserum specific for CA. Samples containing 200 ng of p24 were analyzed. Shown are representative results from one of three independent experiments which exhibited similar outcomes.

Uncleaved MA-CA Impairs Nuclear Entry

I next sought to identify the precise stage in the viral lifecycle at which uncleaved MA-CA impairs infectivity. I started by quantifying virus-cell fusion with the BlaM-Vpr reporter assay. In this approach, reporter viruses were titrated on TZM-bl cells supplemented with CCF4-AM, and fluorescence was measured 16 h after inoculation. I observed efficient fusion of viruses produced from MA-CA plasmid cotransfection, including particles containing only MA-CA (Fig. 2-7A and 2-7B). Immunoblotting of pelleted particles demonstrated that the viruses contained similar quantities of the BlaM-Vpr reporter protein (Fig. 2-7C). I conclude that HIV-1 particles containing uncleaved MA-CA protein are not impaired for fusion with target cells.

I next monitored the effects of MA-CA incorporation on post-fusion steps of infection, including reverse transcription and nuclear entry. Lee and coworkers previously observed impaired reverse transcription with particles containing uncleaved MA-CA, suggesting that the inhibitory protein results in an early defect in infection. I performed a similar experiment but employed quantitative PCR to more precisely quantify the levels of HIV-1 DNA produced in cells during infection. To minimize background PCR signals resulting from the integrated LTR reporter construct present in TZM-bl cells (187), I employed Hela-CD4$^+$ cells that lack endogenous HIV-1 sequences. In control experiments, I observed that the Hela-CD4$^+$ cell line exhibited comparable susceptibility to HIV-1 infection as TZM-bl. Following HIV-1 inoculation of the cells, I quantified the formation of late reverse transcription and 2-LTR circle DNA products (Fig. 2-7D). I observed no significant reduction in late reverse transcripts in cells infected by particles produced from 5 to 10% MA-CA plasmid cotransfection, and a

small but statistically significant reduction with particles produced from 20% MA-CA plasmid cotransfection. In contrast, particles containing only the uncleaved MA-CA protein were completely inactive for reverse transcription. These results suggest that the major antiviral effect of incorporation of uncleaved MA-CA into HIV-1 particles is manifested at a stage following reverse transcription.

Non-integrated HIV-1 2-LTR circle DNA is formed following HIV-1 entry into the cell nucleus; therefore, I quantified 2-LTR circles as an indicator of the efficiency of HIV-1 nuclear entry. I observed significant reductions of 2-LTR circle DNA in cells infected with MA-CA mixed particles (Fig. 2-7D). The magnitude of the observed reduction appeared to parallel the infectivity impairment at low levels of MA-CA plasmid cotransfection, with a discrepancy noted at 20% MA-CA plasmid cotransfection: infectivity was impaired by 99%, while nuclear entry was impaired by only 76%. Therefore, while MA-CA mixed particles exhibit a substantial impairment at nuclear entry, there may be an additional effect at a subsequent step, such as integration.

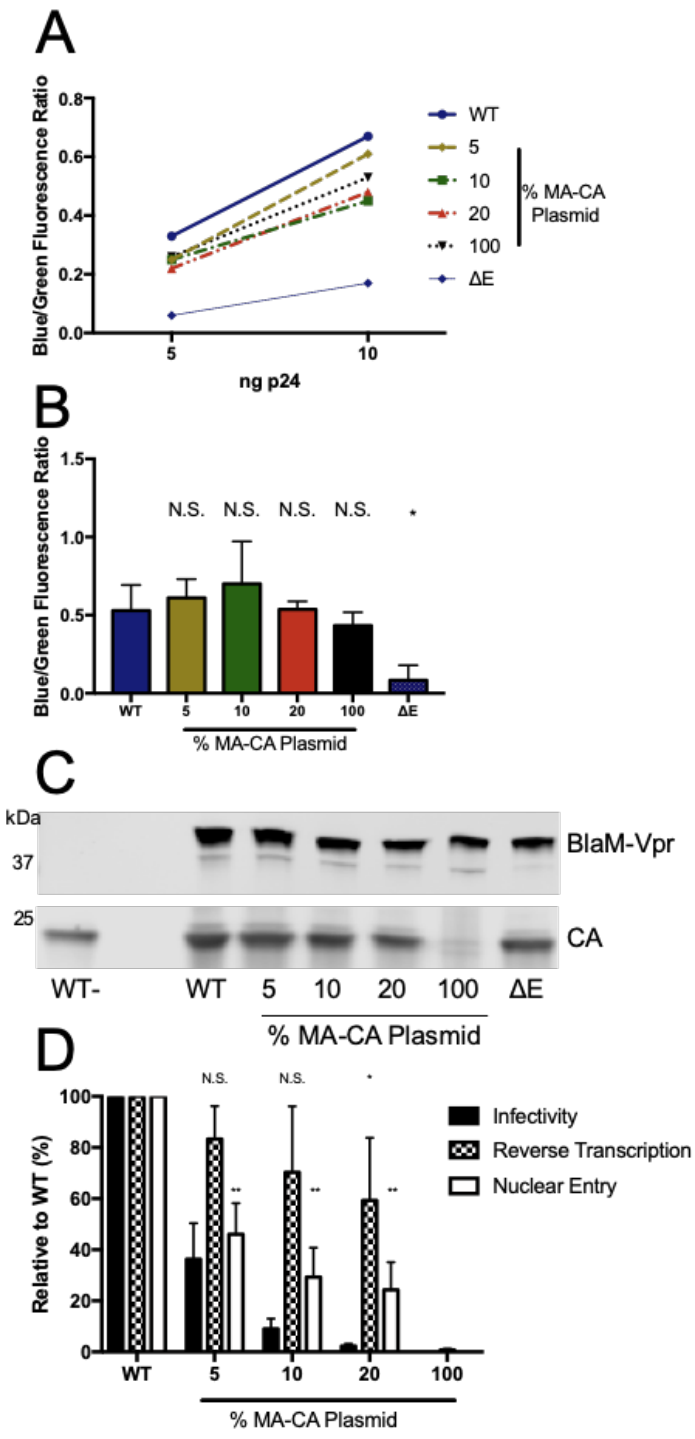
A
Blue/Green Fluorescence Ratio
0.8
0.6
0.4
0.2
0.0
5
10
ng p24
WT
5
10
20
100
ΔE
% MA-CA Plasmid
B
Blue/Green Fluorescence Ratio
1.5
1.0
0.5
0.0
N.S. N.S. N.S. N.S. *
WT 5 10 20 100 ΔE
% MA-CA Plasmid
C
kDa
37
25
BlaM-Vpr
CA
WT- WT 5 10 20 100 ΔE
% MA-CA Plasmid
D
Relative to WT (%)
100
80
60
40
20
0
N.S. N.S. *
** ** **
WT 5 10 20 100
% MA-CA Plasmid
Infectivity
Reverse Transcription
Nuclear Entry

Figure 2-7. MA-CA Mixed Particles Exhibit Impaired Nuclear Entry. (A) Wild-type and MA-CA-containing particles were assayed for fusion with TZM-bl target cells in the BlaM-Vpr reporter assay. The graph shows representative results from one of three independent experiments. (B) Shown are the mean blue/green fluorescence ratios (from assays employing 10 ng of p24) from three independent experiments. Error bars represent standard deviations. N.S.: not significant; *: $p<0.05$ as determined by unpaired t-test. (C) Immunoblot analysis of pelleted particles for CA and BlaM proteins. "WT-" refers to HIV-1 not containing the BlaM-Vpr protein. ΔE refers to the Env-deficient HIV-1 mutant particles. (D) Infectivity, reverse transcription, and nuclear entry of viruses containing uncleaved MA-CA protein. Infectivity was determined by titration on TZM-bl cells and quantification of relative luciferase activity (solid bars). Particles were assayed for synthesis of second-strand transfer DNA (checkered bars) and 2-LTR circle DNA (open bars) 8 h and 24 h post infection of HeLa-$CD4^+$ cells, respectively, by quantitative PCR. Shown are the mean values from 4 independent experiments with copy numbers normalized to that of wild type; error bars represent one standard deviation. N.S.: not-significant; *: $p< 0.05$; **: $p<0.01$ as determined by single-sample t-test with a hypothetical mean of 100.

Uncleaved MA-CA Affects Integration Targeting

As discussed in Chapter 1, CA and CA-host factor interactions have been implicated in integration efficiency and integration targeting in several HIV-1 studies (53, 57, 59, 115, 188-191). To determine whether MA-CA affects HIV-1 integration targeting, I again collaborated with Alan Engelman's lab. Their original integration site sequencing platform amplified viral-host DNA junctions for Illumina sequencing using primers specific to the viral U5 region (189, 192). To enable site sequencing in cells with pre-existing HIV-1 LTR sequences, such as HeLa-P4 (193), they modified the U3 region of pNLX.Luc.R-.ΔAvrII (188) to harbor a heterologous 33 bp sequence derived from the U3 region of equine infectious anemia virus (EIAV) 38 nucleotides in from the HIV-1 terminus after reverse transcription . The resulting NLX.Luc.R-U3-tag virus supported infection at a level that was virtually indistinguishable from the parental NLX.Luc.R- strain. Integration sites determined using genomic DNA isolated 5 d after infection moreover revealed the expected pattern of HIV-1 integration targeting with respect to several genomic annotations including transcription units and local gene density surrounding the integration sites.

To test for possible effects of MA-CA on integration targeting, I cotransfected pNLX.Luc.R-U3-tag with pNL4-3 MA-CA plasmid and inoculated Hela-P4 cells with the resulting 5% MA-CA and 20% MA-CA mixed particles. Four days post inoculation, cellular DNA was extracted and sheared by restriction endonuclease digestion, and sites of HIV-1 integration were mapped to the human genome. To control for possible dilution effects on the tagged provirus, we performed analyses with viruses produced by cotransfection with parallel quantities of the wild type (i.e. untagged) pNL4-3 plasmid.

While 4,495 unique integration sites were mapped for control viruses that lacked added MA-CA sequences, the lower infectivities of 5% and 20% MA-CA viruses (Fig. 2-1A) reduced the recovery of respective integration sites to 1,094 and 205, respectively (Table 2-1). Whereas 81.3% of WT HIV-1 integrations in this experiment mapped to genes, gene-targeting was diminished to ~77% of integrations for both 5% and 20% MA-CA, which was a significant difference for the 5% MA-CA virus ($p = 0.004$). The frequencies at which transcriptional start sites (TSSs) and associated CpG islands were targeted did not vary significantly across the different virus preparations. By contrast, targeting of gene dense regions of chromosomes was significantly affected. While WT on average targeted megabase (Mb) regions that harbored 21.5 genes, MA-CA viruses selected for regions that on average harbored 18.6 genes ($p = 3.6 \times 10^{-12}$ and 1.7×10^{-4} for 5% and 20% MA-CA, respectively). These changes were associated with upticks in targeting of heterochromatic lamina-associated domains (LADs) from 17.2% for the WT to 22.9% ($p = 1.9 \times 10^{-5}$) and 22.4% ($p = 0.055$) for 5% and 20% MA-CA, respectively (Table 2-1). Expectedly, we did not observe significant changes in integration targeting in cells infected with the corresponding viruses that controlled for total DNA content during transfection. These results demonstrate that inclusion of uncleaved MA-CA protein in HIV-1 particles results in a decrease in infection, and that the residual level of infection is associated with altered sites of integration within the host genome.

Table 2-1. Effects Of Uncleaved MA-CA On HIV-1 Integration Site Preferences

Library	Unique Sites	Within Refseq genes (%)[a]	Within 5 kb (+/- 2.5kb) of TSS (%)[a]	Within 5 kb (+/- 2.5 kb) CpG island (%)[a]	Within 5 kb (+/- 2.5 kb) LAD (%)[a]	Average gene density within 1 Mb (+/- 0.5 Mb) of integration sites[b]
WT	4,495	3,653 (81.3)	222 (4.9)	276 (6.1)	774 (17.2)	21.5
5% MA-CA plasmid	1,094	846 (77.3)[c]	51 (4.7)[e]	56 (5.1)[g]	251 (22.9)[i]	18.6[k]
20% MA-CA plasmid	205	157 (76.6)[d]	11 (5.4)[f]	14 (6.8)[h]	46 (22.4)[j]	18.6[l]
RIC[m]	31,846	14,807 (46.5)	1,710 (5.4)	1,932 (6.1)	13,916 (43.7)	9.5

[a]Statistical comparisons performed by Fisher's exact test.
[b]Statistical comparisons performed by Wilcoxon rank-sum test
[c]*p* value vs. WT, 3.79×10^{-3}
[d]*p* value vs. WT, 1.87×10^{-1}
[e]*p* value vs. WT, 7.55×10^{-1}
[f]*p* value vs. WT, 8.27×10^{-1}
[g]*p* value vs. WT, 2.25×10^{-1}
[h]*p* value vs. WT, 9.22×10^{-1}
[i]*p* value vs. WT, 1.90×10^{-5}
[j]*p* value vs. WT, 5.49×10^{-2}
[k]*p* value vs. WT, 3.58×10^{-12}
[l]*p* value vs. WT, 1.65×10^{-4}
[m]Random Integration Control

Integration sequencing and data analysis were performed by Parmit Singh in Alan Engelman's lab.

Genetic Determinants For MA-CA Transdominance

I sought to identify genetic determinants in Gag that are required for MA-CA transdominance to further define its antiviral mechanism. Based on the eccentric morphology of MA-CA containing particles, Lee and coworkers suggested that the MA domain of MA-CA anchors the core to the viral membrane during assembly owing to its membrane-binding activity (150). The Gag polyprotein is myristoylated, which promotes membrane association and is necessary for particle formation (61, 62). Membrane association of Gag also involves electrostatic interactions of N-terminal basic residues in the MA region with acidic phospholipids in the cell membrane (63). Therefore, it is plausible that MA-CA-induced membrane tethering requires one or both of the membrane binding elements in MA. To test this, I created and tested MA-CA plasmids lacking either or both elements. The protein changes included the N-terminal G2A substitution in MA, which prevents myristoylation of Gag, and two large internal deletions in MA that remove the N-terminal basic patch and are compatible with particle assembly: Δ8-126 and Δ8-87 (194). I observed that HIV-1 particles containing uncleaved MA-CA proteins lacking these regions were as impaired for infection as those containing the full-length uncleaved MA-CA protein, across the range of cotransfections (Fig. 2-8A). Therefore, the majority of the coding region of MA, including the N-terminal basic patch (KKQYKLKH), is not required for MA-CA antiviral activity.

To test whether myristoylation of Gag is required, I assayed the infectivity of HIV-1 particles generated by cotransfection of wild type and the myristoylation-defective MA-CA (MA-CA G2A) proviral constructs. The resulting mixed particles were as impaired for infection as those containing the uncleaved MA-CA protein (Fig. 2-8B).

Strong inhibition by the MA-CA G2A construct required the Y132I substitution, as the construct encoding only the G2A substitution was only mildly inhibitory, as previously reported (150). These results indicate that myristoylation of the MA-CA protein is not necessary for its antiviral effect.

Finally, to test the requirement of both membrane-binding elements in MA for MA-CA transdominance, I generated mixed particles with wild type and Δ8-126 MA-CA G2A and Δ8-87 MA-CA G2A constructs. While both non-myristoylated deletion constructs inhibited HIV-1 infectivity, the antiviral potency was 3 to 20-fold less than that of full-length MA-CA (Fig. 2-8C). The Δ8-87 MA-CA G2A protein was incorporated into particles at MA-CA:CA ratios similar to that of full-length MA-CA (Fig. 2-8D). The Δ8-126 MA-CA G2A protein was also incorporated into particles. However, removal of the 8-126 region from the uncleaved MA-CA protein resulted in a protein that I was unable to resolve from CA by SDS-PAGE. Collectively, these results indicate that at least one membrane-binding element of MA is necessary for the antiviral potency of uncleaved MA-CA.

Experiments involving cotransfections of two highly similar plasmids could be affected by host cell-mediated DNA recombination (195). In principle, recombination between the wild type and MA-CA G2A plasmid DNAs could result in segregation of the G2A and Y132I substitutions, potentially confounding the interpretation of the results shown in Figure 2-8. To determine if recombination was a significant factor in my genetic studies, I cotransfected the MA-CA plasmid with a plasmid encoding substitutions (L363I/M367I/M377V) that inhibit cleavage between CA and NC (CA-NC) (196). In this assay, I cotransfected the plasmids at a 1:1 ratio to maximize the

probability of recombination. If recombination occurred within the CA-coding region of the plasmids, it would result in a DNA molecule harboring all four mutations, resulting in particles containing a 48 kDa MA-NC protein. Immunoblotting analysis showed that particles resulting from the cotransfection contained only trace amounts of a band corresponding to uncleaved MA-NC. Similar quantities of this band were observed in particles produced by transfection of either the MA-CA or the CA-NC plasmid alone, suggesting that it did not result from recombination (Fig. 2-8E). These results suggest that DNA recombination in my cotransfection experiments was inefficient and therefore did not result in significant expression of uncleaved MA-CA protein that could be myristoylated.

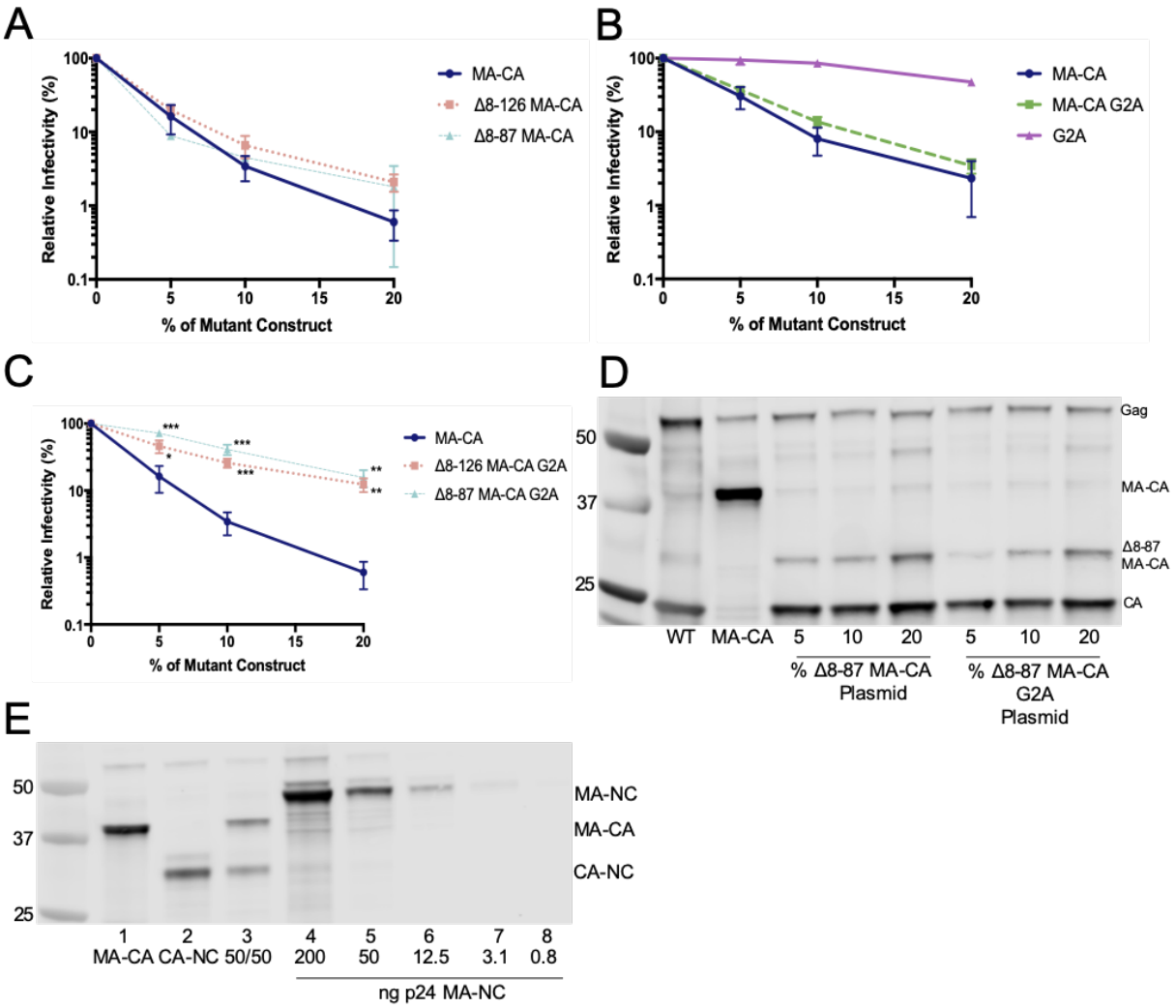

Figure 2-8. MA-CA Antiviral Potency Requires Membrane-Binding Elements In Gag. (A-C) Wild type plasmid DNA was cotransfected with MA-CA plasmids encoding the indicated substitutions or deletions in MA. Infectivity is shown relative to the control virus (0% Mutant Construct). Shown are the mean values of 3 to 6 independent experiments. Error bars represent standard deviations. *: $p<0.05$; **: $p<0.01$; ***: $p<0.001$ as determined by unpaired t-test. (D) CA immunoblot of mutant particles shown in panels A and C. (E) CA immunoblot of the mutant particles produced by transfection with plasmids encoding substitutions preventing cleavage at MA-CA or CA-NC junctions. "50/50" designates particles produced by cotransfection of equal quantities of the MA-CA and CA-NC mutant constructs. Lanes 4-8 contain dilutions of mutant particles produced by transfection of an HIV-1 plasmid encoding both MA-CA and CA-NC substitutions, resulting in production of an uncleaved Gag protein extending from MA through NC.

Discussion

In this study, I employed biochemical and cell-based assays to further define the mechanism by which a substoichiometric amount of uncleaved MA-CA protein potently interferes with HIV-1 infectivity. Using a disulfide crosslinking approach and *in vitro* immunoprecipitation, I obtained evidence for coassembly between CA and MA-CA in particles, and I observed cosedimentation of MA-CA protein with the genome and core proteins. I also showed that uncleaved MA-CA inhibits infection at nuclear entry and alters integration targeting. Finally, I showed that removal of both of the membrane-binding elements of MA reduced the antiviral potency of uncleaved MA-CA.

Post entry events in the HIV-1 lifecycle include reverse transcription, uncoating, intracellular transport, entry into the nucleus, and integration into host chromatin. The role of the capsid during all of these stages has been the subject of numerous studies (for reviews, see (28, 34, 35, 41, 197)). However, a well-defined model of the spatial and temporal aspects of uncoating has yet to emerge. Several genetic studies have coupled the intrinsic stability of the capsid to reverse transcription, nuclear entry, and infectivity (46, 53, 56, 58, 102, 176, 198, 199). The phenotypes I observed in particles containing uncleaved MA-CA protein suggest that coassembly with CA does not reduce the stability of the capsid: such particles exhibited normal levels of core-associated CA, near wild-type levels of late reverse transcription products, and they importantly retained the ability to abrogate restriction by TRIMCyp (176, 182, 185), which requires a stable capsid. However, my results do not preclude the possibility that uncleaved MA-CA hyperstabilizes the capsid lattice, potentially resulting in hyperstable cores that undergo delayed uncoating in target cells. This hypothesis is consistent with reports that CA

substitutions that hyperstabilize the capsid generally result in infection defects manifested after reverse transcription (46, 53).

Both nuclear entry and integration targeting are affected by capsid binding to host cell factors (for reviews, see (28, 34, 35, 41, 197)), and incorporation of uncleaved MA-CA into the assembling viral capsid may affect these interactions, potentially accounting for our observation that these particles were impaired at nuclear entry and exhibited altered integration targeting. Our experiments showed that inclusion of MA-CA marginally decreased integration into genes and gene dense areas of the host chromatin and increased integration near heterochromatic LAD regions. While 5% MA-CA viruses scored significantly different from the WT virus across these metrics, I suspect that 20% MA-CA viral infections failed to attain statistical significance for genes and LAD regions due to the comparatively fewer number of integration sites recovered (Table 2-1). The MA-CA viral phenotype is reminiscent of what occurs with WT virus when host factors Nup153 (188, 200) or Nup358 (190) are depleted from target cells. In both cases, a primary effect is observed at the step of nuclear import (104, 201), which is accompanied by significant integration retargeting away from gene dense chromatin regions (188, 190, 200). This basic phenotype is also observed upon restriction of WT virus by the antiviral protein MxB (189). Although MxB is unlikely to be expressed at inhibitory levels under the conditions of viral infection used herein, recent reports have implicated components of the cellular nuclear import machinery in the mechanism of MxB antiviral activity (55, 202). Therefore, I propose that analysis of the effects of MA-CA coassembly on Nup153 and Nup358 binding to CA *in vitro* or in cells, in the

presence or absence of MxB, may help to inform the molecular mechanism of altered MA-CA integration site targeting observed here.

The eccentric particle morphology defect associated with MA-CA-containing virions is reminiscent of the morphology defect caused by exposing HIV-1-producer cells to ALLINIs or by class II IN mutations (161-168). Despite this similarity, the resulting viral phenotypes appear to be distinct. While the IN-perturbed viruses are defective for reverse transcription (161-168) due to the uncoupling of the vRNP from the capsid shell (203, 204), defective virus that harbored 20% MA-CA was largely competent for reverse transcription (Fig. 2-7D). Possibly, the proposed tethering of MA-CA to the viral membrane (150) helps to stave off rapid loss of the vRNP after virus entry, allowing reverse transcription to proceed largely unfettered. Indeed, my genetic studies revealed a dependence on membrane-binding elements in MA for the antiviral potency of uncleaved MA-CA. Coupled with my observation that MA-CA coassembles with CA and is present in the viral core, I suggest that the core structure remains attached to cellular membranes after virus entry, which could impede its trafficking to the nucleus. I speculate that, upon completion of reverse transcription, the PIC dissociates from the cellular membranes whereby the MA-CA component of the PIC then interferes with CA-Nup interactions, obstructing nuclear entry and integration targeting. I accordingly suggest that membrane tethering of the core and interference with capsid-Nup interactions both contribute to the unique antiviral activity of core-associated MA-CA. Testing the membrane-tethering hypothesis represents an interesting future direction that will require developing appropriate cell fractionation and/or live-cell imaging techniques.

My observation that pseudotyping by VSV-G reduces the antiviral potency of uncleaved MA-CA supports the notion for the involvement of the target cell membrane in the antiviral mechanism. Pseudotyping by VSV-G targets HIV-1 entry to an endocytic route that requires exposure to the low endosomal pH for membrane fusion to be activated (186). Endocytic entry may reduce the inhibition by promoting endosomal transport of the virus within the cell prior to fusion. Additionally, exposure to the low pH of the endosome could facilitate membrane detachment and/or capsid disassembly events required for infection. I suspect that persistent membrane association may also provide a possible explanation for the reduced density of peak CA observed in cores isolated from particles containing uncleaved MA-CA protein (Fig. 5E). A strong association of uncleaved MA-CA protein with the viral membrane could result in retention of lipids despite the exposure to detergent during isolation of the cores, potentially reducing the density of the isolated cores (178). Another possible explanation for the altered density of MA-CA-containing cores is the apparent dissociation of the vRNP from the capsid shell in eccentric viral particles (Fig. 1C). HIV-1 produced in the presence of ALLINIs, and class II IN mutant viruses, both harbor similar morphological defects and exhibit similar changes in core density (161, 204). Cryo-ET analysis of MA-CA-containing virions may help to delineate aspects of the eccentric particle phenotype that differ from those induced by class II IN mutations or ALLINI exposure, the latter of which instill dramatic reverse transcription defects.

Immature HIV-1 particles reportedly contain 2,400 Gag molecules (205), while the mature capsid is comprised of approximately 1,500 CA subunits (67). Thus, proteolytic maturation results in an excess of CA molecules that are not incorporated

into the mature capsid. Given the surplus of Gag subunits in particles, the approximately 480 subunits of uncleaved MA-CA present in a 20% mixed particle represents a fraction of subunits that presumably is unnecessary for a mature capsid to form. Therefore, it is conceivable that the small amounts of uncleaved MA-CA protein present in mixed particles are not incorporated into the mature capsid structure, affecting the core *in trans* through random incorporation, possibly by interfering with normal CA functions. Nonetheless, my cross-linking analysis, *in vitro* binding reactions, and biochemical characterization of isolated cores provide evidence that uncleaved MA-CA coassembles with CA. One possible consequence of MA-CA coassembly with CA into the capsid is disruption of the intermolecular interfaces that construct the mature CA lattice, possibly explaining the morphological assembly defect observed by us and others (150). In a previous study, our lab observed that the HIV-1 CA-binding small molecule BI compound 1 induces aberrant crosslinks at the CTD-CTD three-fold axis in particles capable of disulfide crosslinking (206). By contrast, I did not observe a similar effect of MA-CA capable of the same crosslinking. Additionally, while canonical recombinant 14C/45C CA tubes were not observed when coassembled with MA-CA, hexamer formation was not prohibited. My results suggest that while MA-CA induces morphological assembly defects, the capsids in particles containing uncleaved MA-CA protein are hexameric lattices. This interpretation is also supported by my observation that the particles abrogate restriction by TRIMCyp (182, 185). Nonetheless, a hexameric lattice is not sufficient for a closed capsid structure, which requires inclusion of 12 CA pentamers, which I was unable to test using the engineered disulfide crosslinking approach. It is possible that uncleaved MA-CA incorporation affects the

pentamer structure and intersubunit contacts. Testing this hypothesis will require a novel approach.

Recently, the host small molecule inositol hexakisphosphate (IP6) has been shown to bind both immature Gag and mature CA hexamers during the assembly of each lattice (207-210). Because cleavage at the MA-CA junction is required for β-hairpin formation, incorporation of MA-CA into the CA lattice may inhibit IP6 binding to the hexamer and undermine its potential effects, including modulation of capsid stability and binding of host proteins.

In summary, I have shown that a small quantity of uncleaved MA-CA protein can coassemble with CA during HIV-1 maturation, and that incorporation of uncleaved MA-CA inhibits HIV-1 nuclear entry and affects integration site targeting. Particles containing uncleaved MA-CA exhibit aberrant morphology but have stable capsids and are competent for reverse transcription in target cells. I propose that inclusion of MA-CA in the mature capsid lattice alters capsid-host factor interactions necessary for HIV-1 nuclear import and integration targeting, and that impaired nuclear entry is also exacerbated by tethering to cellular membranes. Accumulation of uncleaved MA-CA may account, at least in part, for the marked reduction in HIV-1 infectivity observed under conditions of partial inhibition of the viral protease (157).

Chapter 3

The Requirement For Target Cell EF1A In HIV-1 Infection Depends On The Viral Env Protein

Introduction

HIV-1 infection is dependent on the biology of its capsid protein. CA monomers form hexameric and pentameric polyproteins, which then assemble into a fullerene cone-shaped container called the capsid. The capsid encases the two copies of the viral RNA genome, viral enzymes, and host proteins. After entry into the host cell, the capsid undergoes a disassembly process, termed uncoating, whereby CA subunits dissociate from the capsid. In addition to uncoating, the events of reverse transcription, nuclear entry, and integration of viral DNA into host chromatin complete the early replication events. CA mutational studies have revealed that capsid intrinsic stability, and thus the uncoating kinetics of the capsid, have direct impacts on the efficiency of infection (42-45, 49), and extensive research has revealed that CA is a determinant of every stage during early replication. While the timing and location of uncoating and reverse transcription have not been agreed upon, growing evidence suggests the two occur together (47, 50, 211) and that host factors are necessary for their efficiencies (125, 131, 212-215). Likewise, CA has also been identified as a determinant of nuclear entry, not only due to its structural integrity (53, 58, 216, 217), but also its ability to interact with host proteins (56, 57, 103, 218-220). Finally, integration also maps genetically to CA (102, 221-225) as well as its ability to interact with host proteins (106,

110, 226-228). The common factor during each replication stage is CA's interaction with host factors. Thus, understanding the roles of the various CA-host factor interactions is required to fully understand HIV-1 biology.

Given its significant roles during early HIV-1 replication, CA and the capsid have been the subject of numerous drug-development campaigns. Several compounds have been identified to bind to the capsid and impair infection at early and late stages (229-234); however, none currently has sufficient potency for therapeutic use. Despite the lack of clinical applicability, these compounds have served useful roles in elucidating capsid functions. One such compound, PF74, has been the focus of numerous studies. PF74 appears to affect the capsid in multiple different ways. At high concentrations (10 μM), PF74 blocks reverse transcription in target cells by inducing premature uncoating (235), while at lower concentrations (2 μM), PF74 impairs nuclear entry of the PIC (236). Unlike the PF74-induced capsid disassembly that occurs in target cells (235), PF74 actually promotes assembly of recombinant CA tubes *in vitro* (229). PF74 binds to an intrahexameric pocket formed between the NTD and CTD of neighboring CA subunits (105, 229, 237, 238), which is also the binding site of the host proteins CPSF6 and Nup153. Experiments have demonstrated that PF74, and another small molecule, BI-2, can compete with CPSF6 and Nup153 for binding (105, 239), and genetic studies have revealed a mutant virus that is resistant to PF74's antiviral activity but displays altered dependence on CPSF6, Nup153, and TNPO3 (240). PF74 has thus been a useful tool to understand host factor requirements for HIV-1 replication.

Upon joining the Aiken Lab, I focused on investigating capsid-host factor interactions. My goal was to identify novel host proteins that bound to assembled CA in

the presence or absence of PF74. A previous graduate student in the lab, Mallori Burse, had developed an *in vitro* binding assay using cell extracts and assemblies of recombinant CA (122). Recombinant CA forms long, hollow tube structures under high salt conditions that can be stabilized via disulfide crosslinks when CA harbors Cys substitutions at residues A14 and E45 (241). Disulfide-crosslinked CA tubes are more stable than WT CA tubes or native capsids and can serve as a suitable analogue for experiments involving host protein binding. To identify host proteins capable of binding CA tubes, I incubated 125 μg of HeLa P4 cytoplasmic extracts with 12 μg of CA assembled under high salt conditions. I then pelleted the binding reactions and separated the proteins by SDS-PAGE. Colloidal Coomassie-stained gels were submitted to Hayes McDonald at the Vanderbilt Mass Spectrometry Research Center for Multidimensional Protein Identification Technology (MuDPIT) analysis. A total of 714 proteins were identified in the binding reactions. One of the most abundant proteins present was elongation factor 1 A (EF1A). Interestingly, when PF74 was present in the binding reaction, the amount of EF1A that pelleted with CA was reduced 4-fold ($p < 0.0001$). I observed that CPSF6 was also reduced nearly four-fold in binding reactions when PF74 was present ($p = 0.0013$), suggesting that PF74 was able to bind to the assembled CA and compete for binding with a known host factor. For the first few years of my graduate work, I focused on the EF1A-CA interaction and on determining if EF1A is required for HIV-1 infection.

EF1A's canonical role in the cell is to enhance translation elongation by catalyzing the delivery of aminoacyl-tRNA to the ribosome (242). Following the delivery of aa-tRNA and subsequent hydrolysis of its bound GTP to GDP, EF1A depends on the

guanine exchange factor EF1B complex to catalyze the exchange back to GTP, where it can then bind aa-tRNA and the repeat the process (243). In addition to its role during translation, EF1A also occupies a myriad of moonlighting functions, a fact that is typically attributed to its high cellular abundance of 1-2% of total cellular protein (244). EF1A occupies the following non-canonical cellular roles: actin binding and bundling (245-247), microtubule stabilization and severing (248-251), nuclear export of aa-tRNA (252, 253), proteolysis (254, 255), and both pro and anti-apoptotic signaling (256-259). Due to its abundance and binding properties with tRNA, it is not surprising that many RNA viruses employ EF1A during infection. EF1A has been shown to bind tRNA-like structures in the genomes of several plant and animal viruses (260-265) as well as binding viral polymerases and proteins (130, 131, 263, 266-269) to enhance infection.

Recently, our lab and others have implicated EF1A as an HIV-1 host factor that modulates early replication events. Initially, EF1A was identified from a yeast-two hybrid screen as a Gag-binding protein at the MA and NC subunits, an interaction speculated to promote viral RNA incorporation into virions (130). A few years later, a former postdoc in the Aiken lab, David Hout, identified EF1A by MOLDI-TOF mass spectrometry from partially-purified cell fractions that stimulated *in vitro* uncoating of purified HIV-1 cores. The uncoating stimulation was abolished when EF1A was immunodepleted from cells, and the uncoating stimulation could be replicated by the addition of recombinant EF1A protein when present with its known cofactor GDP (David Hout, unpublished data). However, no effect on HIV-1 infection was observed when EF1A was depleted from target cells. Thus, no functional role for EF1A during infection was identified. Shortly after these observations were made, David Harrich's group

reported that EF1A coimmunoprecipitated with HIV-1 RT and IN from reverse transcription complexes (RTCs) both *in vitro* and in cells, and that RNAi depletion resulted in decreased reverse transcription (131). The Harrich Lab later reported a direct interaction between EF1A and RT, and the genetic determinants of this interaction were required for efficient reverse transcription. Additionally, they reported that this interaction could be inhibited by the small molecule didemninB (132-134) suggesting that EF1A is required for efficient infection.

In this study, I investigated the binding interaction between CA assemblies and EF1A, and EF1A's requirement for HIV-1 infection. I determined that EF1A-CA binding is substoichiometric and that EF1A depletion resulted in impaired HIV-1 infectivity. However, EF1A was only required for efficient HIV-1 infection when virus harbored native, X4-tropic envelope.

Results

EF1A-Capsid Binding Properties

Upon identifying EF1A from my binding reactions, I set out to perform validation experiments. My first goal was to determine if EF1A could be identified in binding reactions by immunoblotting. I performed the same binding assay as done for the MuDPIT analysis, incubating 125 µg of HeLa P4 cytoplasmic extracts with 12 µg of CA assembled under high salt conditions, with or without 7 µM PF74 or 40 µM BI-2. I then pelleted the reactions, separated the proteins by SDS-PAGE, and probed immunoblots with antisera specific for EF1A and CPSF6. Under identical conditions performed for the MuDPIT experiment, I observed equivalent quantities of EF1A present in binding

assay pellets in the presence and absence of assembled CA and PF74 (Fig. 3-1, compare lanes 1-4 with 5-7, and compare lane 5 with lanes 6 and 7), which suggested that the presence of EF1A in my previous binding assay was due to direct pelleting of the host protein. To determine if any specific interactions occurred during the binding assay, I probed the same membrane for CPSF6. CPSF6 was specifically present in the binding assay pellets when assembled CA was coincubated, but not in the presence of the small molecules PF74 or BI-2 (Fig. 3-1, compare lane 5 with lanes 6 and 7). Thus, the binding assay conditions performed in this experiment were sufficient to identify specific interactions of assembled CA and known host factors, but the original observation of EF1A binding was likely due to background pelleting of the host protein.

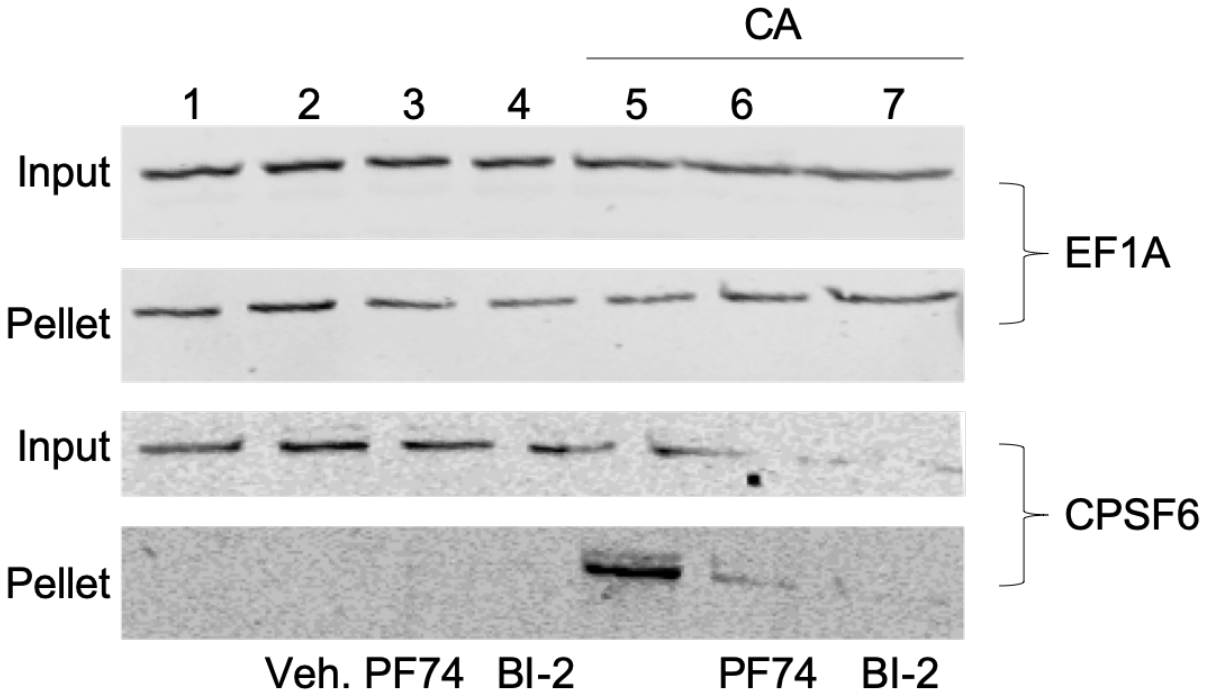

Figure 3-1. EF1A Pellets Independent Of CA. Assembled CA (12.5 µg) was incubated with 125 µg HeLa P4 cytoplasmic extracts for 1 h on ice with or without 7 µM PF74, 40 µM BI-2, or matched vehicle control (Veh.). Reactions were pelleted at 5,000 rpm for 5 min at 4° C. Pelleted proteins were separated by SDS-PAGE. EF1A and CPSF6 proteins were detected by immunoblotting with the appropriate antibodies. Input blots represent 10% of the binding reaction. CA was only added to reactions 5-7 as indicated.

EF1A:CA Stoichiometry

Upon identification of EF1A from my initial binding assay experiments, I hypothesized that the previous reports of EF1A interacting with MA and NC regions in Gag (130) and immunoprecipitating with RT and IN from RTCs (131) could be explained by an interaction with CA, which is common to both Gag and RTCs. However, my immunoblot validation experiments suggested that EF1A identification by mass spectrometry was due to precipitation of the protein. I sought to identify binding conditions that would prevent background EF1A pelleting. After extensive optimization experiments, adjusting temperature, detergents, and centrifugation, I identified binding conditions where EF1A pelleted only when assembled CA was present (Fig. 3-2). I used these conditions to determine the stoichiometry of EF1A to CA. Despite the abundant EF1A identified by mass spectrometry, under stringent binding conditions, I estimated that the EF1A-CA interaction was substoichiometric at 1 molecule of EF1A to 118 molecules of CA. This suggests that the amount of EF1A identified in my initial binding assay did not accurately represent the EF1A-CA interaction, likely due to its high abundance of the host protein (244).

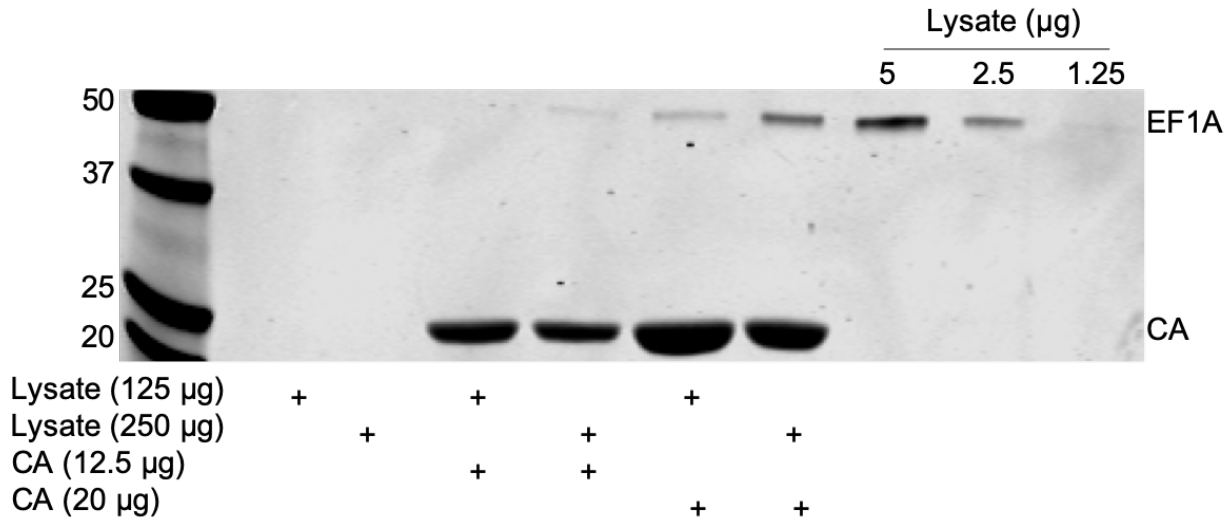

Figure 3-2. Stoichiometry Of EF1A To CA. Assembled CA (12.5 µg or 20 µg) was incubated with HeLa P4 cytoplasmic lysates (125 µg or 250 µg) for 1 h at 37° C in the presence of the non-ionic detergent Brij-58 (0.086%). Reactions were centrifuged at 10,000 rpm for 10 min through layers of 30% and 45% sucrose at 4° C. Pelleted proteins were separated by SDS-PAGE. EF1A and CA proteins were detected by immunoblotting with the appropriate antibodies. All protein species were quantified and compared to a standard curve generated by lysate titrations. EF1A:CA stoichiometry was calculated using the standard curve. Blot represents one of two independent experiments with similar outcomes.

Functional Validation Of EF1A

While I was performing immunoblot validation and optimization experiments, I was also performing functional validation experiments. Warren et al. reported that EF1A was required for reverse transcription in cells (131), which suggests that EF1A is required for infection, despite our lab's unpublished data to the contrary (David Hout and Christopher Aiken, unpublished observations). Nonetheless, I began by performing RNAi-mediated depletion of EF1A in two $CD4^+$ HeLa-derived reporter cell lines: HeLa-P4 and TZM-bl. Lentiviral expression of two different shRNAs resulted in depletion of EF1A to near undetectable levels in both cell types (Fig. 3-3 A, B). Unlike data previously observed in the Aiken Lab, EF1A depletion resulted in up to four-fold inhibition of HIV-1 infection (Fig. 3-3 A, B) in both cell types. Preliminary data in more relevant T cell lines, SupT1 and CEM, also suggest that EF1A promotes HIV-1 infection (Fig. 3-3, panels C and D).

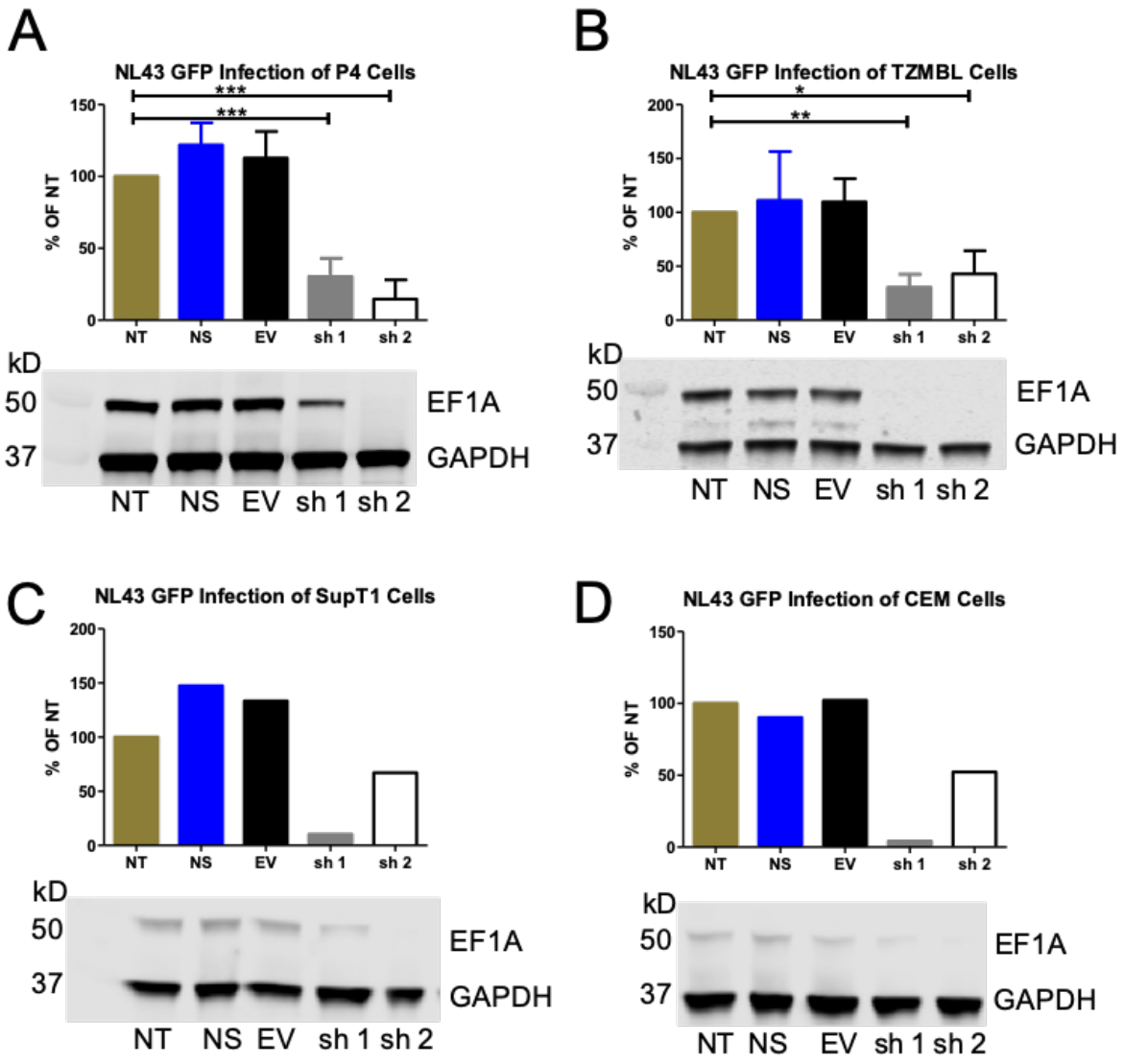

Figure 3-3. EF1A Is Required For HIV-1 Infection. Upper panels. (A) HeLa P4, (B) HeLa TZMBL, (C) SupT1, or (D) CEM cells were transduced with non-silencing (NS), empty vector (EV), or EF1A-targeting shRNAs (sh1 or sh2). NT: Not Transduced. Five days post transduction, cells were challenged with the pNL4-3-based, GFP reporter HIV-1. The percentage of GFP-expressing cells was determined by flow cytometry. Data represents mean % GFP signal normalized to NT samples. Error bars represent SD. * $p<0.05$; ** $p<0.01$; ** $p<0.0001$ as determined by single-sample t-test with a hypothetical mean of 100. N.S.: not significant. For (A) n=13; (B) n=4; (C, D) n=1 independent experiments. Lower panels. Cells were transduced as above. Five days post transfection, whole cell extracts were prepared. Equal masses of protein extracts were separated by SDS-PAGE, and EF1A and GAPDH were detected by sequential immunoblotting with appropriate antibodies.

Envelope Complementation Circumvents The Requirement For EF1A In HIV-1 Infection

My functional data contradicted what was previously observed in our laboratory; however, where Dr. Hout employed an envelope-defective strain of HIV-1 that was pseudotyped with VSV-G for infection, I used an HIV-1 strain expressing its native envelope protein. To determine if the differences in EF1A requirement were due to envelope expression, I infected EF1A-depleted HeLa P4 and TZM-bl cells with HIV-1 expressing a variety of viral envelope proteins that either target viral entry via fusion or endocytosis, (Table 3-1). Unlike infection by HIV-1 expressing native Env, EF1A was not required for infection by HIV-1 expressing the VSV-G protein (Fig. 3-4 A, B). Preliminary data in more relevant T cell lines, Sup T1 and CEM, also suggested that EF1A is not required for HIV-1 infectivity when the virus expresses VSV-G (Fig. 3-4 C, D). Similarly, EF1A was not required for infection by HIV-1 expressing the amphotropic murine leukemia virus (AMLV) envelope protein (Fig. 3-4 E). Interestingly, complementing Env-deficient HIV-1 with an HIV-1 envelope protein (HXB2) resulted in infection that was unaffected by EF1A depletion (Fig. 3-4 F, G). Collectively, these data suggest that complementing Env-deficient HIV-1 with envelope proteins from HIV-1 or other viruses can circumvent the requirement of EF1A in multiple cell types.

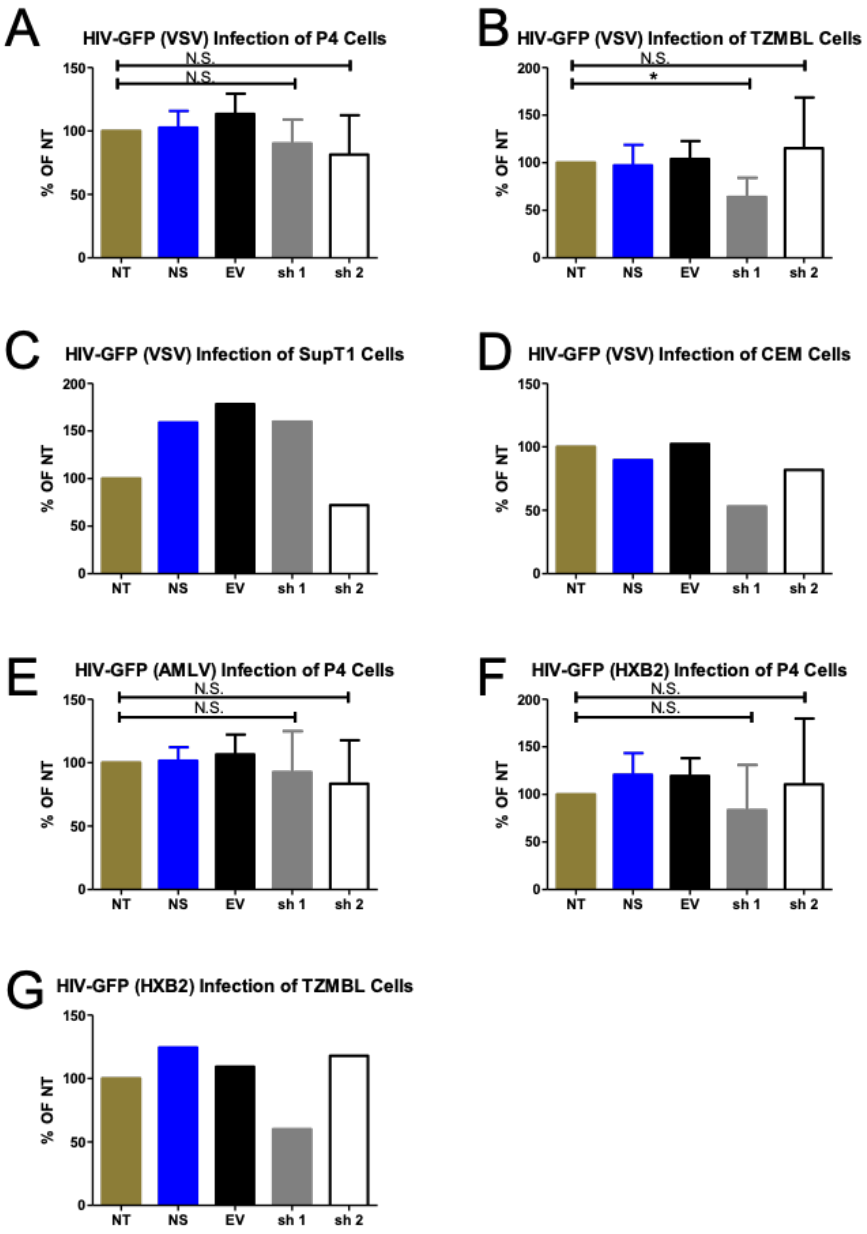

Figure 3-4. EF1A Is Not Required For Complemented HIV-1 Infection. CD4+ (A/E/F) HeLa P4, (B/G) HeLa TZMBL, (C) SupT1, or (D) CEM cells were transduced with non-silencing (NS), empty vector (EV), or EF1A targeted shRNAs (sh 1 or sh 2). NT: Not Transduced. Five days post transduction, cells were challenged with pNL4-3-based, GFP reporter HIV-1 pseudotyped with (A-D) VSV-G, (E) AMLV, or (F-G) HXB2 envelope proteins. GFP-expressing cells were quantified by flow cytometry. Data represents mean % GFP signal normalized to NT samples. Error bars represent SD. * $p<0.05$ as determined by single-sample t-test with a hypothetical mean of 100. N.S. not significant. For (A) n=10; (B) n=4; (C, D, F) n=1; (E) n=4; (G) n=5 independent experiments.

Table 3-1. Viral Envelope Proteins Tested And Their Receptor Proteins

Envelope Protein	Receptor	Entry Method
HIV	CD4	Fusion
VSV	LDLR	Endocytosis
Amphotropic MLV	PiT2	Fusion

HIV-1 Coreceptor Tropism Dictates EF1A Requirement

In all EF1A depletion experiments detailed thus far, I used the pNL4-3 laboratory-adapted strain of HIV-1, which expresses an envelope protein that requires the CXCR4 coreceptor for fusion at the cell membrane (X-4 tropic). To determine if the requirement for EF1A is coreceptor specific, I infected EF1A-depleted HeLa TZM-bl cells with the R5-tropic NL4-3-BaL strain of HIV-1, which requires the CCR5 coreceptor for fusion. Infection was impaired two-fold in cells transduced with one EF1A shRNA, but no impairment was observed when EF1A was depleted by a second shRNA (Fig. 3-5), suggesting a minor role for EF1A in R5-tropic HIV-1 infection.

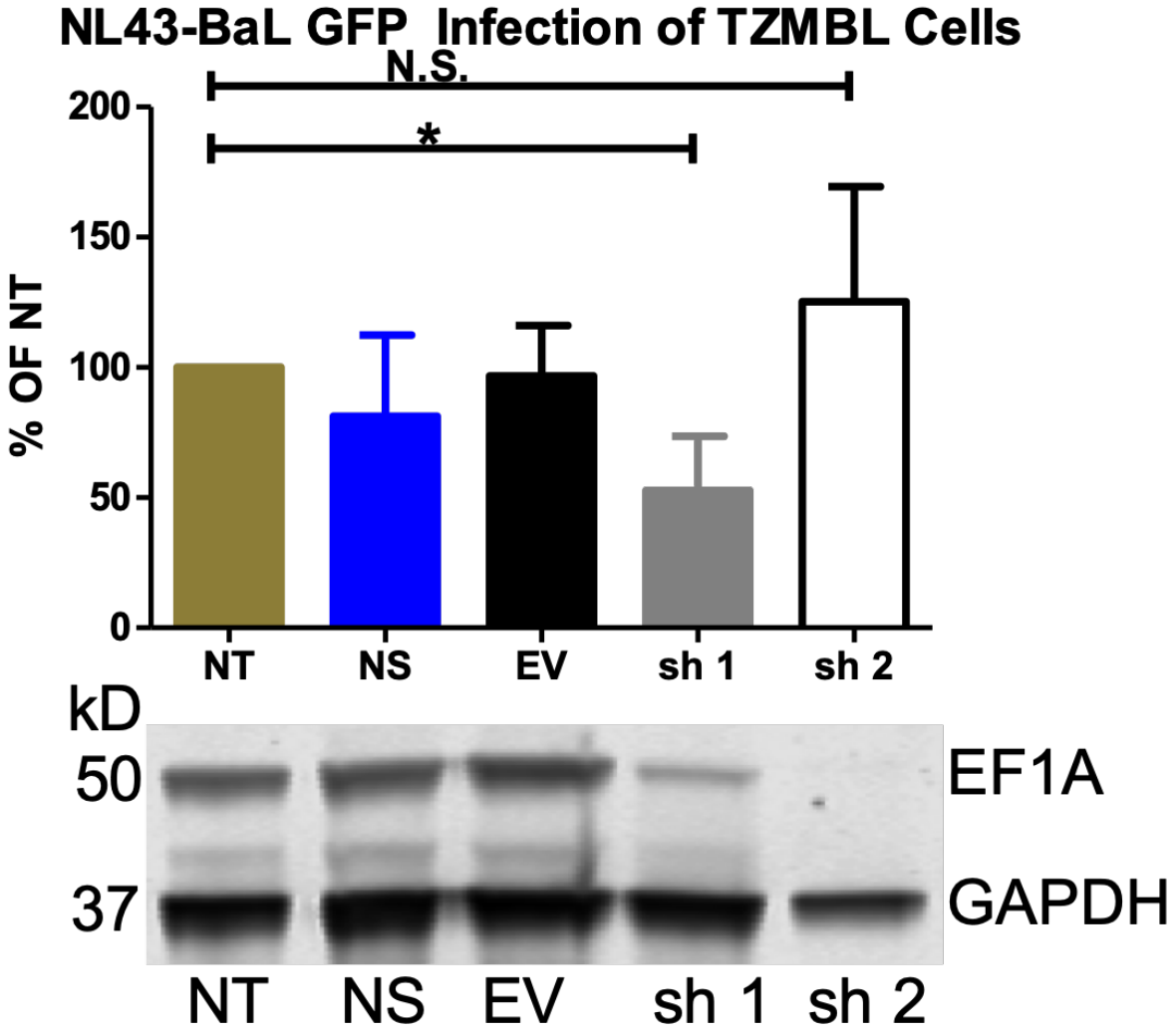

Figure 3-5. EF1A Is Not Required For R5-Tropic HIV-1 Infection. Upper panel. CD4+ HeLa TZMBL cells were transduced with non-silencing (NS), empty vector (EV), or EF1A targeted shRNAs (sh 1 or sh 2). NT: Not Transduced. Five days post transduction, cells were challenged with pNL4-3-BaL-based, GFP reporter HIV-1. GFP-expressing cells were quantified by flow cytometry. Data represents mean % GFP signal normalized to NT samples. Error bars represent SD. * $p<0.05$ as determined by single-sample t-test with a hypothetical mean of 100. N.S. not significant. n=4 independent experiments. Lower panel. Cells were transduced as above. Five days post transfection, whole cell extracts were prepared. Equal masses of protein extracts were separated by SDS-PAGE, and EF1A and GAPDH were detected by sequential immunoblotting with appropriate antibodies.

EF1A Functions During Early Stages Of Infection

A fundamental difference between the HIV-1 strain bearing native envelope and the Env-deficient, complemented strains of HIV-1 tested is the ability of the native HIV-1 particles to replicate in infected cells and then proceed to infect neighboring cells in multiple rounds. By contrast, while the complemented viruses are competent for single round infections, progeny virus-like particles produced by infected cells do not bear any envelope protein and the infection cannot spread. Thus, it was possible that the infection impairment of native HIV-1 in EF1A-depleted cells occurred during a second or third round of infection, consistent with a producer cell effect. To determine if EF1A is required during a single round of infection, I prevented HIV-1 replication by treating cells with the protease inhibitor Crixivan (Crix) at the time of infection (Fig. 3-6 A) or by inhibiting fusion by the addition of dextran sulfate (DS) (Fig. 3-6 A) or the small molecule AMD3100 (AMD) (Fig. 3-6 B, C) at two hours post inoculation. Limiting HIV-1 infection to a single round did not affect the inhibition resulting from EF1A depletion, which suggests that EF1A is required during the initial infection.

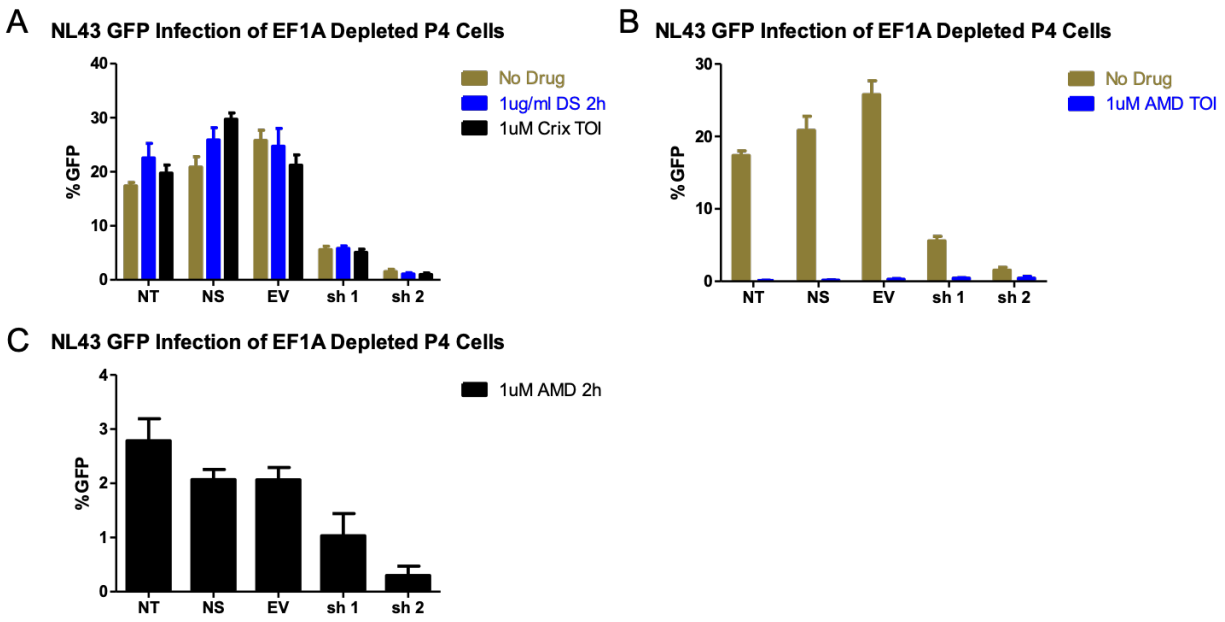

Figure 3-6. EF1A Is Required During Early Replication Events. CD4+ HeLa P4 cells were transduced with non-silencing (NS), empty vector (EV), or EF1A targeted shRNAs (sh1 or sh2). NT: Not Transduced. Five days post transduction, cells were challenged with pNL4-3-based, GFP reporter HIV-1 and compounds targeting the viral protease (Crixivan (Crix)) or fusion (dextran sulfate (DS) or AMD3100 (AMD)) were either added at time of infection (TOI) or 2 h post infection. Error bars represent SD. The data in each graph represent one experiment with three technical replicates.

EF1A Depletion Affects CD4 Surface Expression

EF1A has diverse functions in the cell. It is possible that its depletion would affect the function or expression of proteins relevant to HIV-1 infection. I therefore asked whether EF1A depletion affects CD4 surface expression. EF1A-depleted HeLa P4 and TZM-bl cells were stained with a FITC-labelled antibody specific for CD4, and CD4 surface expression was quantified by flow cytometry. One of the EF1A shRNAs did not affect CD4 surface expression in either cell type, while a second shRNA resulted in a maximum two-fold reduction in CD4 staining (Fig. 3-7 A, B).

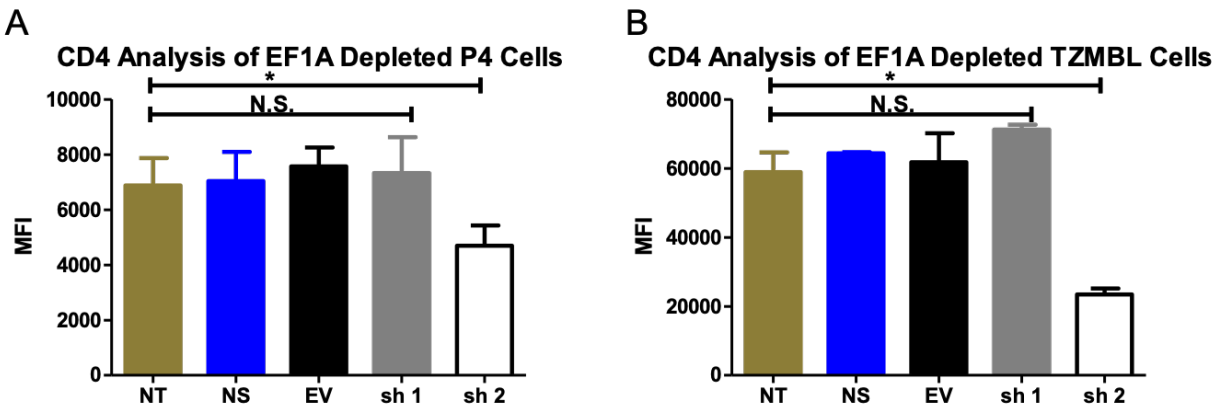

Figure 3-7. EF1A Depletion Affects CD4 Surface Expression In Hela Cells. CD4+ (A) HeLa-P4 or (B) TZMBL cells were transduced with non-silencing (NS), empty vector (EV), or EF1A targeted shRNAs (sh1 or sh2). NT: Not Transduced. Five days post transduction, cells were collected and stained with FITC-labeled CD4 antibody and analyzed by flow cytometry. Shown are the mean fluorescence intensities (MFI) of FITC-positive cells. Error bars represent SD. * $p<0.05$ as determined by unpaired t-test. N.S.: not significant. For (A) n=8; (B) n=2 independent experiments.

EF1A Depletion Does Not Specifically Affect Integrated Provirus Translation

The infection experiments detailed thus far involve flow cytometry counting of cells expressing GFP. GFP expression results from HIV-1 integration into host chromatin and subsequent expression via cellular processes. Thus, the infection experiments reveal whether or not HIV-1 has entered the cells and undergone all early events: reverse transcription, uncoating, nuclear entry, and integration. Because the read-out for infection requires GFP expression from the cell, it is possible that the perceived infection inhibition observed in EF1A depleted cells could be explained by a global inhibition of protein synthesis. To test this hypothesis, I performed biosynthetically labelled EF1A-depleted cells with ^{35}S (Fig. 3-8 A). Compared to non-transduced cells, global protein synthesis was reduced for all cells transduced with shRNAs. However, global protein synthesis was reduced to comparable levels in cells transduced with EF1A shRNAs and cells transduced with empty and non-targeting control shRNAs. This suggests that EF1A depletion did not specifically impair global protein synthesis. Moreover, flow plots from infected, EF1A-depleted cells revealed that the mean fluorescence intensity of GFP-positive cells was comparable to infected control cells (Fig. 3-8 B). Together, these data suggest that EF1A depletion does not impair integrated provirus translation.

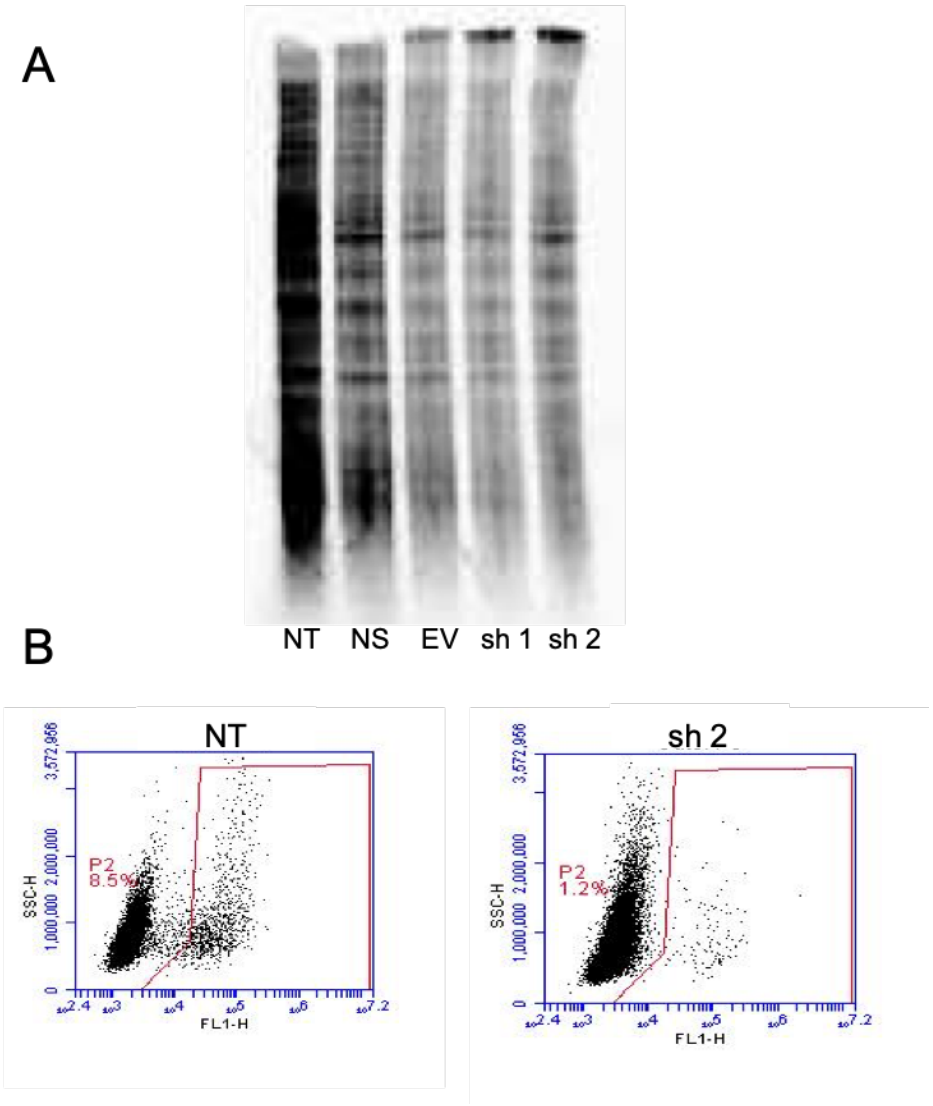

Figure 3-8. EF1A Does Not Specifically Impair Proviral GFP Expression. CD4+ HeLa P4 cells were transduced with non-silencing (NS), empty vector (EV), or EF1A targeted shRNAs (sh 1 or sh 2). NT=Not Transduced. (A) Five days post transduction, cells were metabolically labeled with ^{35}S for 90 min, cells were collected, and whole cell lysates were prepared. Equal masses of cellular proteins were separated by SDS-PAGE, and labeled protein was detected with a phosphorimager. Shown are the data from one experiment. (B) Five days post transduction, cells were challenged with pNL4-3-based, GFP reporter HIV-1. GFP-expressing cells were quantified by flow cytometry. Shown are the flow plots of cells gated for GFP expression for cells not transduced or transduced with EF1A shRNA sh 2. These plots are representative of 13 independent experiments with similar outcomes.

Discussion

In this study, I examined the binding properties between EF1A and assembled HIV-1 CA. I determined that binding between EF1A and CA is at a very low stoichiometry. I also examined the requirement of EF1A for efficient HIV-1 infection. EF1A was required for efficient infection by an X4-tropic strain of HIV-1 in two $CD4^+$ HeLa cell lines, and preliminary data suggests a role for EF1A in two T cell lines. The requirement for EF1A occurs during early stages of HIV-1 infection; however, this effect was altered by changing the viral envelope.

Interpretation of my studies of EF1A represented a challenge. How might HIV-1 utilize an abundant, cytoplasmic host protein during infection in an Env-dependent manner? According to published data, EF1A depletion in target cells impairs reverse transcription (131). Additionally, EF1A was reported to bind directly to RT, and disruption of this interaction, either by RT point substitutions or by small-molecule inhibition, also resulted in reduced HIV-1 reverse transcription (132-134). Collectively, these data suggest a model of EF1A functioning during reverse transcription. How then might different viral envelopes affect the requirement for EF1A during reverse transcription? One possibility is the different routes of entry that envelope proteins dictate upon receptor recognition. The HIV-1 envelope protein directs entry via fusion at the outer membrane, while the VSV-G protein mediates infection via an endocytic entry route (114). The low pH environment of the endosome may stimulate uncoating and/or reverse transcription in an EF1A-independent manner. Alternatively, there may be an as yet undefined repository of EF1A in endosomes that may serve as a concentrated source of the host protein, even under knockdown conditions. However,

complementation experiments involving env proteins from AMLV and even HIV-1 indicated that EF1A was dispensable for infection, (Fig. 3-4), when entry occurred via fusion at the membrane. In this case, reverse transcription and uncoating would occur in the cytoplasm with abundant access to EF1A.

Based on my results, I would speculate that EF1A may have a previously unidentified role during viral fusion. It is possible that EF1A depletion may affect one or more host factors required for HIV-1 attachment and/or fusion. I tested this hypothesis by quantifying surface-expressed levels of CD4 on HeLa P4 and HeLa TZM-bl cells. While EF1A depletion resulted in a statistically-significant reduction in CD4 expression, this phenotype was only observed when one shRNA was transduced, and not when a second shRNA was transduced that also resulted in EF1A depletion (Fig. 3-7). Therefore, the results were difficult to interpret. Quantifying surface-expressed CXCR4 may be more informative in EF1A depleted cells to address this hypothesis, as X4-tropic HIV-1 was more affected by EF1A depletion than an R5-tropic strain of HIV-1 (Fig. 3-5).

EF1A may affect viral entry directly. One report has demonstrated that EF1A can localize to the exterior of fibroblasts and function as a receptor for fibronectin (270). While the cells used in this study are not fibroblasts, and to my knowledge, EF1A has not been identified at the surface of other cell types, it is possible that EF1A may have a direct role during virus attachment and or fusion. Indeed, prior to CD4 binding, initial HIV-1 contact can be mediated by heparan sulfate proteoglycans (271), integrins (272, 273), or the macrophage pattern recognition receptor DC-SIGN (9, 274). Thus, there is precedent for non-CD4 proteins involved in HIV-1 attachment to target cells. An immediate future direction for this project will be to assay viral fusion in EF1A-depleted

cells to directly test whether EF1A functions during entry. If this hypothesis is true, why might HXB2-complemented HIV-1 or AMLV-complemented virus abrogate the necessity for EF1A? Env-deficient viruses that are complemented, or pseudotyped, to express a receptor *in trans* often express much more of that receptor than what is natively found on a particle. Therefore, I would speculate that if EF1A functions during early attachment or fusion of HIV-1, complementing particles to express more envelope protein may obviate the need for EF1A.

EF1A membrane localization has also been demonstrated by the prokaryotic analogue EF-Tu protein, which can function as a receptor protein to infect mammalian cells (275-279). Therefore, if EF1A is expressed on the surface of HEK293T cells, HIV-1 generated by transfection may harbor EF1A on its surface and potentially act as a receptor-like protein. If true, HIV-1 particles generated during infection of EF1A-depleted HeLa cells may have subsequent infection inhibition due to a lack of surface-expressed EF1A. In this case, the effects of EF1A depletion would be manifested during a second round of infection; however, my data do not support this hypothesis (Fig. 3-6).

In summary, I have observed that EF1A promotes HIV-1 infection when the virus bears an X4-tropic envelope. While I have not determined the mechanism by which the identity of the viral envelope influences the requirement for EF1A in HIV-1 infection, I have obtained evidence for a novel function of EF1A during HIV-1 infection. Much of my discussion has been speculative on what has been a disparate set of observations that does not necessarily support the reported requirement for EF1A in HIV-1 reverse

transcription. Nevertheless, work on this project taught me valuable lessons in both perseverance and the value of things left unfinished.

Chapter 4

Summary And Future Directions

My graduate thesis research has focused on two different aspects of HIV-1 biology: host factor utilization, and maturation. In Chapter 2, I detailed the mechanism by which small amounts of uncleaved MA-CA protein potently inhibits HIV-1 infection; and in Chapter 3, I described how I identified EF1A as a host factor required for X4-tropic HIV-1 infectivity.

The MA-CA antiviral mechanism project (Chapter 2) was based on several previous studies investigating the inhibitory effects of Gag cleavage mutants. HIV-1 PR inhibitors are successful therapeutics (156) because Gag and Gag-Pol cleavage is required for generating infectious virions (157). Maturation inhibitors, typified by the small molecule bevirimat, also prevent Gag cleavage by binding to the CA-SP1 Gag cleavage site and preventing PR activity (78, 158-160). Gag cleavage can also be inhibited by replacement of the P1 residue at each cleavage site with Ile (280). With exception to the NC-SP2 cleavage site (150), mutation at each HIV-1 Gag cleavage site completely inhibits virus infectivity. Based on the necessity of Gag cleavage for replication, several investigators (Volker Vogt, Ronald Swanstrom, Eric Freed, and Hans-Georg Krausslich) hypothesized that Gag cleavage mutants could function as a transdominant inhibitor of HIV-1 infection.

Transdominant inhibition of HIV-1 infection has been previously explored for other viral genes, including Tat (281), Rev (282-286), and even Gag (173, 287).

Transdominant inhibition by cleavage mutants was first observed in MLV when the p12-CA cleavage was blocked (170). Shortly after this, studies on HIV-1 Gag indicated that the MA-CA (150, 172) and CA-SP1 (171) cleavage mutants were potently transdominant. However, no extensive mechanistic details were revealed. My work on this subject directly relates to that reported by Lee et al. (150), who showed that the MA-CA cleavage mutant, Y132I, potently inhibits HIV-1 infectivity when particles are generated by cotransfection of WT and Y132I proviral plasmids. They reported that the resulting particles exhibited early defects in reverse transcription and that the particles' cores were eccentrically located. My goal for this project was to more precisely define the mechanism by which a small amount of uncleaved MA-CA protein potently interfered with HIV-1 infectivity, in order to better understand the molecular events required for proper HIV-1 maturation.

Based on the reverse transcription impairment reported by Lee et al., I hypothesized that virions containing uncleaved MA-CA protein would have unstable cores. However, using biochemical fractionation (Fig. 2-5) and a complementary, cell-based assay (Fig. 2-6) I observed that the cores are stable. Further investigation revealed no major reverse transcription impairment by MA-CA mixed particles; rather, I observed a strong impairment to nuclear entry (Fig. 2-7). Using a disulfide crosslinking approach (Fig. 2-2) and immunoprecipitation (Fig. 2-3), I determined that uncleaved MA-CA and cleaved CA proteins coassemble within virus particles to form a mixed capsid. I hypothesized that this coassembly would perturb the intermolecular CA-CA interfaces necessary for capsid assembly. However, using a disulfide crosslinking approach (Fig. 2-4), I did not observe perturbations to any of the known CA-CA

interfaces, which suggests that uncleaved MA-CA protein does not inhibit CA hexamer assembly, despite my observations that particle morphology is aberrant (Fig. 2-1). In collaborative experiments with Parmit Singh and Greg Sowd (present and former members of Alan Engelman's group at the Dana Farber Cancer Institute), I also determined that particles bearing uncleaved MA-CA have marginally decreased integration into genes and gene dense areas of the host chromatin and increased integration near heterochromatic LAD regions (Table 2-1), phenotypes shared with WT virus infections of cells where the nuclear pore proteins Nup153 and Nup358 where depleted (188, 190, 200). Finally, my genetic experiments revealed that both MA myristoylation and the N-terminal basic patch are required for the antiviral potency of MA-CA.

Based on my data, I propose a model involving two, non-mutually exclusive mechanisms for the antiviral action of uncleaved MA-CA protein (Fig. 4-1), both of which involve association of MA-CA with the assembled viral capsid. I propose that the membrane-binding elements of MA—the myristate and the N-terminal basic patch—result in tethering of the core to the cellular membrane upon fusion. Retention at the membrane results in reverse transcription and partial uncoating at the cellular periphery rather than either *en route* to the nucleus and/or at the nuclear pore. Thus, a significant fraction of reverse transcribed proviral genomes fail to make it to the nucleus. However, the membrane retention does not appear to account for the full antiviral effect of MA-CA, since nuclear import is reduced by about 75% of the wild type at a dose that inhibited infectivity by 95%. Therefore, based on the altered integration targeting I observed, I propose that the remaining proviruses that do make it to the nucleus are

impaired for integration owing to impaired interactions with the nuclear pore complex, which results in poor penetration into chromatin-dense regions.

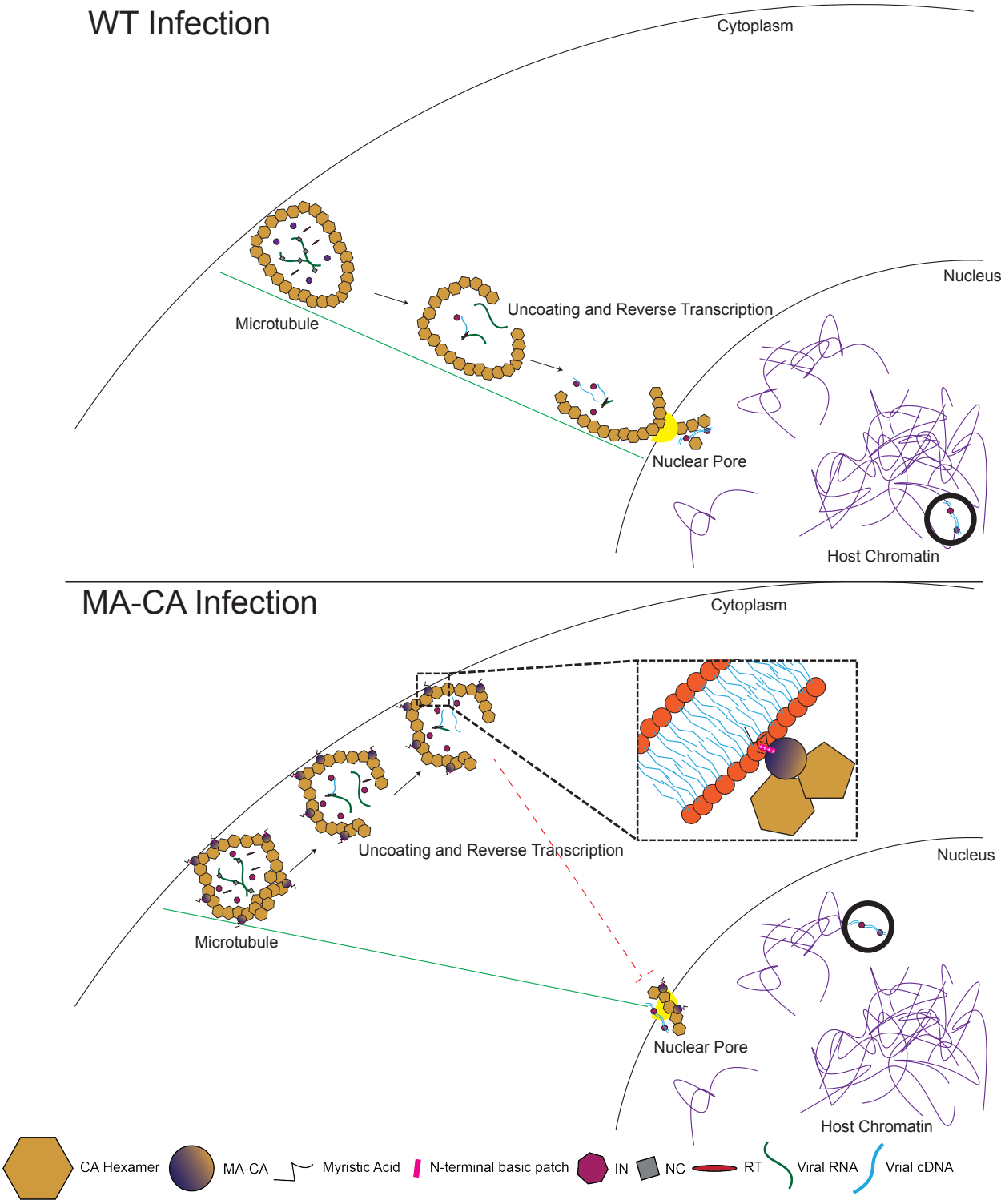
WT Infection
Cytoplasm
Microtubule
Uncoating and Reverse Transcription
Nucleus
Nuclear Pore
Host Chromatin
MA-CA Infection
Cytoplasm
Uncoating and Reverse Transcription
Nucleus
Microtubule
Nuclear Pore
Host Chromatin
CA Hexamer
MA-CA
Myristic Acid
N-terminal basic patch
IN
NC
RT
Viral RNA
Vrial cDNA

Figure 4-1. Model For Uncleaved MA-CA Protein Inhibition Of HIV-1 Infection. HIV-1 enters target cells by fusion. The viral core is transported to the nucleus where uncoating and reverse transcription occur. The viral preintegration complex enters the nucleus at the nuclear pore complex, and proviral DNA integrates into gene dense areas of the host chromatin. MA-CA mixed viruses enters via fusion, and MA-CA-containing cores are tethered to the membrane via myristic acid and a basic patch of residues. Reverse transcription occurs and uncoating, but nuclear entry is impaired. Viral cDNA that does enter the nucleus integrates into peripheral heterochromatin. Inset depicts interaction between myristic acid and positive residues of MA with the lipid bilayer.

Two elements of my proposed model remain to be tested and serve as future directions for this project. I hypothesize that the membrane-binding elements of MA tether the MA-CA-mixed core to the cellular membrane upon fusion. Currently, there are no reported assays for detecting core detachment from membranes, so testing this hypothesis will require development and optimization of new methods. Assembled Gag has been identified from cellular membranes isolated by fractionation experiments (288, 289). This approach is a logical starting point, and, indeed, I attempted this experiment several times. However, I quickly became aware of the scope of development this approach would require in order to generate interpretable data. The necessary variables to consider are not limited to cell count, time course of infection, and MOI of virus necessary for adequate signal to noise. Presently, this approach is plagued by a lack of obvious positive and negative controls. Perhaps a suitable negative control would be a virus that cannot fuse with the membrane, such as an Env-defective mutant. However, the degree to which the mutant virus associates with cell membranes would first have to be determined. An appropriate positive control is more difficult to imagine. Full MA-CA mutants (i.e. not cotransfected particles) may serve, since all of the MA would be associated with the immature core; although this would have to be limited to MA-CA and MA-SP1, since MA-NC cleavage is required for fusion (290).

Microscopy could serve as an alternative approach to test the membrane-tethering hypothesis. We have spoken with Dr. Zandrea Ambrose (Univ. of Pittsburgh) and Dr. Ashwanth Francis (Emory University) about potential collaborations involving live-cell imaging of infected cells (291, 292). With the appropriate localization markers, live-cell imaging would reveal if and how long cores remain tethered to the membrane

as well as the trafficking patterns associated with transport to the nucleus. As with the biochemical approach, significant development and optimization would be required to generate interpretable data, including the identification of suitable controls.

The second aspect of my proposed model that remains to be tested involves the nuclear import of MA-CA-mixed preintegration complexes. I determined that MA-CA cotransfection results in a nuclear entry impairment (Fig. 2-7), and our integration targeting data are reminiscent of WT infection of cells depleted of Nup153 and Nup358 (Table 2-1). I hypothesize that uncleaved MA-CA, present in the PIC, interferes with the CA-Nup interactions necessary for nuclear entry. Both Nup153 and Nup358 bind to the capsid and are involved in nuclear entry (55-57, 103-106). To test my hypothesis, I would perform *in vitro* binding assays with the recombinant CA and MA-CA assembled proteins described in Chapter 2 and cellular extracts and perform binding assays with immunoprecipitation. Similarly, I would infect cells with MA-CA-mixed viruses and perform immunoprecipitations with cellular extracts. The same experiment(s) could be performed for other elements of the nuclear pore complex, as recent reports have indicated that multiple nucleoporins and host factors can facilitate nuclear entry (55, 56). When I assayed mixed virus for nuclear entry, I observed a small amount of 2LTR circles (Fig. 2-7). While the reduction to nuclear entry accounted for the majority of the infection impairment, a small amount of nuclear entry occurred, even for the 20% MA-CA mixed viruses. If MA-CA interferes with the CA-Nup interactions necessary for nuclear entry, how did any PIC enter the nucleus? All infection experiments utilized HeLa cells, capable of cell division. It is possible that MA-CA PICs integrated while the host chromatin was accessible during division. To test this hypothesis, I would infect

cells treated with aphidicolin, preventing cell division. I would then determine if the small amount of nuclear entry was still occurring. These hypotheses and proposed experiments are based on the speculation that uncleaved MA-CA protein is part of the PIC. This could be easily tested by isolating PICs from infected cells and immunoblotting for MA-CA.

Understanding the antiviral effects of uncleaved MA-CA protein reveal the strict requirements for Gag cleavage during maturation and reinforce the models for CA-host factor interactions. Compounds directed at blocking the MA-CA cleavage site may represent a potent therapeutic avenue (293), since only small amounts of uncleaved MA-CA are required to inhibit infection. I also speculate that an MA-CA mimetic may also represent a novel therapy. An uncleavable MA-CA analogue produced in infected cells may render progeny virions non-viable. I imagine that a proof of concept could be performed by cotransfecting an MA-CA truncation construct with WT plasmid and then determine if uncleaved MA-CA was incorporated into harvested particles. While I have demonstrated that MA-CA coassembles with CA, I do not know if MA-CA coassembles with Gag, as other elements, such as NC and the viral RNA, participate in Gag assembly. Nevertheless, uncleaved MA-CA may hold promise for future antiviral therapeutics and greater understanding of HIV-1 biology.

My initial thesis project focused on CA-host factor interactions. Using *in vitro* binding assays and mass spectrometry, I identified EF1A as a capsid-binding host factor. However, I realized that EF1A was likely a false-positive in the mass spectrometry data, as EF1A was present in binding assay pellets independent of CA (Fig. 3-1). After months of optimization trials, I developed a new binding and

centrifugation procedure that eliminated the EF1A background pelleting, and I determined that the EF1A-CA interaction is substoichiometric at 118 molecules of CA to 1 molecule of EF1A (Fig. 3-2). While developing the new binding assay methods, I also performed functional validation experiments. I observed that EF1A depletion in HeLa P4 and TZM-bl cells significantly impaired HIV-1_{pNL4-3} infectivity (Fig. 3-3). Interestingly, the same depleted cells were permissive for HIV-1 infection where the virus harbored complemented envelope proteins, either from HIV-1 or other viruses (Fig. 3-4 and 3-5). Further investigation revealed a small decrease in surface CD4 expression in EF1A depleted cells (Fig. 3-7).

Based on my data, I hypothesize that EF1A depletion results in a fusion impairment. To test this hypothesis, I would perform the fusion assay used in Chapter 2 of my thesis and, if successfully developed, complement the experiment with live-cell imaging analysis to visualize the extent of entry. The latter analysis may reveal interesting insights into the kinetics of entry and how EF1A may affect it. I would also perform staining and flow cytometry experiments to determine if CXCR4 surface expression is specifically down-regulated in EF1A-depleted cells. I have performed preliminary experiments in SupT1 and CEM T cell lines, which suggest that EF1A is necessary for infection. However, it is possible that EF1A depletion in HeLa cells results in infection-related artifacts. Thus, functional validation experiments will be necessary in primary $CD4^+$ T cells to determine how relevant EF1A is to HIV-1 infection.

The most recent reports on EF1A related to HIV-1 suggest an important role for EF1A during reverse transcription (132-134). Collectively, the reports demonstrate an interaction between EF1A and RT, and that when this interaction is inhibited, either by

RT mutation or small molecule, reverse transcription in target cells is impaired. Additionally, Warren et al. reported that VSV-G pseudotyped HIV-1 was impaired for reverse transcription in HEK293T cells when EF1A was depleted by siRNA knock down (131). My observations in $CD4^+$ HeLa cells contradicted this report and suggested that the viral envelope and/or method of entry can obviate the need for EF1A during infection. Had I continued to work on this project, I may have revealed an unknown connection between envelope and post-entry replication events. However, at the time, there were too many intangibles related to this line of investigation, I was spending too much time and effort trying to establish a functioning fusion assay, and there was no clear path towards publication of this story. Ultimately, I decided that transitioning to the MA-CA project was in my best interest, and I thank my mentor and committee members their support and the chance to start over.

Chapter 5

Materials And Methods

Plasmids

All viruses tested in this study were generated from pNL4-3 or R9 proviral clones, which are isogenic in the Gag coding region. The pNL4-3 MA-CA plasmid harbors the single Y132I substitution in Gag (178). The following substitutions were generated by PCR overlap in pNL4-3 and pNL4-3 MA-CA constructs: in MA, G2A; in CA, A14C and E45C. The following deletions in MA were generated in wild type, MA-CA, and MA-CA G2A pNL4-3 plasmids by overlap PCR: removal of codons 8-126 and 8-87. For constructs in which 8-126 and 8-87 were deleted, a Ser/Arg (TCTCGT) motif was inserted concomitant with the removal in a single phase of overlap PCR. Constructions of the pNL4-3 CA-NC plasmid (196) and pNL4-3 MA-NC plasmid (290) were described previously. pNL4-3ΔE encodes a frameshift at the NdeI restriction site in *env*, resulting in Env-deficient particles. Plasmid pNLX.Luc.R-U3-tag, which was derived from pNLX.Luc.R-.ΔAvrII using overlap PCR, is also *env*-deficient and additionally carries the gene for Firefly luciferase in the viral *nef* position (188). The resulting PCR product, digested with XhoI and NgoMIV, was ligated with XhoI/NgoMIV-digested pNLX.Luc.R-.ΔAvrII DNA. The accuracy of mutagenesis was confirmed by DNA sequencing of all PCR-amplified regions.

Env-deficient viruses were pseudotyped with the vesicular stomatitis virus G (VSV-G) protein by cotransfection with pHCMV-G (294), the amphotropic murine

leukemia virus envelope protein by cotransfection with pSV-A-MLV-*env* (295), or the HIV-1 HXB2 envelope protein by cotransfection with pIIIEnv3-1 (296). Reporter-based infection assays employed HIV-GFP, a pNL4-3-based construct that harbors an *env* frameshift mutation and encodes green fluorescent protein (GFP) in place of *nef* (297), NL4-3-BaL-GFP, which was generated by transferring the SalI to BamHI fragment from R9-BaL to NL4-3 GFP, or HIV-Luc generated from pNLX.Luc.R-.ΔAvrII. BlaM-Vpr-reporter viruses used in virus-cell fusion assays were generated by cotransfection with the pMM310 plasmid, as previously described (290).

The recombinant 14C/45C CA protein was generated by introduction of Cys codons into pET21a HIV-1 CA at positions 14 and 45 (174). The recombinant MA-CA protein was generated by introducing the MA-CA coding region of pNL4-3 into the pET21a vector via restriction enzymes NdeI and XhoI.

Cells And viruses

TZM-bl cells were obtained through the NIH AIDS Reagent Program, Division of AIDS, NIAID, NIH (Cat# 8129) from Dr. John C. Kappes, and Dr. Xiaoyun Wu, and Tranzyme Inc (187, 298-301). HeLa-P4 cells were the generous gift of F. Clavel (193). SupT1 and CEM cells were the generous gift of Didier Trono. Owl Monkey Kidney (OMK) and human embryonic kidney (HEK) 293T cells were purchased from the American Type Culture Collection. HeLa-$CD4^+$ cells were generated by transducing HeLa cells with a pBABE-puro (302) vector encoding CD4. Single cell clones were grown, and cells were selected for growth with puromycin (1 μg/ml). Adherent cells were cultured at 37°C, 5% CO_2 in Dulbecco's modified eagle medium (DMEM)

(Cellgro), and non-adherent cells (SupT1, CEM) were cultured in RPMI supplemented with 10% fetal bovine serum (FBS), penicillin (50 IU/ml), and streptomycin (50 µg/ml). Virus stocks used for infectivity, cell fusion, abrogation of restriction, and protein cross-linking analyses were produced by calcium phosphate transfection of HEK293T cells (303). Virus stocks for thin-section EM analysis and HIV-Luc virions used to test infectivity of the U3-tagged virus for integration site sequencing were produced via PolyJet (SignaGen Laboratories) transfection (115). Virus stocks used for isolation of cores and integration targeting analysis were generated by polyethylenimine (PEI) transfection owing to the need for higher particle yields. Briefly, 10 µg of plasmid DNA was added to 900 µl Opti-Mem (gibco) and 40 µg PEI, incubated for 15 min at room temperature, and subsequently added to 3 million 293T cells. Cells were incubated at 37°C, 5% CO_2 for 6 h and subsequently washed in phosphate-buffered saline (PBS), and 6 ml media was replaced. Cell supernatants were harvested 48 h post transfection. Viruses used for quantification of reverse transcription products and 2-long terminal repeat (LTR) circles by qPCR were generated by transfection using the TransIT-293 transfection reagent (Mirus), according to the manufacturer's protocol, to minimize contamination of the virus stocks by transfected plasmid DNA. For cotransfection experiments, the total amount of DNA transfected was kept constant between experiments, using 20 µg total DNA per dish for calcium phosphate, 10 µg total DNA for PEI, and 15 µg total DNA for TransIT-293 transfections. VSV-G-pseudotyped HIV-1 particles were generated by cotransfection of 20 µg of proviral DNA with 5 µg of pHCMV-G DNA. Culture supernatants were filtered through 0.45 µm pore-size syringe filters, and aliquots were frozen and stored at -80°C only once per use. The CA content

of virus stocks was quantified by a p24-specific enzyme-linked immunosorbent assay (ELISA) (304), where viral samples were initially diluted in 2X Laemmli buffer (347mM Tris-HCl [pH 6.8], 22% glycerol, .0167% bromophenol blue, 4.4% sodium dodecyl sulfate (SDS)) containing 10% 2-mercaptoethanol (BME) and heated to 95°C for 5 min prior to serial dilution.

Virion Morphology Analysis

HIV-1 particles produced by transfection were pelleted at 26,000 rpm (115,000 x *g*) at 4°C for 2.5 h with a Beckman SW32 Ti rotor. Viral pellets were collected in 1 ml of PBS and subsequently pelleted at 45,000 rpm (125,000 x *g*) at 4°C for 30 min in a Beckman TLA 55 rotor. Viral pellets were fixed overnight at 4°C in electron microscopy (EM)-grade (Electron Microscopy Sciences) fixative agents (1.25% paraformaldehyde, 2.5% glutaraldehyde, 0.03% picric acid, 0.1 M sodium cacodylate buffer (pH 7.4)). Ultrathin (~60 nm) were cut on a Reichert Ultracut-S microtome, transferred to copper grids stained with lead citrate, and observed using a JEOL 1200EX microscope with an AMT 2k charge-coupled device camera. Images were captured at 30,000X magnification and were visually inspected to classify viral particles as mature, immature, eccentric, or empty. Virus particle classification was conducted using blinded samples, and over 100 particles were counted per virus preparation. Linear regression analysis of the eccentric particles was performed using GraphPad Prism software.

Virus-Cell Fusion Assay

Viral fusion was assayed as before (290) with modification. Briefly, we inoculated 10,000 HeLa TZM-bl cells, seeded the day prior, in a black-walled 96 well plate with dilutions of Blam-Vpr-reporter viruses in DMEM free of FBS, penicillin, and streptomycin but containing HEPES (10 mM) and DEAE-dextran (20 µg/ml). Diluted viruses (100 µl) were added to cells and cultured for 2 h at 37°C to allow for virus fusion. CCF4-AM (Invitrogen) was then added to a final concentration of 0.94 µM and incubated at room temperature for 16 h in the dark. Supernatants were removed and replaced with 100 µl PBS, and fluorescence was quantified at 450 nm and 520 nm with a BMG Fluostar microplate fluorometer with excitation at 410 nm. The extent of fusion was determined as the resulting ratio of blue-to-green fluorescence in each culture. These ratios were calculated following subtraction of averaged background values of uninoculated (blue values) and cell-free, PBS-containing quadruplicate wells (green background). Duplicate determinations were performed for each virus dilution.

Assay Of HIV Infectivity

Viral infectivity was determined by titrating virus stocks on TZM-bl cells and assaying expression of luciferase reporter activity in cell lysates or by using p24-matched levels of luciferase-containing constructs to infect HEK293T cells (115). Cells (10,000 per well) were seeded in black-walled 96 well plates and inoculated with 10-fold serial dilutions of HIV-1_{NL4-3} in culture medium containing 20 µg/ml DEAE-dextran in 100 µl total volume. 48 h after inoculation, cells were washed once in PBS and lysed in 30 µl TBS (50mM Tris-HCl [pH 7.8], 130 mM NaCl, 10 mM KCl, 5 mM $MgCl_2$) containing

0.5% Triton X-100. Luminescence was determined using an Lmax luminometer (Molecular Devices) for 5 sec after injection of 200 µl Solution 1 (75mM Tris-HCl [pH 8], 8.3 mM MgOAc, 4 mM ATP) and 80 µl Solution 2 (1 mM D-Luciferin (GoldBio)). Infectivity values were determined as the ratio of Arbitrary Light Units (ALU) per ng p24 at doses of virus corresponding to the linear range of luciferase signals from each assay. The infectivity of particles containing uncleaved MA-CA was calculated as a percentage of the corresponding wild type values. For abrogation of restriction experiments, single-cycle assays of viral infectivity were performed with 10,000 OMK cells plated one day prior to infection in 96 well plates with 100 µl volumes of HIV-1ΔE(VSV), co-inoculated with HIV-GFP(VSV) (2 ng p24). Sixteen hours after inoculation, cells were washed in PBS and culture media replaced. 48 h post infection, cells were detached with trypsin and fixed overnight in PBS containing 4% fresh paraformaldehyde. GFP expression in OMK cells was analyzed by flow cytometry on an Accuri C6 flow cytometer, analyzing a minimum of 5,000 cells per sample.

Isolation Of HIV-1 Cores

Viral cores were isolated from concentrated HIV-1 particles as previously described (177). Supernatants from transfected 293T cells were concentrated by centrifugation in a Beckman SW32-Ti rotor at 32,000 rpm (175,000 X *g* at r_{max}) at 4°C for 3 h. Pelleted virions were resuspended in 0.4 ml of 1X STE buffer (10 mM Tris-HCl [pH 7.4], 100 mM NaCl, and 1 mM EDTA) and incubated on ice for 3 h. The concentrated virions were then centrifuged at 32,000 rpm (187,000 X *g*) for 16 h at 4°C through an 11 ml 30%-70% linear sucrose gradient overlaid with 1% Triton X-100.

Fractions (1 ml) were collected from the top of the gradient. The CA content in each fraction was quantified by p24 ELISA. HIV-1 RNA in each fraction was quantified by RT-qPCR. Prior to concentration of the particles and core isolation, transfected cell supernatants were treated with 20 µg/ml DNase I and 10 mM $MgCl_2$ for 1 h at 37°C. RNA was isolated from each fraction with Trizol reagent (Invitrogen) according to the manufacturer's protocol. cDNA was synthesized from extracted RNA by RT-PCR using a cDNA Reverse Transcription kit (Applied Biosystems) according to the manufacturer's protocol. cDNA from each fraction was analyzed by quantitative PCR using an MX-3000P thermocycler (Stratagene) utilizing SYBR green chemistry (ABI). First strand-transfer reverse transcripts were amplified using forward (5'-AGCAGCTGCTTTTTGCCTGTACT-3') and reverse (5'-ACACAACAGACGGGCACACAC-3') primers, and copy numbers were interpolated from a standard curve produced with dilutions of wild type R9 plasmid DNA. HIV-1 proteins in each gradient fraction were analyzed by immunoblotting after concentrating the protein samples by precipitation with trichloroacetic acid (TCA). Briefly, 500 µl of gradient fractions were diluted in 500 µl PBS. 250 µl of 30% TCA was added, and samples were incubated on ice for 30 min. Precipitated proteins were pelleted at 13,000 rpm for 5 min. Pellets were washed twice in a 1:1 ethanol:ether mix. Pellets were resuspended in Laemmli buffer.

Immunoblotting Analysis

Proteins were separated on 4-20% SurePAGE bis-tris polyacrylamide gradient gels (Genscript) and electrophoretically transferred to nitrocellulose membranes (Perkin

Elmer). Blots were subsequently blocked in blocking buffer (Li-COR) diluted 50% with PBS. Membranes were washed in PBS containing 0.2% Tween 20 thrice for 5 min between antibody incubations. For immunoblotting analysis of pelleted viral particles, samples were normalized by p24 levels (determined by ELISA) with proteins dissolved in 2X Laemmli buffer containing 10% BME and incubated for 5 min at 95°C (reducing conditions) or dissolved in Laemmli buffer without BME and not heated (non-reducing conditions). Samples from TCA-precipitated gradient fractions were loaded onto gels with equal volumes between samples. Membranes were probed with the following antibodies: HIV-1 CA (mouse monoclonal, 183-H12-5C, NIH AIDS Research and Reference Program (305), 4 μg/ml); HIV-1 NC (polyclonal goat serum, received from Dr. Robert Gorelick 1:1000 dilution); HIV-1 MA (polyclonal rabbit serum, 4811 NIH AIDS Research and Reference Program (306), 1:500 dilution); and HIV-1 RT (polyclonal rabbit serum, 6195 NIH AIDS Research and Reference Program, 1:1000 dilution). Rabbit antiserum against HIV-1 IN was raised in animals inoculated with 2 μg purified recombinant protein (307), which was subsequently affinity purified over an IN-containing column (Thermo Fisher). The resulting antibody was used at 1:5,000 dilution. BlaM-Vpr was detected with beta-lactamase antibody (mouse monoclonal, QED Bioscience Inc. 15720, 2.8 μg/ml). EF1A was detected with EF1A antibody (mouse monoclonal, Millipore. Clone CBP-KK1; 05-235, 2.5 μg/ml). GAPDH was detected by GAPDH antibody (mouse monoclonal, Santa Cruz Biotechnology. 0411, SC-47724, 100 ng/ml). Immunoblots were probed with the appropriate infrared (IR) dye-conjugated secondary antibodies at 100 ng/ml (Li-COR Biosciences), and bound antibodies were detected by scanning with a Li-COR Odyssey imaging system. Protein

band quantification was determined via pixel intensity analysis using Li-COR Image Studio 3.1 employing background subtraction by the top and bottom, median background method.

Quantification Of Reverse Transcribed Products And 2-LTR Circles In Infected Cells

Duplicate cultures of 100,000 Hela-CD4 cells were inoculated with 150 ng p24 of HIV-1 particles in 12-well plates. Cell monolayers were rinsed in PBS and detached with trypsin 8 h after virus inoculation (for second-strand transfer analysis) or 24 h post inoculation (for 2-LTR circle analysis). Cell pellets were treated with qPCR lysis buffer (10 mM Tris-HCl [pH 8], 0.2 mM $CaCl_2$, 1 mM EDTA, 0.001% TX-100, 0.001% SDS, 1 mg/ml proteinase K) for 1 h at 57°C. Proteinase K was then inactivated by heating the samples at 95°C for 15 min. As a control to detect contaminating plasmid DNA, the RT inhibitor Efavirenz (1 μM) was added to parallel infections in all experiments analyzing second-strand transfer. Either 25 μM IN inhibitor 118-D-24 (NIH AIDS Research and Reference Program (308, 309)) or 1 μM Raltegravir (a generous gift from Dr. Chandravanu Dash) was added to all samples in experiments analyzing 2-LTR circles. Prior to all infections for qPCR analysis, virus stocks were treated with 20 μg/ml DNaseI, 10 mM $MgCl_2$ at 37°C for 1 h to reduce contaminating plasmid DNA. HIV-1 DNA was detected in each sample with SYBR green chemistry on a Stratagene MX3000p instrument. Second-strand transfer DNA was amplified using
forward primer: 5'-TGTGTGCCCGTCTGTTGTGT-3' and
reverse primer: 5'-GAGTCCTGCGTCGAGAGATC-3'. 2-LTR circle DNA was amplified

using forward primer: 5'-AACTAGGGAACCCACTGCTTAAG-3' and reverse primer: 5'-TCCACAGATCAAGGATATCTTGTC-3'. Second strand transfer copy numbers of cDNA were interpolated from a standard curve using HIV-1 plasmid DNA as a standard. 2-LTR circle copy numbers of cDNA were interpolated from a standard curve using p2LTR plasmid DNA (310) as a standard.

Recombinant Protein Purification And Immunoprecipitation

The HIV-1 proteins MA-CA and CA were expressed from the pET21a-MA-CA construct and the pET21a-CA construct, which encodes A14C/E45C substitutions in CA. The plasmids were transformed into competent *E. coli* BL21 cells, grown in 2 L of LB to OD_{600} of 0.6, and expression was induced by the addition of 1 mM IPTG (isopropyl-B-D-thiogalactopyranoside; Gold Biotechnology) and cultures were subsequently incubated for 8 h at 25°C. Cells were lysed by sonication (Sonic Dismembrator ultrasonic processor (Fisher Scientific)), and lysates were cleared by centrifugation for 1 h at 40,000 X *g* at 4°C. CA protein was purified by anion-exchange chromatography as described (174). MA-CA protein was purified as described (155), with the following modifications. MA-CA protein was precipitated from the bacterial lysate by addition of ammonium sulfate to 25%-34% of saturation, and the precipitate was pelleted and dissolved in 30 ml Buffer A (25 mM Tris-HCl (pH 8.0), 50 mM NaCl, 5 mM BME, protease inhibitor cocktail tablet (Roche)), dialyzed against 1 L of Buffer A overnight at 4°C, clarified by centrifugation for 30 min at 27000 X *g*, and then subjected to anion-exchange chromatography using a 5 ml UNOsphere ^{TM} Q cartridge (Bio Rad). MA-CA protein was present in the flow-through and subsequently spontaneously

precipitated. The precipitate was pelleted and dissolved in 5 ml of STE buffer containing 5 mM BME and 0.2% DPC (N-dodecylphosphocholine). DPC was removed by two rounds of dialysis against 1 L of 50 mM Tris-HCl pH7.4, 1 M NaCl at 4°C for 16 h, and the sample was subsequently concentrated to 0.8 ml with an Amicon Utracel-10K filter unit (Millipore). The final yield of MA-CA protein was approximately 3 mg, with a purity of greater than 95% as determined by SDS-polyacrylamide gel electrophoresis (PAGE) and staining with Coomassie blue.

Recombinant CA and MA-CA proteins were assembled in 50 mM Tris-HCl (pH 8.0), 1 M NaCl at 37°C for 1 h at 0.8 mg/ml each, and assembled proteins were pelleted by centrifugation at 5,000 X *g* for 5 min at 4°C. The supernatant was removed, and the pelleted assembled protein was resuspended in 25 mM Tris-HCl (pH 8.0), 0.5 M NaCl. Immunoprecipitation was performed with Pierce™ protein A/G magnetic beads (Thermo Scientific) per the manufacturer's instructions. Beads (200 µg) were coated with 5 µl anti-MA antibody (rabbit polyclonal, 4811 NIH AIDS Research and Reference Program) for 1 h at room temperature in wash buffer (25 mM Tris-HCl (pH 8.0), 0.5 M NaCl, 0.05% Tween-20). 15 µl of each resuspended assembly or coassembly reaction was added to coated beads and incubated for 16 h at 4°C in 25 mM Tris-HCl (pH 8.0), 0.5 M NaCl. The beads were washed thrice in wash buffer. Beads were resuspended in 30 µl of 2X Laemmli buffer containing 10% BME and incubated for 10 min at 95°C. Beads were removed from the sample by magnet prior to SDS-PAGE and immunoblotting.

Visual Inspection Of Recombinant CA And MA-CA Assembly Reactions

Recombinant CA and MA-CA proteins were assembled as above at 0.8 mg/ml each, pelleted, supernatants removed, and pelleted reactions resuspended in 25 mM Tris-HCl (pH 8.0), 0.5 M NaCl. To check tube assembly, reactions were visualized by negative-stain EM after staining with 0.7% uranyl formate, and images were collected with an FEI Morgagni electron microscope at 100 kV at a magnification of 4,400 X or 2,200 X. Images were recorded on an AMT 100X 100 charge-coupled device camera.

Integration Site Analysis

In preliminary experiments, genomic DNA was extracted from HEK293T cells infected with VSV-G-pseudotyped HIV-$1_{NLX.Luc.R-}$ or HIV-$1_{NLX.Luc.R-U3-tag}$ using the DNeasy Blood and Tissue Kit (Qiagen). To sequence U5-cell DNA junctions, genomic DNA was digested with MseI and BglII (192). For U3-cell junctions, DNA isolated from cells infected with HIV-$1_{NLX.Luc.R-U3-tag}$ was digested with AvrII, NheI-HF, SpeI-HF, and BamHI-HF. Following digestion, fragmented DNA was ligated to adapters and subjected to consecutive rounds of ligation-mediated (LM)-PCR, essentially as previously described (192) using 16 independent PCR reactions for each primer pair during both rounds of PCR.

Plasmid pNLX.Luc.R-U3-tag was cotransfected with either pNL4-3 or pNL4-3 MA-CA plasmid and pHCMV-G to produce pseudotyped HIV-1 particles, which were then used (12.5 ng of p24) to inoculate 0.5 million HeLa-P4 cells. Cells were subsequently cultured for 4 days, and cellular DNA was extracted (QIAGEN DNeasy Blood and Tissue Kit). The DNA was processed for LM-PCR and Illumina sequencing essentially

as described above and as in references (59, 192). Read pairs from 150 bp paired end sequencing were selected for U3 LTR sequences in the first read (read 1) and linker DNA (read 2) in the second read. After trimming both LTR and linker sequences, reads were aligned to human genome build hg19 by BWA-MEM aligner with pair end option (311). MA-CA virus experiments compiled results from two independent infections, and the alignment outputs from both experiments were combined to generate single alignment files to map integration sites. For preliminary work with the U3-tagged virus, only read1 information was aligned using the Hisat aligner (312). BWA-aligned reads were filtered to remove unmapped reads using the –F 4 option in SAMtools (313), while secondary alignment and reads with low MAPQ score were removed using –F 256 –q 1 options. The paired end analysis filtered for reads that were properly distanced and directed towards each other on the same chromosome; reads where the distance between the integration site and the linker ligation site was > 900 bp were omitted from analysis. Unique reads across pipelines were selected and converted into the BED format. To account for the 5 bp duplication of genomic DNA associated with HIV-1 integration, the left interval of the BED format was determined by adding 2 to the integration site if the site was on the genomic positive strand and by subtracting 2 from the site if it was on the negative strand. Similarly, the right interval of the BED format was obtained by adding 3 to the integration site if the site was on the positive strand and by subtracting 3 if the site was on the negative strand. Distribution of integration sites with respect to various genomic features of the human genome was analyzed using BEDtools as described previously (192). The computation random integration control (RIC) was similarly mapped using DNA fragments generated following digestion of hg19

with restriction endonucleases AvrII, NheI, Spe, and BamHI in silico. Statistical analyses were performed as described previously (192).

Cytoplasmic Extracts Of Hela P4 Cells

HeLa P4 cells were grown to confluency in 50 10 cm dishes. Cells were washed once in PBS and detached with Trypsin. Cells were collected in DMEM and pelleted at 3,300 rpm for 5 min at 4°C. Pellets were resuspended in cold PBS and multiple pellets were combined, pelleted again, and resuspended in 12.5ml of Lysis Buffer (10 mM Tris HCl pH 8.0, 1.5 mM $MgCl_2$, 10 mM KCl, 0.5 mM EDTA pH 8.0, protease inhibitor tablets (Roche)). Cells were lysed by sonication, and lysis was determined by Trypan Blue staining. Cell nuclei were pelleted at 14,000 X *g* for 30 min at 4°C. Protein concentration was determined by absorbance at 280 nm.

***in vitro* Binding Assays Of Recombinant CA And Cell Extracts**

Purified 14C/45C CA was purified as above and assembled in a dialysis cup for 1 h at 4°C in Buffer 1 (1 M NaCl, 50 mM Tris HCl pH 8.0, 20 mM BME) and transferred to Buffer 2 (1 M NaCl, 50 mM Tris HCl pH 8.0) for 16 h at 4°C. Assembled protein was pelleted at 5,000 X *g* for 5 min at 4°C. Pelleted protein was resuspended in Binding Buffer (50 mM Tris HCl pH 8.0, 150 mM NaCl, 5 mM $MgCl_2$, 0.5 mM EDTA). CA (12.5 µg) was added to lysates (125 µg) binding buffer, and in some cases, 7 µM PF74, 40 µM BI-2, or matched DMSO control (0.5%), and reactions were incubated on ice for 1 h with gentle mixing every 15 min. Binding reactions were pelleted at 5,000 X *g* for 5 min at 4°C, resuspended in binding buffer and pelleted again. Reaction pellets were

resuspended in 15 µl of 2X Laemmli buffer containing 10% BME and incubated for 5 min at 95°C. Immunoblotting was performed as above. The binding reactions prepared for mass spectrometry were performed as above. The proteins were separated by SDS-PAGE and stained with colloidal Coomassie. Gels were submitted to Hayes McDonald at the Vanderbilt Mass Spectrometry Research Center for Multidimensional Protein Identification Technology (MuDPIT) analysis.

Alternative binding assays utilized the same CA and lysate conditions as above in Binding Buffer 2(50 mM Tris HCl pH 8.0, 150 mM NaCl, 5 mM $MgCl_2$, 0.5 mM EDTA, 0.086% Brij-58 (10X CMC)). Binding reactions proceeded for 1h at 37°C with gentle mixing every 15 min. Reactions were overlayed atop layers of 45% and 30% sucrose solutions (prepared in Binding Buffer 2) and centrifuged at 10,000 rpm for 10 min at 4°C. Reaction pellets were resuspended in 15 µl of 2X Laemmli buffer containing 10% BME and incubated for 5 min at 95°C. Immunoblotting was performed as above.

EF1A Depletion Experiments

EF1A shRNA pLKO.1 vectors were purchased from GE Healthcare, Dharmacon (TRC EEF1A1, RHS4533-EG1915). Lentiviruses were generated by PEI cotransfection of pLKO.1 (20 µg), psPAX2 (15 µg), and pHCMV-G (5 µg) plasmid DNAs. HeLa P4, HeLa TZM-bl, SupT1, and CEM cells were transduced with 500 ng p24 of the resulting lentiviruses in media supplemented with 8 µg/ml Polybrene. Cells were incubated for 48 h at 37°C, 5% CO_2. 48 h after transduction, cells were collected and plated in media containing 1 µg/ml puromycin. 48 h after selection with puromycin, cells were collected, counted, and plated for immunoblot analysis (500,000 cells) in 10 cm dishes, or single-

cycle infection (15,000 cells) in 96 well plates. Five days post transduction, cells were analyzed in the following ways. First, cell extracts were prepared with RIPA buffer (150mM NaCl, 1% NP40, 0.5% sodium deoxycholate, 0.1% SDS, 50 mM Tris HCl pH 8.0), and protein concentration was determined by BCA assay. Immunoblots of extracts were performed as detailed above. Second, cells were infected with viruses listed above. 48 h post infection, cells were detached with trypsin and fixed overnight in PBS containing 4% fresh paraformaldehyde. GFP expression in cells was analyzed by flow cytometry on an Accuri C6 flow cytometer, analyzing a minimum of 5,000 cells per sample. Third, cells were stained with a FITC-labelled human CD4 antibody (mouse monoclonal, BD Biosciences, clone RPA-T4, Lot 3303851, Cat 555346, 1:5 dilution) in PBS containing 2% FBS, on ice for 30 min with gentle mixing every 5 min. Cells were pelleted, resuspended in PBS/FBS, twice, with a final resuspension in 4% PFA, stored 16 h at 4°C. FITC-labelled cells were analyzed by flow cytometry as above. Fourth, cells were biosynthetically labelled with ^{35}S. Cells were washed twice in labelling media (DMEM without L-cysteine and L-methionine) and then incubated in labeling media for 15 min at 37°C 5% CO_2. Following incubation and aspiration, labeling media containing 0.2 mCi/ml was added to cells and incubated for 90 min at 37°C 5% CO_2. Cells were washed twice in cold PBS, and cell extracts were prepared in cell lysis buffer (50 mM Tris HCl pH 7.5, 100mM NaCl, 1% NP40, protease inhibitor tablets (Roche); nuclei were pelleted by centrifugation at 14,000 X *g* for 5 min at 4°C. Supernatants were collected, and protein concentration was determined by BCA. Proteins were separated by SDS-PAGE. The gel was fixed in 30% methanol, 10% acetic acid mix for 30 min at room temperature, followed by two incubations in water for 15 min, and a final incubation in

Fluorenhance for 30 min. Dried gels were exposed to x-ray film for 36 h at -80°C, and the film was imaged with a phosphorimager.

Statistical Analysis

Analysis was performed with GraphPad Prism 7 software (GraphPad, La Jolla, CA, USA). Comparisons were performed with unpaired t-test or single-sample t-test with a hypothetical mean when comparing normalized data. Integration site sequencing and MuDPIT comparisons were performed with Fisher's exact test. All tests were considered statistically significant at $p<0.05$.

REFERENCES

1. Comeau AM, Hatfull GF, Krisch HM, Lindell D, Mann NH, Prangishvili D. 2008. Exploring the prokaryotic virosphere. Res Microbiol 159:306-13.
2. Meyer TJ, Rosenkrantz JL, Carbone L, Chavez SL. 2017. Endogenous Retroviruses: With Us and against Us. Front Chem 5:23.
3. Barre-Sinoussi F, Chermann JC, Rey F, Nugeyre MT, Chamaret S, Gruest J, Dauguet C, Axler-Blin C, Vezinet-Brun F, Rouzioux C, Rozenbaum W, Montagnier L. 1983. Isolation of a T-lymphotropic retrovirus from a patient at risk for acquired immune deficiency syndrome (AIDS). Science 220:868-71.
4. Gallo RC, Montagnier L. 2003. The discovery of HIV as the cause of AIDS. N Engl J Med 349:2283-5.
5. WHO. 2018. HIV/AIDS. https://www.who.int/news-room/fact-sheets/detail/hiv-aids. Accessed
6. UNAIDS. 2017. Epidemic transition metrics. http://aidsinfo.unaids.org. Accessed
7. Shaw GM, Hunter E. 2012. HIV transmission. Cold Spring Harb Perspect Med 2.
8. Dalgleish AG, Beverley PC, Clapham PR, Crawford DH, Greaves MF, Weiss RA. 1984. The CD4 (T4) antigen is an essential component of the receptor for the AIDS retrovirus. Nature 312:763-7.
9. Geijtenbeek TB, van Kooyk Y. 2003. DC-SIGN: a novel HIV receptor on DCs that mediates HIV-1 transmission. Curr Top Microbiol Immunol 276:31-54.
10. Lackner AA, Lederman MM, Rodriguez B. 2012. HIV pathogenesis: the host. Cold Spring Harbor perspectives in medicine 2:a007005-a007005.
11. Fauci AS, Pantaleo G, Stanley S, Weissman D. 1996. Immunopathogenic Mechanisms of HIV Infection. Annals of Internal Medicine 124:654-663.
12. de Wolf F, Spijkerman I, Schellekens PT, Langendam M, Kuiken C, Bakker M, Roos M, Coutinho R, Miedema F, Goudsmit J. 1997. AIDS prognosis based on HIV-1 RNA, CD4+ T-cell count and function: markers with reciprocal predictive value over time after seroconversion. Aids 11:1799-806.
13. Mellors JW, Rinaldo CR, Gupta P, White RM, Todd JA, Kingsley LA. 1996. Prognosis in HIV-1 Infection Predicted by the Quantity of Virus in Plasma. Science 272:1167.
14. Cummins NW, Badley AD. 2014. Making sense of how HIV kills infected CD4 T cells: implications for HIV cure. Molecular and cellular therapies 2:20-20.
15. Kumar P. 2013. Long term non-progressor (LTNP) HIV infection. The Indian journal of medical research 138:291-293.
16. Arts EJ, Hazuda DJ. 2012. HIV-1 antiretroviral drug therapy. Cold Spring Harb Perspect Med 2:a007161.
17. Collier AC, Coombs RW, Schoenfeld DA, Bassett RL, Timpone J, Baruch A, Jones M, Facey K, Whitacre C, McAuliffe VJ, Friedman HM, Merigan TC, Reichman RC, Hooper C, Corey L. 1996. Treatment of human immunodeficiency virus infection with saquinavir, zidovudine, and zalcitabine. AIDS Clinical Trials Group. N Engl J Med 334:1011-7.

18. D'Aquila RT, Hughes MD, Johnson VA, Fischl MA, Sommadossi JP, Liou SH, Timpone J, Myers M, Basgoz N, Niu M, Hirsch MS. 1996. Nevirapine, zidovudine, and didanosine compared with zidovudine and didanosine in patients with HIV-1 infection. A randomized, double-blind, placebo-controlled trial. National Institute of Allergy and Infectious Diseases AIDS Clinical Trials Group Protocol 241 Investigators. Ann Intern Med 124:1019-30.
19. Staszewski S, Miller V, Rehmet S, Stark T, De Cree J, De Brabander M, Peeters M, Andries K, Moeremans M, De Raeymaeker M, Pearce G, Van den Broeck R, Verbiest W, Stoffels P. 1996. Virological and immunological analysis of a triple combination pilot study with loviride, lamivudine and zidovudine in HIV-1-infected patients. Aids 10:F1-7.
20. Allers K, Hutter G, Hofmann J, Loddenkemper C, Rieger K, Thiel E, Schneider T. 2011. Evidence for the cure of HIV infection by CCR5Delta32/Delta32 stem cell transplantation. Blood 117:2791-9.
21. Hutter G, Nowak D, Mossner M, Ganepola S, Mussig A, Allers K, Schneider T, Hofmann J, Kucherer C, Blau O, Blau IW, Hofmann WK, Thiel E. 2009. Long-term control of HIV by CCR5 Delta32/Delta32 stem-cell transplantation. N Engl J Med 360:692-8.
22. Gupta RK, Abdul-Jawad S, McCoy LE, Mok HP, Peppa D, Salgado M, Martinez-Picado J, Nijhuis M, Wensing AMJ, Lee H, Grant P, Nastouli E, Lambert J, Pace M, Salasc F, Monit C, Innes AJ, Muir L, Waters L, Frater J, Lever AML, Edwards SG, Gabriel IH, Olavarria E. 2019. HIV-1 remission following CCR5Delta32/Delta32 haematopoietic stem-cell transplantation. Nature doi:10.1038/s41586-019-1027-4.
23. Coffin JM HS, Varmus HE, editors. 1997. Retroviruses, *on* Cold Spring Harbor Laboratory Press. https://www.ncbi.nlm.nih.gov/books/NBK19376/. Accessed
24. Zhu P, Liu J, Bess J, Jr., Chertova E, Lifson JD, Grise H, Ofek GA, Taylor KA, Roux KH. 2006. Distribution and three-dimensional structure of AIDS virus envelope spikes. Nature 441:847-52.
25. Balliet JW, Kolson DL, Eiger G, Kim FM, McGann KA, Srinivasan A, Collman R. 1994. Distinct effects in primary macrophages and lymphocytes of the human immunodeficiency virus type 1 accessory genes vpr, vpu, and nef: mutational analysis of a primary HIV-1 isolate. Virology 200:623-31.
26. Yan J, Shun MC, Hao C, Zhang Y, Qian J, Hrecka K, DeLucia M, Monnie C, Ahn J, Skowronski J. 2018. HIV-1 Vpr Reprograms CLR4(DCAF1) E3 Ubiquitin Ligase to Antagonize Exonuclease 1-Mediated Restriction of HIV-1 Infection. MBio 9.
27. Yan J, Shun MC, Zhang Y, Hao C, Skowronski J. 2019. HIV-1 Vpr counteracts HLTF-mediated restriction of HIV-1 infection in T cells. Proc Natl Acad Sci U S A 116:9568-9577.
28. Campbell EM, Hope TJ. 2015. HIV-1 capsid: the multifaceted key player in HIV-1 infection. Nat Rev Microbiol 13:471-83.
29. Freed EO. 2015. HIV-1 assembly, release and maturation. Nat Rev Microbiol 13:484-96.
30. Seelamgari A, Maddukuri A, Berro R, de la Fuente C, Kehn K, Deng L, Dadgar S, Bottazzi ME, Ghedin E, Pumfery A, Kashanchi F. 2004. Role of viral regulatory and accessory proteins in HIV-1 replication. Front Biosci 9:2388-413.
31. Karn J, Stoltzfus CM. 2012. Transcriptional and posttranscriptional regulation of HIV-1 gene expression. Cold Spring Harb Perspect Med 2:a006916.

32. Wilen CB, Tilton JC, Doms RW. 2012. HIV: cell binding and entry. Cold Spring Harbor perspectives in medicine 2:a006866.
33. Wilen CB, Tilton JC, Doms RW. 2012. HIV: cell binding and entry. Cold Spring Harb Perspect Med 2.
34. Ambrose Z, Aiken C. 2014. HIV-1 uncoating: connection to nuclear entry and regulation by host proteins. Virology 454-455:371-9.
35. Yamashita M, Engelman AN. 2017. Capsid-Dependent Host Factors in HIV-1 Infection. Trends Microbiol 25:741-755.
36. Carnes SK, Zhou J, Aiken C. 2018. HIV-1 Engages a Dynein-Dynactin-BICD2 Complex for Infection and Transport to the Nucleus. Journal of virology 92:e00358-18.
37. Fernandez J, Portilho DM, Danckaert A, Munier S, Becker A, Roux P, Zambo A, Shorte S, Jacob Y, Vidalain P-O, Charneau P, Clavel F, Arhel NJ. 2015. Microtubule-associated proteins 1 (MAP1) promote human immunodeficiency virus type I (HIV-1) intracytoplasmic routing to the nucleus. The Journal of biological chemistry 290:4631-4646.
38. Lehmann M, Nikolic DS, Piguet V. 2011. How HIV-1 takes advantage of the cytoskeleton during replication and cell-to-cell transmission. Viruses 3:1757-1776.
39. Sabo Y, Walsh D, Barry DS, Tinaztepe S, de Los Santos K, Goff SP, Gundersen GG, Naghavi MH. 2013. HIV-1 induces the formation of stable microtubules to enhance early infection. Cell Host Microbe 14:535-46.
40. Yoder A, Guo J, Yu D, Cui Z, Zhang X-E, Wu Y. 2011. Effects of Microtubule Modulators on HIV-1 Infection of Transformed and Resting CD4 T Cells. Journal of Virology 85:3020-3024.
41. Arhel N. 2010. Revisiting HIV-1 uncoating. Retrovirology 7:96.
42. Forshey B, von Schwedler U, Sundquist W, Aiken C. 2002. Formation of a human immunodeficiency virus type 1 core of optimal stability is crucial for viral replication. J Virol 76:5667 - 5677.
43. Reicin AS, Ohagen A, Yin L, Hoglund S, Goff SP. 1996. The role of Gag in human immunodeficiency virus type 1 virion morphogenesis and early steps of the viral life cycle. Journal of Virology 70:8645-8652.
44. Rihn SJ, Wilson SJ, Loman NJ, Alim M, Bakker SE, Bhella D, Gifford RJ, Rixon FJ, Bieniasz PD. 2013. Extreme genetic fragility of the HIV-1 capsid. PLoS Pathog 9:e1003461.
45. von Schwedler UK, Stray KM, Garrus JE, Sundquist WI. 2003. Functional Surfaces of the Human Immunodeficiency Virus Type 1 Capsid Protein. Journal of Virology 77:5439-5450.
46. Yang R, Shi J, Byeon IJ, Ahn J, Sheehan JH, Meiler J, Gronenborn AM, Aiken C. 2012. Second-site suppressors of HIV-1 capsid mutations: restoration of intracellular activities without correction of intrinsic capsid stability defects. Retrovirology 9:30.
47. Hulme AE, Perez O, Hope TJ. 2011. Complementary assays reveal a relationship between HIV-1 uncoating and reverse transcription. Proceedings of the National Academy of Sciences 108:9975-9980.
48. Rankovic S, Varadarajan J, Ramalho R, Aiken C, Rousso I. 2017. Reverse Transcription Mechanically Initiates HIV-1 Capsid Disassembly. Journal of Virology 91:e00289-17.

49. Tang S, Murakami T, Agresta BE, Campbell S, Freed EO, Levin JG. 2001. Human immunodeficiency virus type 1 N-terminal capsid mutants that exhibit aberrant core morphology and are blocked in initiation of reverse transcription in infected cells. J Virol 75:9357-66.
50. Yang Y, Fricke T, Diaz-Griffero F. 2013. Inhibition of Reverse Transcriptase Activity Increases Stability of the HIV-1 Core. Journal of Virology 87:683-687.
51. Hu WS, Hughes SH. 2012. HIV-1 reverse transcription. Cold Spring Harb Perspect Med 2.
52. Bukrinsky MI, Sharova N, Dempsey MP, Stanwick TL, Bukrinskaya AG, Haggerty S, Stevenson M. 1992. Active nuclear import of human immunodeficiency virus type 1 preintegration complexes. Proc Natl Acad Sci U S A 89:6580-4.
53. Dismuke DJ, Aiken C. 2006. Evidence for a functional link between uncoating of the human immunodeficiency virus type 1 core and nuclear import of the viral preintegration complex. J Virol 80:3712-20.
54. Fouchier RAM, Malim MH. 1999. Nuclear Import of Human Immunodeficiency Virus Type-1 Preintegration Complexes, p 275-299. *In* Rlaramorosch K, Murphy FA, Shawn AJ (ed), Advances in Virus Research, vol 52. Academic Press.
55. Kane M, Rebensburg SV, Takata MA, Zang TM, Yamashita M, Kvaratskhelia M, Bieniasz PD. 2018. Nuclear pore heterogeneity influences HIV-1 infection and the antiviral activity of MX2. Elife 7.
56. Lee K, Ambrose Z, Martin TD, Oztop I, Mulky A, Julias JG, Vandegraaff N, Baumann JG, Wang R, Yuen W, Takemura T, Shelton K, Taniuchi I, Li Y, Sodroski J, Littman DR, Coffin JM, Hughes SH, Unutmaz D, Engelman A, KewalRamani VN. 2010. Flexible use of nuclear import pathways by HIV-1. Cell Host Microbe 7:221-33.
57. Schaller T, Ocwieja KE, Rasaiyaah J, Price AJ, Brady TL, Roth SL, Hue S, Fletcher AJ, Lee K, KewalRamani VN, Noursadeghi M, Jenner RG, James LC, Bushman FD, Towers GJ. 2011. HIV-1 capsid-cyclophilin interactions determine nuclear import pathway, integration targeting and replication efficiency. PLoS Pathog 7:e1002439.
58. Yamashita M, Emerman M. 2004. Capsid is a dominant determinant of retrovirus infectivity in nondividing cells. J Virol 78:5670-8.
59. Achuthan V, Perreira JM, Sowd GA, Puray-Chavez M, McDougall WM, Paulucci-Holthauzen A, Wu X, Fadel HJ, Poeschla EM, Multani AS, Hughes SH, Sarafianos SG, Brass AL, Engelman AN. 2018. Capsid-CPSF6 Interaction Licenses Nuclear HIV-1 Trafficking to Sites of Viral DNA Integration. Cell Host Microbe 24:392-404.e8.
60. Fenouillet E, Jones IM. 1995. The glycosylation of human immunodeficiency virus type 1 transmembrane glycoprotein (gp41) is important for the efficient intracellular transport of the envelope precursor gp160. J Gen Virol 76 (Pt 6):1509-14.
61. Bryant M, Ratner L. 1990. Myristoylation-dependent replication and assembly of human immunodeficiency virus 1. Proc Natl Acad Sci U S A 87:523-7.
62. Göttlinger HG, Sodroski JG, Haseltine WA. 1989. Role of capsid precursor processing and myristoylation in morphogenesis and infectivity of human immunodeficiency virus type 1. Proceedings of the National Academy of Sciences of the United States of America 86:5781-5785.

63. Zhou W, Parent LJ, Wills JW, Resh MD. 1994. Identification of a membrane-binding domain within the amino-terminal region of human immunodeficiency virus type 1 Gag protein which interacts with acidic phospholipids. Journal of virology 68:2556-2569.
64. Sundquist WI, Krausslich HG. 2012. HIV-1 assembly, budding, and maturation. Cold Spring Harb Perspect Med 2:a006924.
65. Pettit SC, Moody MD, Wehbie RS, Kaplan AH, Nantermet PV, Klein CA, Swanstrom R. 1994. The p2 domain of human immunodeficiency virus type 1 Gag regulates sequential proteolytic processing and is required to produce fully infectious virions. Journal of Virology 68:8017-8027.
66. Briggs JAG, Riches JD, Glass B, Bartonova V, Zanetti G, Kräusslich H-G. 2009. Structure and assembly of immature HIV. Proceedings of the National Academy of Sciences 106:11090-11095.
67. Briggs JAG, Simon MN, Gross I, Kräusslich H-G, Fuller SD, Vogt VM, Johnson MC. 2004. The stoichiometry of Gag protein in HIV-1. Nature Structural &Amp; Molecular Biology 11:672.
68. Wright ER, Schooler JB, Ding HJ, Kieffer C, Fillmore C, Sundquist WI, Jensen GJ. 2007. Electron cryotomography of immature HIV-1 virions reveals the structure of the CA and SP1 Gag shells. The EMBO Journal 26:2218-2226.
69. Briggs JAG, Wilk T, Welker R, Kräusslich H-G, Fuller SD. 2003. Structural organization of authentic, mature HIV-1 virions and cores. The EMBO Journal 22:1707-1715.
70. Ganser BK, Li S, Klishko VY, Finch JT, Sundquist WI. 1999. Assembly and Analysis of Conical Models for the HIV-1 Core. Science 283:80-83.
71. Li S, Hill CP, Sundquist WI, Finch JT. 2000. Image reconstructions of helical assemblies of the HIV-1 CA protein. Nature 407:409.
72. Pornillos O, Ganser-Pornillos BK, Kelly BN, Hua Y, Whitby FG, Stout CD, Sundquist WI, Hill CP, Yeager M. 2009. X-Ray Structures of the Hexameric Building Block of the HIV Capsid. Cell 137:1282-1292.
73. Pornillos O, Ganser-Pornillos BK, Yeager M. 2011. Atomic-level modelling of the HIV capsid. Nature 469:424.
74. Benjamin J, Ganser-Pornillos BK, Tivol WF, Sundquist WI, Jensen GJ. 2005. Three-dimensional Structure of HIV-1 Virus-like Particles by Electron Cryotomography. Journal of Molecular Biology 346:577-588.
75. Bharat TAM, Davey NE, Ulbrich P, Riches JD, de Marco A, Rumlova M, Sachse C, Ruml T, Briggs JAG. 2012. Structure of the immature retroviral capsid at 8 Å resolution by cryo-electron microscopy. Nature 487:385.
76. Briggs JA, Krausslich HG. 2011. The molecular architecture of HIV. J Mol Biol 410:491-500.
77. de Marco A, Müller B, Glass B, Riches JD, Kräusslich H-G, Briggs JAG. 2010. Structural Analysis of HIV-1 Maturation Using Cryo-Electron Tomography. PLOS Pathogens 6:e1001215.
78. Keller PW, Adamson CS, Heymann JB, Freed EO, Steven AC. 2011. HIV-1 Maturation Inhibitor Bevirimat Stabilizes the Immature Gag Lattice. Journal of Virology 85:1420-1428.

79. Keller PW, Huang RK, England MR, Waki K, Cheng N, Heymann JB, Craven RC, Freed EO, Steven AC. 2013. A Two-Pronged Structural Analysis of Retroviral Maturation Indicates that Core Formation Proceeds by a Disassembly-Reassembly Pathway Rather than a Displacive Transition. Journal of Virology 87:13655-13664.
80. Woodward CL, Cheng SN, Jensen GJ. 2015. Electron Cryotomography Studies of Maturing HIV-1 Particles Reveal the Assembly Pathway of the Viral Core. Journal of Virology 89:1267-1277.
81. Frank GA, Narayan K, Bess Jr JW, Del Prete GQ, Wu X, Moran A, Hartnell LM, Earl LA, Lifson JD, Subramaniam S. 2015. Maturation of the HIV-1 core by a non-diffusional phase transition. Nature Communications 6:5854.
82. Meng X, Zhao G, Yufenyuy E, Ke D, Ning J, DeLucia M, Ahn J, Gronenborn AM, Aiken C, Zhang P. 2012. Protease Cleavage Leads to Formation of Mature Trimer Interface in HIV-1 Capsid. PLOS Pathogens 8:e1002886.
83. Ning J, Erdemci-Tandogan G, Yufenyuy EL, Wagner J, Himes BA, Zhao G, Aiken C, Zandi R, Zhang P. 2016. In vitro protease cleavage and computer simulations reveal the HIV-1 capsid maturation pathway. Nature Communications 7:13689.
84. Gamble TR, Yoo S, Vajdos FF, von Schwedler UK, Worthylake DK, Wang H, McCutcheon JP, Sundquist WI, Hill CP. 1997. Structure of the Carboxyl-Terminal Dimerization Domain of the HIV-1 Capsid Protein. Science 278:849-853.
85. Ganser-Pornillos BK, Cheng A, Yeager M. 2007. Structure of Full-Length HIV-1 CA: A Model for the Mature Capsid Lattice. Cell 131:70-79.
86. Byeon I-JL, Meng X, Jung J, Zhao G, Yang R, Ahn J, Shi J, Concel J, Aiken C, Zhang P, Gronenborn AM. 2009. Structural Convergence between CryoEM and NMR Reveals Novel Intersubunit Interactions Critical for HIV-1 Capsid Function. Cell 139:780-790.
87. Lanman J, Lam TT, Barnes S, Sakalian M, Emmett MR, Marshall AG, Prevelige PE. 2003. Identification of Novel Interactions in HIV-1 Capsid Protein Assembly by High-resolution Mass Spectrometry. Journal of Molecular Biology 325:759-772.
88. Lanman J, Sexton J, Sakalian M, Prevelige JPE. 2002. Kinetic Analysis of the Role of Intersubunit Interactions in Human Immunodeficiency Virus Type 1 Capsid Protein Assembly In Vitro. Journal of Virology 76:6900-6908.
89. Yufenyuy EL, Aiken C. 2013. The NTD-CTD intersubunit interface plays a critical role in assembly and stabilization of the HIV-1 capsid. Retrovirology 10:29-29.
90. Worthylake DK, Wang H, Yoo S, Sundquist WI, Hill CP. 1999. Structures of the HIV-1 capsid protein dimerization domain at 2.6 A resolution. Acta Crystallographica Section D 55:85-92.
91. Ganser-Pornillos BK, von Schwedler UK, Stray KM, Aiken C, Sundquist WI. 2004. Assembly properties of the human immunodeficiency virus type 1 CA protein. J Virol 78:2545-52.
92. Dharan A, Opp S, Abdel-Rahim O, Keceli SK, Imam S, Diaz-Griffero F, Campbell EM. 2017. Bicaudal D2 facilitates the cytoplasmic trafficking and nuclear import of HIV-1 genomes during infection. Proc Natl Acad Sci U S A 114:E10707-e10716.
93. Jayappa KD, Ao Z, Wang X, Mouland AJ, Shekhar S, Yang X, Yao X. 2015. Human immunodeficiency virus type 1 employs the cellular dynein light chain 1 protein for

reverse transcription through interaction with its integrase protein. Journal of virology 89:3497-3511.
94. Lukic Z, Dharan A, Fricke T, Diaz-Griffero F, Campbell EM. 2014. HIV-1 uncoating is facilitated by dynein and kinesin 1. J Virol 88:13613-25.
95. Malikov V, da Silva ES, Jovasevic V, Bennett G, de Souza Aranha Vieira DA, Schulte B, Diaz-Griffero F, Walsh D, Naghavi MH. 2015. HIV-1 capsids bind and exploit the kinesin-1 adaptor FEZ1 for inward movement to the nucleus. Nat Commun 6:6660.
96. Pawlica P, Berthoux L. 2014. Cytoplasmic dynein promotes HIV-1 uncoating. Viruses 6:4195-4211.
97. Katz RA, Greger JG, Skalka AM. 2005. Effects of cell cycle status on early events in retroviral replication. J Cell Biochem 94:880-9.
98. Weinberg JB, Matthews TJ, Cullen BR, Malim MH. 1991. Productive human immunodeficiency virus type 1 (HIV-1) infection of nonproliferating human monocytes. The Journal of Experimental Medicine 174:1477-1482.
99. Zhang Z, Schuler T, Zupancic M, Wietgrefe S, Staskus KA, Reimann KA, Reinhart TA, Rogan M, Cavert W, Miller CJ, Veazey RS, Notermans D, Little S, Danner SA, Richman DD, Havlir D, Wong J, Jordan HL, Schacker TW, Racz P, Tenner-Racz K, Letvin NL, Wolinsky S, Haase AT. 1999. Sexual transmission and propagation of SIV and HIV in resting and activated CD4+ T cells. Science 286:1353-7.
100. Yamashita M, Emerman M. 2005. The cell cycle independence of HIV infections is not determined by known karyophilic viral elements. PLoS Pathog 1:e18.
101. Yamashita M, Emerman M. 2006. Retroviral infection of non-dividing cells: old and new perspectives. Virology 344:88-93.
102. Yamashita M, Perez O, Hope TJ, Emerman M. 2007. Evidence for Direct Involvement of the Capsid Protein in HIV Infection of Nondividing Cells. PLOS Pathogens 3:e156.
103. Brass AL, Dykxhoorn DM, Benita Y, Yan N, Engelman A, Xavier RJ, Lieberman J, Elledge SJ. 2008. Identification of host proteins required for HIV infection through a functional genomic screen. Science 319:921-6.
104. Matreyek KA, Engelman A. 2011. The requirement for nucleoporin NUP153 during human immunodeficiency virus type 1 infection is determined by the viral capsid. J Virol 85:7818-27.
105. Matreyek KA, Yücel SS, Li X, Engelman A. 2013. Nucleoporin NUP153 Phenylalanine-Glycine Motifs Engage a Common Binding Pocket within the HIV-1 Capsid Protein to Mediate Lentiviral Infectivity. PLOS Pathogens 9:e1003693.
106. De Iaco A, Luban J. 2011. Inhibition of HIV-1 infection by TNPO3 depletion is determined by capsid and detectable after viral cDNA enters the nucleus. Retrovirology 8:98.
107. De Iaco A, Santoni F, Vannier A, Guipponi M, Antonarakis S, Luban J. 2013. TNPO3 protects HIV-1 replication from CPSF6-mediated capsid stabilization in the host cell cytoplasm. Retrovirology 10:20.
108. Shah VB, Shi J, Hout DR, Oztop I, Krishnan L, Ahn J, Shotwell MS, Engelman A, Aiken C. 2013. The Host Proteins Transportin SR2/TNPO3 and Cyclophilin A Exert Opposing Effects on HIV-1 Uncoating. Journal of Virology 87:422-432.

109. Thys W, De Houwer S, Demeulemeester J, Taltynov O, Vancraenenbroeck R, Gerard M, De Rijck J, Gijsbers R, Christ F, Debyser Z. 2011. Interplay between HIV entry and transportin-SR2 dependency. Retrovirology 8:7.
110. Zhou L, Sokolskaja E, Jolly C, James W, Cowley SA, Fassati A. 2011. Transportin 3 promotes a nuclear maturation step required for efficient HIV-1 integration. PLoS Pathog 7:e1002194.
111. Fricke T, Valle-Casuso JC, White TE, Brandariz-Nunez A, Bosche WJ, Reszka N, Gorelick R, Diaz-Griffero F. 2013. The ability of TNPO3-depleted cells to inhibit HIV-1 infection requires CPSF6. Retrovirology 10:46.
112. Henning MS, Dubose BN, Burse MJ, Aiken C, Yamashita M. 2014. In vivo functions of CPSF6 for HIV-1 as revealed by HIV-1 capsid evolution in HLA-B27-positive subjects. PLoS Pathog 10:e1003868.
113. Saito A, Henning MS, Serrao E, Dubose BN, Teng S, Huang J, Li X, Saito N, Roy SP, Siddiqui MA, Ahn J, Tsuji M, Hatziioannou T, Engelman AN, Yamashita M. 2016. Capsid-CPSF6 Interaction Is Dispensable for HIV-1 Replication in Primary Cells but Is Selected during Virus Passage In Vivo. J Virol 90:6918-6935.
114. Aiken C. 1997. Pseudotyping human immunodeficiency virus type 1 (HIV-1) by the glycoprotein of vesicular stomatitis virus targets HIV-1 entry to an endocytic pathway and suppresses both the requirement for Nef and the sensitivity to cyclosporin A. J Virol 71:5871-7.
115. Sowd GA, Serrao E, Wang H, Wang W, Fadel HJ, Poeschla EM, Engelman AN. 2016. A critical role for alternative polyadenylation factor CPSF6 in targeting HIV-1 integration to transcriptionally active chromatin. Proc Natl Acad Sci U S A 113:E1054-63.
116. Bosco DA, Eisenmesser EZ, Pochapsky S, Sundquist WI, Kern D. 2002. Catalysis of cis/trans isomerization in native HIV-1 capsid by human cyclophilin A. Proceedings of the National Academy of Sciences 99:5247-5252.
117. Vajdos FF, Yoo S, Houseweart M, Sundquist WI, Hill CP. 1997. Crystal structure of cyclophilin A complexed with a binding site peptide from the HIV-1 capsid protein. Protein Sci 6:2297-307.
118. Wang P, Heitman J. 2005. The cyclophilins. Genome Biology 6:226.
119. Luban J, Bossolt KL, Franke EK, Kalpana GV, Goff SP. 1993. Human immunodeficiency virus type 1 Gag protein binds to cyclophilins A and B. Cell 73:1067-78.
120. Braaten D, Ansari H, Luban J. 1997. The hydrophobic pocket of cyclophilin is the binding site for the human immunodeficiency virus type 1 Gag polyprotein. J Virol 71:2107-13.
121. Braaten D, Franke EK, Luban J. 1996. Cyclophilin A is required for an early step in the life cycle of human immunodeficiency virus type 1 before the initiation of reverse transcription. Journal of Virology 70:3551-3560.
122. Henning MS, Dubose BN, Burse MJ, Aiken C, Yamashita M. 2014. In Vivo Functions of CPSF6 for HIV-1 as Revealed by HIV-1 Capsid Evolution in HLA-B27-Positive Subjects. PLOS Pathogens 10:e1003868.
123. Franke EK, Luban J. 1996. Inhibition of HIV-1 replication by cyclosporine A or related compounds correlates with the ability to disrupt the Gag-cyclophilin A interaction. Virology 222:279-82.

124. Liu C, Perilla JR, Ning J, Lu M, Hou G, Ramalho R, Himes BA, Zhao G, Bedwell GJ, Byeon IJ, Ahn J, Gronenborn AM, Prevelige PE, Rousso I, Aiken C, Polenova T, Schulten K, Zhang P. 2016. Cyclophilin A stabilizes the HIV-1 capsid through a novel non-canonical binding site. Nat Commun 7:10714.
125. Braaten D, Franke EK, Luban J. 1996. Cyclophilin A is required for the replication of group M human immunodeficiency virus type 1 (HIV-1) and simian immunodeficiency virus SIV(CPZ)GAB but not group O HIV-1 or other primate immunodeficiency viruses. J Virol 70:4220-7.
126. Li Y, Kar AK, Sodroski J. 2009. Target cell type-dependent modulation of human immunodeficiency virus type 1 capsid disassembly by cyclophilin A. Journal of virology 83:10951-10962.
127. Yin L, Braaten D, Luban J. 1998. Human immunodeficiency virus type 1 replication is modulated by host cyclophilin A expression levels. Journal of virology 72:6430-6436.
128. Lin T-Y, Emerman M. 2008. Determinants of cyclophilin A-dependent TRIM5 alpha restriction against HIV-1. Virology 379:335-341.
129. Stremlau M, Song B, Javanbakht H, Perron M, Sodroski J. 2006. Cyclophilin A: An auxiliary but not necessary cofactor for TRIM5α restriction of HIV-1. Virology 351:112-120.
130. Cimarelli A, Luban J. 1999. Translation elongation factor 1-alpha interacts specifically with the human immunodeficiency virus type 1 Gag polyprotein. J Virol 73:5388-401.
131. Warren K, Wei T, Li D, Qin F, Warrilow D, Lin M-H, Sivakumaran H, Apolloni A, Abbott CM, Jones A, Anderson JL, Harrich D. 2012. Eukaryotic elongation factor 1 complex subunits are critical HIV-1 reverse transcription cofactors. Proceedings of the National Academy of Sciences 109:9587-9592.
132. Li D, Wei T, Rawle DJ, Qin F, Wang R, Soares DC, Jin H, Sivakumaran H, Lin M-H, Spann K, Abbott CM, Harrich D. 2015. Specific Interaction between eEF1A and HIV RT Is Critical for HIV-1 Reverse Transcription and a Potential Anti-HIV Target. PLOS Pathogens 11:e1005289.
133. Li D, Wei T, Jin H, Rose A, Wang R, Lin M-H, Spann K, Harrich D. 2015. Binding of the eukaryotic translation elongation factor 1A with the 5'UTR of HIV-1 genomic RNA is important for reverse transcription. Virology journal 12:118-118.
134. Rawle DJ, Li D, Swedberg JE, Wang L, Soares DC, Harrich D. 2018. HIV-1 Uncoating and Reverse Transcription Require eEF1A Binding to Surface-Exposed Acidic Residues of the Reverse Transcriptase Thumb Domain. MBio 9.
135. Malim MH, Bieniasz PD. 2012. HIV Restriction Factors and Mechanisms of Evasion. Cold Spring Harbor perspectives in medicine 2:a006940-a006940.
136. Lascano J, Uchil PD, Mothes W, Luban J. 2016. TRIM5 Retroviral Restriction Activity Correlates with the Ability To Induce Innate Immune Signaling. Journal of Virology 90:308-316.
137. Pertel T, Hausmann S, Morger D, Zuger S, Guerra J, Lascano J, Reinhard C, Santoni FA, Uchil PD, Chatel L, Bisiaux A, Albert ML, Strambio-De-Castillia C, Mothes W, Pizzato M, Grutter MG, Luban J. 2011. TRIM5 is an innate immune sensor for the retrovirus capsid lattice. Nature 472:361-5.

138. Stremlau M, Owens CM, Perron MJ, Kiessling M, Autissier P, Sodroski J. 2004. The cytoplasmic body component TRIM5alpha restricts HIV-1 infection in Old World monkeys. Nature 427:848-53.
139. Stremlau M, Perron M, Lee M, Li Y, Song B, Javanbakht H, Diaz-Griffero F, Anderson DJ, Sundquist WI, Sodroski J. 2006. Specific recognition and accelerated uncoating of retroviral capsids by the TRIM5α restriction factor. Proceedings of the National Academy of Sciences 103:5514-5519.
140. Wu X, Anderson JL, Campbell EM, Joseph AM, Hope TJ. 2006. Proteasome inhibitors uncouple rhesus TRIM5alpha restriction of HIV-1 reverse transcription and infection. Proceedings of the National Academy of Sciences of the United States of America 103:7465-7470.
141. Anderson JL, Campbell EM, Wu X, Vandegraaff N, Engelman A, Hope TJ. 2006. Proteasome inhibition reveals that a functional preintegration complex intermediate can be generated during restriction by diverse TRIM5 proteins. Journal of virology 80:9754-9760.
142. Dietrich EA, Jones-Engel L, Hu S-L. 2010. Evolution of the Antiretroviral Restriction Factor TRIMCyp in Old World Primates. PLOS ONE 5:e14019.
143. Wilson SJ, Webb BLJ, Ylinen LMJ, Verschoor E, Heeney JL, Towers GJ. 2008. Independent evolution of an antiviral TRIMCyp in rhesus macaques. Proceedings of the National Academy of Sciences 105:3557-3562.
144. Busnadiego I, Kane M, Rihn SJ, Preugschas HF, Hughes J, Blanco-Melo D, Strouvelle VP, Zang TM, Willett BJ, Boutell C, Bieniasz PD, Wilson SJ. 2014. Host and Viral Determinants of Mx2 Antiretroviral Activity. Journal of Virology 88:7738-7752.
145. Fricke T, White TE, Schulte B, de Souza Aranha Vieira DA, Dharan A, Campbell EM, Brandariz-Nuñez A, Diaz-Griffero F. 2014. MxB binds to the HIV-1 core and prevents the uncoating process of HIV-1. Retrovirology 11:68.
146. Goujon C, Moncorge O, Bauby H, Doyle T, Ward CC, Schaller T, Hue S, Barclay WS, Schulz R, Malim MH. 2013. Human MX2 is an interferon-induced post-entry inhibitor of HIV-1 infection. Nature 502:559-62.
147. Kane M, Yadav SS, Bitzegeio J, Kutluay SB, Zang T, Wilson SJ, Schoggins JW, Rice CM, Yamashita M, Hatziioannou T, Bieniasz PD. 2013. MX2 is an interferon-induced inhibitor of HIV-1 infection. Nature 502:563-6.
148. King MC, Raposo G, Lemmon MA. 2004. Inhibition of nuclear import and cell-cycle progression by mutated forms of the dynamin-like GTPase MxB. Proc Natl Acad Sci U S A 101:8957-62.
149. Liu Z, Pan Q, Ding S, Qian J, Xu F, Zhou J, Cen S, Guo F, Liang C. 2013. The interferon-inducible MxB protein inhibits HIV-1 infection. Cell Host Microbe 14:398-410.
150. Lee S-K, Harris J, Swanstrom R. 2009. A Strongly Transdominant Mutation in the Human Immunodeficiency Virus Type 1 gag Gene Defines an Achilles Heel in the Virus Life Cycle. Journal of Virology 83:8536-8543.
151. Anderson-Daniels J, Singh PK, Sowd GA, Li W, Engelman AN, Aiken C. 2019. Dominant negative MA-CA fusion protein is incorporated into HIV-1 cores and inhibits nuclear entry of viral preintegration complexes. J Virol doi:10.1128/jvi.01118-19.

152. McQuade T, Tomasselli A, Liu L, Karacostas V, Moss B, Sawyer T, Heinrikson R, Tarpley W. 1990. A synthetic HIV-1 protease inhibitor with antiviral activity arrests HIV-like particle maturation. Science 247:454-456.
153. Lee S-K, Potempa M, Kolli M, Özen A, Schiffer CA, Swanstrom R. 2012. Context Surrounding Processing Sites Is Crucial in Determining Cleavage Rate of a Subset of Processing Sites in HIV-1 Gag and Gag-Pro-Pol Polyprotein Precursors by Viral Protease. The Journal of Biological Chemistry 287:13279-13290.
154. Kräusslich HG, Ingraham RH, Skoog MT, Wimmer E, Pallai PV, Carter CA. 1989. Activity of purified biosynthetic proteinase of human immunodeficiency virus on natural substrates and synthetic peptides. Proceedings of the National Academy of Sciences of the United States of America 86:807-811.
155. von Schwedler UK, Stemmler TL, Klishko VY, Li S, Albertine KH, Davis DR, Sundquist WI. 1998. Proteolytic refolding of the HIV-1 capsid protein amino-terminus facilitates viral core assembly. The EMBO Journal 17:1555-1568.
156. Anderson J, Schiffer C, Lee S-K, Swanstrom R. 2009. Viral Protease Inhibitors, p 85-110. *In* Kräusslich H-G, Bartenschlager R (ed), Antiviral Strategies doi:10.1007/978-3-540-79086-0_4. Springer Berlin Heidelberg, Berlin, Heidelberg.
157. Kaplan AH, Zack JA, Knigge M, Paul DA, Kempf DJ, Norbeck DW, Swanstrom R. 1993. Partial inhibition of the human immunodeficiency virus type 1 protease results in aberrant virus assembly and the formation of noninfectious particles. Journal of Virology 67:4050-4055.
158. Blair WS, Cao J, Fok-Seang J, Griffin P, Isaacson J, Jackson RL, Murray E, Patick AK, Peng Q, Perros M, Pickford C, Wu H, Butler SL. 2009. New Small-Molecule Inhibitor Class Targeting Human Immunodeficiency Virus Type 1 Virion Maturation. Antimicrobial Agents and Chemotherapy 53:5080-5087.
159. Li F, Goila-Gaur R, Salzwedel K, Kilgore NR, Reddick M, Matallana C, Castillo A, Zoumplis D, Martin DE, Orenstein JM, Allaway GP, Freed EO, Wild CT. 2003. PA-457: A potent HIV inhibitor that disrupts core condensation by targeting a late step in Gag processing. Proceedings of the National Academy of Sciences 100:13555-13560.
160. Zhou J, Yuan X, Dismuke D, Forshey BM, Lundquist C, Lee K-H, Aiken C, Chen CH. 2004. Small-Molecule Inhibition of Human Immunodeficiency Virus Type 1 Replication by Specific Targeting of the Final Step of Virion Maturation. Journal of Virology 78:922-929.
161. Balakrishnan M, Yant SR, Tsai L, O'Sullivan C, Bam RA, Tsai A, Niedziela-Majka A, Stray KM, Sakowicz R, Cihlar T. 2013. Non-catalytic site HIV-1 integrase inhibitors disrupt core maturation and induce a reverse transcription block in target cells. PLoS One 8:e74163.
162. Desimmie BA, Schrijvers R, Demeulemeester J, Borrenberghs D, Weydert C, Thys W, Vets S, Van Remoortel B, Hofkens J, De Rijck J, Hendrix J, Bannert N, Gijsbers R, Christ F, Debyser Z. 2013. LEDGINs inhibit late stage HIV-1 replication by modulating integrase multimerization in the virions. Retrovirology 10:57.
163. Engelman A. 1999. In vivo analysis of retroviral integrase structure and function. Adv Virus Res 52:411-26.
164. Fontana J, Jurado KA, Cheng N, Ly NL, Fuchs JR, Gorelick RJ, Engelman AN, Steven AC. 2015. Distribution and Redistribution of HIV-1 Nucleocapsid Protein in Immature,

Mature, and Integrase-Inhibited Virions: a Role for Integrase in Maturation. J Virol 89:9765-80.
165. Jurado KA, Wang H, Slaughter A, Feng L, Kessl JJ, Koh Y, Wang W, Ballandras-Colas A, Patel PA, Fuchs JR, Kvaratskhelia M, Engelman A. 2013. Allosteric integrase inhibitor potency is determined through the inhibition of HIV-1 particle maturation. Proc Natl Acad Sci U S A 110:8690-5.
166. Kessl JJ, Kutluay SB, Townsend D, Rebensburg S, Slaughter A, Larue RC, Shkriabai N, Bakouche N, Fuchs JR, Bieniasz PD, Kvaratskhelia M. 2016. HIV-1 Integrase Binds the Viral RNA Genome and Is Essential during Virion Morphogenesis. Cell 166:1257-1268.e12.
167. Le Rouzic E, Bonnard D, Chasset S, Bruneau JM, Chevreuil F, Le Strat F, Nguyen J, Beauvoir R, Amadori C, Brias J, Vomscheid S, Eiler S, Levy N, Delelis O, Deprez E, Saib A, Zamborlini A, Emiliani S, Ruff M, Ledoussal B, Moreau F, Benarous R. 2013. Dual inhibition of HIV-1 replication by integrase-LEDGF allosteric inhibitors is predominant at the post-integration stage. Retrovirology 10:144.
168. Sharma A, Slaughter A, Jena N, Feng L, Kessl JJ, Fadel HJ, Malani N, Male F, Wu L, Poeschla E, Bushman FD, Fuchs JR, Kvaratskhelia M. 2014. A new class of multimerization selective inhibitors of HIV-1 integrase. PLoS Pathog 10:e1004171.
169. Oshima M, Muriaux D, Mirro J, Nagashima K, Dryden K, Yeager M, Rein A. 2004. Effects of Blocking Individual Maturation Cleavages in Murine Leukemia Virus Gag. Journal of Virology 78:1411-1420.
170. Rulli SJ, Jr., Muriaux D, Nagashima K, Mirro J, Oshima M, Baumann JG, Rein A. 2006. Mutant murine leukemia virus Gag proteins lacking proline at the N-terminus of the capsid domain block infectivity in virions containing wild-type Gag. Virology 347:364-71.
171. Checkley MA, Luttge BG, Soheilian F, Nagashima K, Freed EO. 2010. The capsid-spacer peptide 1 Gag processing intermediate is a dominant-negative inhibitor of HIV-1 maturation. Virology 400:137-144.
172. Müller B, Anders M, Akiyama H, Welsch S, Glass B, Nikovics K, Clavel F, Tervo H-M, Keppler OT, Kräusslich H-G. 2009. HIV-1 Gag Processing Intermediates Trans-dominantly Interfere with HIV-1 Infectivity. The Journal of Biological Chemistry 284:29692-29703.
173. Trono D, Feinberg MB, Baltimore D. 1989. HIV-1 Gag mutants can dominantly interfere with the replication of the wild-type virus. Cell 59:113-120.
174. Pornillos O, Ganser-Pornillos BK, Banumathi S, Hua Y, Yeager M. 2010. Disulfide Bond Stabilization of the Hexameric Capsomer of Human Immunodeficiency Virus. Journal of Molecular Biology 401:985-995.
175. Zhao G, Perilla JR, Yufenyuy EL, Meng X, Chen B, Ning J, Ahn J, Gronenborn AM, Schulten K, Aiken C, Zhang P. 2013. Mature HIV-1 capsid structure by cryo-electron microscopy and all-atom molecular dynamics. Nature 497:643.
176. Forshey BM, von Schwedler U, Sundquist WI, Aiken C. 2002. Formation of a human immunodeficiency virus type 1 core of optimal stability is crucial for viral replication. J Virol 76:5667-77.
177. Shah VB, Aiken C. 2011. In vitro uncoating of HIV-1 cores. Journal of visualized experiments : JoVE doi:10.3791/3384:3384.

178. Wyma DJ, Kotov A, Aiken C. 2000. Evidence for a stable interaction of gp41 with Pr55(Gag) in immature human immunodeficiency virus type 1 particles. Journal of virology 74:9381-9387.
179. Nisole S, Lynch C, Stoye JP, Yap MW. 2004. A Trim5-cyclophilin A fusion protein found in owl monkey kidney cells can restrict HIV-1. Proceedings of the National Academy of Sciences of the United States of America 101:13324-13328.
180. Sayah DM, Sokolskaja E, Berthoux L, Luban J. 2004. Cyclophilin A retrotransposition into TRIM5 explains owl monkey resistance to HIV-1. Nature 430:569.
181. Cowan S, Hatziioannou T, Cunningham T, Muesing MA, Gottlinger HG, Bieniasz PD. 2002. Cellular inhibitors with Fv1-like activity restrict human and simian immunodeficiency virus tropism. Proceedings of the National Academy of Sciences 99:11914-11919.
182. Forshey BM, Shi J, Aiken C. 2005. Structural Requirements for Recognition of the Human Immunodeficiency Virus Type 1 Core during Host Restriction in Owl Monkey Cells. Journal of Virology 79:869-875.
183. Hatziioannou T, Cowan S, Goff SP, Bieniasz PD, Towers GJ. 2003. Restriction of multiple divergent retroviruses by Lv1 and Ref1. The EMBO Journal 22:385-394.
184. Towers GJ, Hatziioannou T, Cowan S, Goff SP, Luban J, Bieniasz PD. 2003. Cyclophilin A modulates the sensitivity of HIV-1 to host restriction factors. Nature Medicine 9:1138.
185. Shi J, Aiken C. 2006. Saturation of TRIM5α-mediated restriction of HIV-1 infection depends on the stability of the incoming viral capsid. Virology 350:493-500.
186. Aiken C. 1997. Pseudotyping human immunodeficiency virus type 1 (HIV-1) by the glycoprotein of vesicular stomatitis virus targets HIV-1 entry to an endocytic pathway and suppresses both the requirement for Nef and the sensitivity to cyclosporin A. Journal of Virology 71:5871-5877.
187. Wei X, Decker JM, Liu H, Zhang Z, Arani RB, Kilby JM, Saag MS, Wu X, Shaw GM, Kappes JC. 2002. Emergence of Resistant Human Immunodeficiency Virus Type 1 in Patients Receiving Fusion Inhibitor (T-20) Monotherapy. Antimicrobial Agents and Chemotherapy 46:1896-1905.
188. Koh Y, Wu X, Ferris AL, Matreyek KA, Smith SJ, Lee K, KewalRamani VN, Hughes SH, Engelman A. 2013. Differential Effects of Human Immunodeficiency Virus Type 1 Capsid and Cellular Factors Nucleoporin 153 and LEDGF/p75 on the Efficiency and Specificity of Viral DNA Integration. Journal of Virology 87:648-658.
189. Matreyek KA, Wang W, Serrao E, Singh PK, Levin HL, Engelman A. 2014. Host and viral determinants for MxB restriction of HIV-1 infection. Retrovirology 11:90.
190. Ocwieja KE, Brady TL, Ronen K, Huegel A, Roth SL, Schaller T, James LC, Towers GJ, Young JAT, Chanda SK, König R, Malani N, Berry CC, Bushman FD. 2011. HIV Integration Targeting: A Pathway Involving Transportin-3 and the Nuclear Pore Protein RanBP2. PLOS Pathogens 7:e1001313.
191. Saito A, Ferhadian D, Sowd GA, Serrao E, Shi J, Halambage UD, Teng S, Soto J, Siddiqui MA, Engelman AN, Aiken C, Yamashita M. 2016. Roles of Capsid-Interacting Host Factors in Multimodal Inhibition of HIV-1 by PF74. J Virol 90:5808-5823.
192. Serrao E, Cherepanov P, Engelman AN. 2016. Amplification, Next-generation Sequencing, and Genomic DNA Mapping of Retroviral Integration Sites. Journal of visualized experiments : JoVE doi:10.3791/53840:53840.

193. Charneau P, Alizon M, Clavel F. 1992. A second origin of DNA plus-strand synthesis is required for optimal human immunodeficiency virus replication. J Virol 66:2814-20.
194. Reil H, Bukovsky AA, Gelderblom HR, Göttlinger HG. 1998. Efficient HIV-1 replication can occur in the absence of the viral matrix protein. The EMBO Journal 17:2699-2708.
195. Bandyopadhyay PK, Watanabe S, Temin HM. 1984. Recombination of transfected DNAs in vertebrate cells in culture. Proc Natl Acad Sci U S A 81:3476-80.
196. Wiegers K, Rutter G, Kottler H, Tessmer U, Hohenberg H, Kräusslich H-G. 1998. Sequential Steps in Human Immunodeficiency Virus Particle Maturation Revealed by Alterations of Individual Gag Polyprotein Cleavage Sites. Journal of Virology 72:2846-2854.
197. Fassati A. 2012. Multiple roles of the capsid protein in the early steps of HIV-1 infection. Virus Res 170:15-24.
198. Ambrose Z, Lee K, Ndjomou J, Xu H, Oztop I, Matous J, Takemura T, Unutmaz D, Engelman A, Hughes SH, KewalRamani VN. 2012. Human Immunodeficiency Virus Type 1 Capsid Mutation N74D Alters Cyclophilin A Dependence and Impairs Macrophage Infection. Journal of Virology 86:4708-4714.
199. Xu H, Franks T, Gibson G, Huber K, Rahm N, Strambio De Castillia C, Luban J, Aiken C, Watkins S, Sluis-Cremer N, Ambrose Z. 2013. Evidence for biphasic uncoating during HIV-1 infection from a novel imaging assay. Retrovirology 10:70-70.
200. Di Nunzio F, Fricke T, Miccio A, Valle-Casuso JC, Perez P, Souque P, Rizzi E, Severgnini M, Mavilio F, Charneau P, Diaz-Griffero F. 2013. Nup153 and Nup98 bind the HIV-1 core and contribute to the early steps of HIV-1 replication. Virology 440:8-18.
201. Zhang R, Mehla R, Chauhan A. 2010. Perturbation of host nuclear membrane component RanBP2 impairs the nuclear import of human immunodeficiency virus -1 preintegration complex (DNA). PLoS One 5:e15620.
202. Dicks MDJ, Betancor G, Jimenez-Guardeno JM, Pessel-Vivares L, Apolonia L, Goujon C, Malim MH. 2018. Multiple components of the nuclear pore complex interact with the amino-terminus of MX2 to facilitate HIV-1 restriction. PLoS Pathog 14:e1007408.
203. Koneru PC, Francis AC, Deng N, Rebensburg SV, Hoyte AC, Lindenberger J, Adu-Ampratwum D, Larue RC, Wempe MF, Engelman AN, Lyumkis D, Fuchs JR, Levy RM, Melikyan GB, Kvaratskhelia M. 2019. HIV-1 integrase tetramers are the antiviral target of pyridine-based allosteric integrase inhibitors. Elife 8.
204. Madison MK, Lawson DQ, Elliott J, Ozanturk AN, Koneru PC, Townsend D, Errando M, Kvaratskhelia M, Kutluay SB. 2017. Allosteric HIV-1 Integrase Inhibitors Lead to Premature Degradation of the Viral RNA Genome and Integrase in Target Cells. J Virol 91.
205. Carlson LA, Briggs JA, Glass B, Riches JD, Simon MN, Johnson MC, Muller B, Grunewald K, Krausslich HG. 2008. Three-dimensional analysis of budding sites and released virus suggests a revised model for HIV-1 morphogenesis. Cell Host Microbe 4:592-9.
206. Wang W, Zhou J, Halambage UD, Jurado KA, Jamin AV, Wang Y, Engelman AN, Aiken C. 2017. Inhibition of HIV-1 Maturation via Small Molecule Targeting of the Amino-Terminal Domain in the Viral Capsid Protein. Journal of Virology doi:10.1128/jvi.02155-16.

207. Campbell S, Fisher RJ, Towler EM, Fox S, Issaq HJ, Wolfe T, Phillips LR, Rein A. 2001. Modulation of HIV-like particle assembly in vitro by inositol phosphates. Proceedings of the National Academy of Sciences 98:10875-10879.
208. Datta SAK, Zhao Z, Clark PK, Tarasov S, Alexandratos JN, Campbell SJ, Kvaratskhelia M, Lebowitz J, Rein A. 2007. Interactions between HIV-1 Gag Molecules in Solution: An Inositol Phosphate-mediated Switch. Journal of Molecular Biology 365:799-811.
209. Dick RA, Zadrozny KK, Xu C, Schur FKM, Lyddon TD, Ricana CL, Wagner JM, Perilla JR, Ganser-Pornillos BK, Johnson MC, Pornillos O, Vogt VM. 2018. Inositol phosphates are assembly co-factors for HIV-1. Nature 560:509-512.
210. Mallery DL, Marquez CL, McEwan WA, Dickson CF, Jacques DA, Anandapadamanaban M, Bichel K, Towers GJ, Saiardi A, Bocking T, James LC. 2018. IP6 is an HIV pocket factor that prevents capsid collapse and promotes DNA synthesis. Elife 7.
211. Arfi V, Lienard J, Nguyen X-N, Berger G, Rigal D, Darlix J-L, Cimarelli A. 2009. Characterization of the Behavior of Functional Viral Genomes during the Early Steps of Human Immunodeficiency Virus Type 1 Infection. Journal of Virology 83:7524-7535.
212. Braaten D, Luban J. 2001. Cyclophilin A regulates HIV-1 infectivity, as demonstrated by gene targeting in human T cells. Embo j 20:1300-9.
213. Ptak RG, Gallay PA, Jochmans D, Halestrap AP, Ruegg UT, Pallansch LA, Bobardt MD, de Bethune MP, Neyts J, De Clercq E, Dumont JM, Scalfaro P, Besseghir K, Wenger RM, Rosenwirth B. 2008. Inhibition of human immunodeficiency virus type 1 replication in human cells by Debio-025, a novel cyclophilin binding agent. Antimicrob Agents Chemother 52:1302-17.
214. Rosenwirth B, Billich A, Datema R, Donatsch P, Hammerschmid F, Harrison R, Hiestand P, Jaksche H, Mayer P, Peichl P, et al. 1994. Inhibition of human immunodeficiency virus type 1 replication by SDZ NIM 811, a nonimmunosuppressive cyclosporine analog. Antimicrob Agents Chemother 38:1763-72.
215. Warrilow D, Meredith L, Davis A, Burrell C, Li P, Harrich D. 2008. Cell Factors Stimulate Human Immunodeficiency Virus Type 1 Reverse Transcription In Vitro. Journal of Virology 82:1425-1437.
216. Fassati A, Goff SP. 1999. Characterization of Intracellular Reverse Transcription Complexes of Moloney Murine Leukemia Virus. Journal of Virology 73:8919-8925.
217. Fassati A, Goff SP. 2001. Characterization of intracellular reverse transcription complexes of human immunodeficiency virus type 1. J Virol 75:3626-35.
218. König R, Zhou Y, Elleder D, Diamond TL, Bonamy GMC, Irelan JT, Chiang C-y, Tu BP, De Jesus PD, Lilley CE, Seidel S, Opaluch AM, Caldwell JS, Weitzman MD, Kuhen KL, Bandyopadhyay S, Ideker T, Orth AP, Miraglia LJ, Bushman FD, Young JA, Chanda SK. 2008. Global analysis of host-pathogen interactions that regulate early stage HIV-1 replication. Cell 135:49-60.
219. Lee K, Mulky A, Yuen W, Martin TD, Meyerson NR, Choi L, Yu H, Sawyer SL, Kewalramani VN. 2012. HIV-1 capsid-targeting domain of cleavage and polyadenylation specificity factor 6. J Virol 86:3851-60.
220. Price AJ, Fletcher AJ, Schaller T, Elliott T, Lee K, KewalRamani VN, Chin JW, Towers GJ, James LC. 2012. CPSF6 defines a conserved capsid interface that modulates HIV-1 replication. PLoS Pathog 8:e1002896.

221. Qi M, Yang R, Aiken C. 2008. Cyclophilin A-dependent restriction of human immunodeficiency virus type 1 capsid mutants for infection of nondividing cells. J Virol 82:12001-8.
222. Schaller T, Ylinen LM, Webb BL, Singh S, Towers GJ. 2007. Fusion of cyclophilin A to Fv1 enables cyclosporine-sensitive restriction of human and feline immunodeficiency viruses. J Virol 81:10055-63.
223. Vozzolo L, Loh B, Gane PJ, Tribak M, Zhou L, Anderson I, Nyakatura E, Jenner RG, Selwood D, Fassati A. 2010. Gyrase B inhibitor impairs HIV-1 replication by targeting Hsp90 and the capsid protein. J Biol Chem 285:39314-28.
224. Yamashita M, Emerman M. 2009. Cellular restriction targeting viral capsids perturbs human immunodeficiency virus type 1 infection of nondividing cells. J Virol 83:9835-43.
225. Yap MW, Dodding MP, Stoye JP. 2006. Trim-cyclophilin A fusion proteins can restrict human immunodeficiency virus type 1 infection at two distinct phases in the viral life cycle. J Virol 80:4061-7.
226. Krishnan L, Matreyek KA, Oztop I, Lee K, Tipper CH, Li X, Dar MJ, Kewalramani VN, Engelman A. 2010. The requirement for cellular transportin 3 (TNPO3 or TRN-SR2) during infection maps to human immunodeficiency virus type 1 capsid and not integrase. J Virol 84:397-406.
227. Valle-Casuso JC, Di Nunzio F, Yang Y, Reszka N, Lienlaf M, Arhel N, Perez P, Brass AL, Diaz-Griffero F. 2012. TNPO3 is required for HIV-1 replication after nuclear import but prior to integration and binds the HIV-1 core. J Virol 86:5931-6.
228. Zaitseva L, Cherepanov P, Leyens L, Wilson SJ, Rasaiyaah J, Fassati A. 2009. HIV-1 exploits importin 7 to maximize nuclear import of its DNA genome. Retrovirology 6:11.
229. Blair WS, Pickford C, Irving SL, Brown DG, Anderson M, Bazin R, Cao J, Ciaramella G, Isaacson J, Jackson L, Hunt R, Kjerrstrom A, Nieman JA, Patick AK, Perros M, Scott AD, Whitby K, Wu H, Butler SL. 2010. HIV Capsid is a Tractable Target for Small Molecule Therapeutic Intervention. PLOS Pathogens 6:e1001220.
230. Kelly BN, Kyere S, Kinde I, Tang C, Howard BR, Robinson H, Sundquist WI, Summers MF, Hill CP. 2007. Structure of the Antiviral Assembly Inhibitor CAP-1 Complex with the HIV-1 CA Protein. Journal of Molecular Biology 373:355-366.
231. Lamorte L, Titolo S, Lemke CT, Goudreau N, Mercier J-F, Wardrop E, Shah VB, von Schwedler UK, Langelier C, Banik SSR, Aiken C, Sundquist WI, Mason SW. 2013. Discovery of Novel Small-Molecule HIV-1 Replication Inhibitors That Stabilize Capsid Complexes. Antimicrobial Agents and Chemotherapy 57:4622-4631.
232. Sticht J, Humbert M, Findlow S, Bodem J, Müller B, Dietrich U, Werner J, Kräusslich H-G. 2005. A peptide inhibitor of HIV-1 assembly in vitro. Nature Structural & Molecular Biology 12:671-677.
233. Tang C, Loeliger E, Kinde I, Kyere S, Mayo K, Barklis E, Sun Y, Huang M, Summers MF. 2003. Antiviral Inhibition of the HIV-1 Capsid Protein. Journal of Molecular Biology 327:1013-1020.
234. Zhang H, Zhao Q, Bhattacharya S, Waheed AA, Tong X, Hong A, Heck S, Curreli F, Goger M, Cowburn D, Freed EO, Debnath AK. 2008. A Cell-penetrating Helical Peptide as a Potential HIV-1 Inhibitor. Journal of Molecular Biology 378:565-580.

235. Shi J, Zhou J, Shah VB, Aiken C, Whitby K. 2011. Small-molecule inhibition of human immunodeficiency virus type 1 infection by virus capsid destabilization. J Virol 85:542-9.
236. Peng K, Muranyi W, Glass B, Laketa V, Yant SR, Tsai L, Cihlar T, Muller B, Krausslich HG. 2014. Quantitative microscopy of functional HIV post-entry complexes reveals association of replication with the viral capsid. Elife 3:e04114.
237. Bhattacharya A, Alam SL, Fricke T, Zadrozny K, Sedzicki J, Taylor AB, Demeler B, Pornillos O, Ganser-Pornillos BK, Diaz-Griffero F, Ivanov DN, Yeager M. 2014. Structural basis of HIV-1 capsid recognition by PF74 and CPSF6. Proc Natl Acad Sci U S A 111:18625-30.
238. Price AJ, Jacques DA, McEwan WA, Fletcher AJ, Essig S, Chin JW, Halambage UD, Aiken C, James LC. 2014. Host cofactors and pharmacologic ligands share an essential interface in HIV-1 capsid that is lost upon disassembly. PLoS Pathog 10:e1004459.
239. Fricke T, Buffone C, Opp S, Valle-Casuso J, Diaz-Griffero F. 2014. BI-2 destabilizes HIV-1 cores during infection and Prevents Binding of CPSF6 to the HIV-1 Capsid. Retrovirology 11:120.
240. Zhou J, Price AJ, Halambage UD, James LC, Aiken C. 2015. HIV-1 Resistance to the Capsid-Targeting Inhibitor PF74 Results in Altered Dependence on Host Factors Required for Virus Nuclear Entry. J Virol 89:9068-79.
241. Pornillos O, Ganser-Pornillos BK, Banumathi S, Hua Y, Yeager M. 2010. Disulfide bond stabilization of the hexameric capsomer of human immunodeficiency virus. J Mol Biol 401:985-95.
242. Carvalho MD, Carvalho JF, Merrick WC. 1984. Biological characterization of various forms of elongation factor 1 from rabbit reticulocytes. Arch Biochem Biophys 234:603-11.
243. Pittman YR, Valente L, Jeppesen MG, Andersen GR, Patel S, Kinzy TG. 2006. Mg2+ and a key lysine modulate exchange activity of eukaryotic translation elongation factor 1B alpha. J Biol Chem 281:19457-68.
244. Condeelis J. 1995. Elongation factor 1 alpha, translation and the cytoskeleton. Trends Biochem Sci 20:169-70.
245. Liu G, Tang J, Edmonds BT, Murray J, Levin S, Condeelis J. 1996. F-actin sequesters elongation factor 1alpha from interaction with aminoacyl-tRNA in a pH-dependent reaction. J Cell Biol 135:953-63.
246. Munshi R, Kandl KA, Carr-Schmid A, Whitacre JL, Adams AE, Kinzy TG. 2001. Overexpression of translation elongation factor 1A affects the organization and function of the actin cytoskeleton in yeast. Genetics 157:1425-36.
247. Yang F, Demma M, Warren V, Dharmawardhane S, Condeelis J. 1990. Identification of an actin-binding protein from Dictyostelium as elongation factor 1a. Nature 347:494-6.
248. Durso NA, Cyr RJ. 1994. A calmodulin-sensitive interaction between microtubules and a higher plant homolog of elongation factor-1 alpha. Plant Cell 6:893-905.
249. Moore RC, Durso NA, Cyr RJ. 1998. Elongation factor-1alpha stabilizes microtubules in a calcium/calmodulin-dependent manner. Cell Motil Cytoskeleton 41:168-80.
250. Ohta K, Toriyama M, Miyazaki M, Murofushi H, Hosoda S, Endo S, Sakai H. 1990. The mitotic apparatus-associated 51-kDa protein from sea urchin eggs is a GTP-binding protein and is immunologically related to yeast polypeptide elongation factor 1 alpha. J Biol Chem 265:3240-7.

251. Shiina N, Gotoh Y, Kubomura N, Iwamatsu A, Nishida E. 1994. Microtubule severing by elongation factor 1 alpha. Science 266:282-5.
252. Grosshans H, Hurt E, Simos G. 2000. An aminoacylation-dependent nuclear tRNA export pathway in yeast. Genes Dev 14:830-40.
253. Murthi A, Shaheen HH, Huang HY, Preston MA, Lai TP, Phizicky EM, Hopper AK. 2010. Regulation of tRNA bidirectional nuclear-cytoplasmic trafficking in Saccharomyces cerevisiae. Mol Biol Cell 21:639-49.
254. Chuang SM, Chen L, Lambertson D, Anand M, Kinzy TG, Madura K. 2005. Proteasome-mediated degradation of cotranslationally damaged proteins involves translation elongation factor 1A. Mol Cell Biol 25:403-13.
255. Gonen H, Smith CE, Siegel NR, Kahana C, Merrick WC, Chakraburtty K, Schwartz AL, Ciechanover A. 1994. Protein synthesis elongation factor EF-1 alpha is essential for ubiquitin-dependent degradation of certain N alpha-acetylated proteins and may be substituted for by the bacterial elongation factor EF-Tu. Proc Natl Acad Sci U S A 91:7648-52.
256. Duttaroy A, Bourbeau D, Wang XL, Wang E. 1998. Apoptosis rate can be accelerated or decelerated by overexpression or reduction of the level of elongation factor-1 alpha. Exp Cell Res 238:168-76.
257. Lamberti A, Longo O, Marra M, Tagliaferri P, Bismuto E, Fiengo A, Viscomi C, Budillon A, Rapp UR, Wang E, Venuta S, Abbruzzese A, Arcari P, Caraglia M. 2007. C-Raf antagonizes apoptosis induced by IFN-alpha in human lung cancer cells by phosphorylation and increase of the intracellular content of elongation factor 1A. Cell Death Differ 14:952-62.
258. Ruest LB, Marcotte R, Wang E. 2002. Peptide elongation factor eEF1A-2/S1 expression in cultured differentiated myotubes and its protective effect against caspase-3-mediated apoptosis. J Biol Chem 277:5418-25.
259. Talapatra S, Wagner JD, Thompson CB. 2002. Elongation factor-1 alpha is a selective regulator of growth factor withdrawal and ER stress-induced apoptosis. Cell Death Differ 9:856-61.
260. Blackwell JL, Brinton MA. 1997. Translation elongation factor-1 alpha interacts with the 3' stem-loop region of West Nile virus genomic RNA. J Virol 71:6433-44.
261. Davis WG, Blackwell JL, Shi PY, Brinton MA. 2007. Interaction between the cellular protein eEF1A and the 3'-terminal stem-loop of West Nile virus genomic RNA facilitates viral minus-strand RNA synthesis. J Virol 81:10172-87.
262. Dreher TW, Uhlenbeck OC, Browning KS. 1999. Quantitative assessment of EF-1alpha.GTP binding to aminoacyl-tRNAs, aminoacyl-viral RNA, and tRNA shows close correspondence to the RNA binding properties of EF-Tu. J Biol Chem 274:666-72.
263. Li Z, Pogany J, Tupman S, Esposito AM, Kinzy TG, Nagy PD. 2010. Translation elongation factor 1A facilitates the assembly of the tombusvirus replicase and stimulates minus-strand synthesis. PLoS Pathog 6:e1001175.
264. Matsuda D, Yoshinari S, Dreher TW. 2004. eEF1A binding to aminoacylated viral RNA represses minus strand synthesis by TYMV RNA-dependent RNA polymerase. Virology 321:47-56.

265. Sikora D, Greco-Stewart VS, Miron P, Pelchat M. 2009. The hepatitis delta virus RNA genome interacts with eEF1A1, p54(nrb), hnRNP-L, GAPDH and ASF/SF2. Virology 390:71-8.
266. Harris KS, Xiang W, Alexander L, Lane WS, Paul AV, Wimmer E. 1994. Interaction of poliovirus polypeptide 3CDpro with the 5' and 3' termini of the poliovirus genome. Identification of viral and cellular cofactors needed for efficient binding. J Biol Chem 269:27004-14.
267. Kou YH, Chou SM, Wang YM, Chang YT, Huang SY, Jung MY, Huang YH, Chen MR, Chang MF, Chang SC. 2006. Hepatitis C virus NS4A inhibits cap-dependent and the viral IRES-mediated translation through interacting with eukaryotic elongation factor 1A. J Biomed Sci 13:861-74.
268. Yamaji Y, Kobayashi T, Hamada K, Sakurai K, Yoshii A, Suzuki M, Namba S, Hibi T. 2006. In vivo interaction between Tobacco mosaic virus RNA-dependent RNA polymerase and host translation elongation factor 1A. Virology 347:100-8.
269. Yamaji Y, Sakurai K, Hamada K, Komatsu K, Ozeki J, Yoshida A, Yoshii A, Shimizu T, Namba S, Hibi T. 2010. Significance of eukaryotic translation elongation factor 1A in tobacco mosaic virus infection. Arch Virol 155:263-8.
270. Itagaki K, Naito T, Iwakiri R, Haga M, Miura S, Saito Y, Owaki T, Kamiya S, Iyoda T, Yajima H, Iwashita S, Ejiri S, Fukai F. 2012. Eukaryotic translation elongation factor 1A induces anoikis by triggering cell detachment. J Biol Chem 287:16037-46.
271. Saphire AC, Bobardt MD, Zhang Z, David G, Gallay PA. 2001. Syndecans serve as attachment receptors for human immunodeficiency virus type 1 on macrophages. J Virol 75:9187-200.
272. Arthos J, Cicala C, Martinelli E, Macleod K, Van Ryk D, Wei D, Xiao Z, Veenstra TD, Conrad TP, Lempicki RA, McLaughlin S, Pascuccio M, Gopaul R, McNally J, Cruz CC, Censoplano N, Chung E, Reitano KN, Kottilil S, Goode DJ, Fauci AS. 2008. HIV-1 envelope protein binds to and signals through integrin alpha4beta7, the gut mucosal homing receptor for peripheral T cells. Nat Immunol 9:301-9.
273. Cicala C, Martinelli E, McNally JP, Goode DJ, Gopaul R, Hiatt J, Jelicic K, Kottilil S, Macleod K, O'Shea A, Patel N, Van Ryk D, Wei D, Pascuccio M, Yi L, McKinnon L, Izulla P, Kimani J, Kaul R, Fauci AS, Arthos J. 2009. The integrin alpha4beta7 forms a complex with cell-surface CD4 and defines a T-cell subset that is highly susceptible to infection by HIV-1. Proc Natl Acad Sci U S A 106:20877-82.
274. Geijtenbeek TB, Kwon DS, Torensma R, van Vliet SJ, van Duijnhoven GC, Middel J, Cornelissen IL, Nottet HS, KewalRamani VN, Littman DR, Figdor CG, van Kooyk Y. 2000. DC-SIGN, a dendritic cell-specific HIV-1-binding protein that enhances trans-infection of T cells. Cell 100:587-97.
275. Balasubramanian S, Kannan TR, Baseman JB. 2008. The surface-exposed carboxyl region of Mycoplasma pneumoniae elongation factor Tu interacts with fibronectin. Infect Immun 76:3116-23.
276. Dallo SF, Kannan TR, Blaylock MW, Baseman JB. 2002. Elongation factor Tu and E1 beta subunit of pyruvate dehydrogenase complex act as fibronectin binding proteins in Mycoplasma pneumoniae. Mol Microbiol 46:1041-51.

277. Granato D, Bergonzelli GE, Pridmore RD, Marvin L, Rouvet M, Corthésy-Theulaz IE. 2004. Cell surface-associated elongation factor Tu mediates the attachment of Lactobacillus johnsonii NCC533 (La1) to human intestinal cells and mucins. Infection and immunity 72:2160-2169.
278. Jacobson GR, Rosenbusch JP. 1976. Abundance and membrane association of elongation factor Tu in E. coli. Nature 261:23-26.
279. Kunert A, Losse J, Gruszin C, Huhn M, Kaendler K, Mikkat S, Volke D, Hoffmann R, Jokiranta TS, Seeberger H, Moellmann U, Hellwage J, Zipfel PF. 2007. Immune evasion of the human pathogen Pseudomonas aeruginosa: elongation factor Tuf is a factor H and plasminogen binding protein. J Immunol 179:2979-88.
280. Pettit SC, Henderson GJ, Schiffer CA, Swanstrom R. 2002. Replacement of the P1 Amino Acid of Human Immunodeficiency Virus Type 1 Gag Processing Sites Can Inhibit or Enhance the Rate of Cleavage by the Viral Protease. Journal of Virology 76:10226-10233.
281. Green M, Ishino M, Loewenstein PM. 1989. Mutational analysis of HIV-1 Tat minimal domain peptides: identification of trans-dominant mutants that suppress HIV-LTR-driven gene expression. Cell 58:215-23.
282. Bahner I, Sumiyoshi T, Kagoda M, Swartout R, Peterson D, Pepper K, Dorey F, Reiser J, Kohn DB. 2007. Lentiviral vector transduction of a dominant-negative Rev gene into human CD34+ hematopoietic progenitor cells potently inhibits human immunodeficiency virus-1 replication. Mol Ther 15:76-85.
283. Bevec D, Dobrovnik M, Hauber J, Bohnlein E. 1992. Inhibition of human immunodeficiency virus type 1 replication in human T cells by retroviral-mediated gene transfer of a dominant-negative Rev trans-activator. Proc Natl Acad Sci U S A 89:9870-4.
284. Cordelier P, Van Bockstaele E, Calarota SA, Strayer DS. 2003. Inhibiting AIDS in the central nervous system: gene delivery to protect neurons from HIV. Mol Ther 7:801-10.
285. Malim MH, Bohnlein S, Hauber J, Cullen BR. 1989. Functional dissection of the HIV-1 Rev trans-activator--derivation of a trans-dominant repressor of Rev function. Cell 58:205-14.
286. Strayer DS, Branco F, Landre J, BouHamdan M, Shaheen F, Pomerantz RJ. 2002. Combination genetic therapy to inhibit HIV-1. Mol Ther 5:33-41.
287. Furuta RA, Shimano R, Ogasawara T, Inubushi R, Amano K, Akari H, Hatanaka M, Kawamura M, Adachi A. 1997. HIV-1 capsid mutants inhibit the replication of wild-type virus at both early and late infection phases. FEBS Lett 415:231-4.
288. Sandefur S, Varthakavi V, Spearman P. 1998. The I domain is required for efficient plasma membrane binding of human immunodeficiency virus type 1 Pr55Gag. J Virol 72:2723-32.
289. Spearman P, Wang JJ, Vander Heyden N, Ratner L. 1994. Identification of human immunodeficiency virus type 1 Gag protein domains essential to membrane binding and particle assembly. J Virol 68:3232-42.
290. Wyma DJ, Jiang J, Shi J, Zhou J, Lineberger JE, Miller MD, Aiken C. 2004. Coupling of Human Immunodeficiency Virus Type 1 Fusion to Virion Maturation: a Novel Role of the gp41 Cytoplasmic Tail. Journal of Virology 78:3429-3435.
291. Francis AC, Melikyan GB. 2018. Live-Cell Imaging of Early Steps of Single HIV-1 Infection. Viruses 10.

292. Xu H, Franks T, Gibson G, Huber K, Rahm N, Strambio De Castillia C, Luban J, Aiken C, Watkins S, Sluis-Cremer N, Ambrose Z. 2013. Evidence for biphasic uncoating during HIV-1 infection from a novel imaging assay. Retrovirology 10:70.
293. Lee SK, Cheng N, Hull-Ryde E, Potempa M, Schiffer CA, Janzen W, Swanstrom R. 2013. A sensitive assay using a native protein substrate for screening HIV-1 maturation inhibitors targeting the protease cleavage site between the matrix and capsid. Biochemistry 52:4929-40.
294. Yee J-K, Friedmann T, Burns JC. 1994. Chapter 5 Generation of High-Titer Pseudotyped Retroviral Vectors with Very Broad Host Range, p 99-112. *In* Roth MG (ed), Methods in Cell Biology, vol 43. Academic Press.
295. Landau NR, Page KA, Littman DR. 1991. Pseudotyping with human T-cell leukemia virus type I broadens the human immunodeficiency virus host range. J Virol 65:162-9.
296. Sodroski J, Goh WC, Rosen C, Campbell K, Haseltine WA. 1986. Role of the HTLV-III/LAV envelope in syncytium formation and cytopathicity. Nature 322:470-474.
297. He J, Chen Y, Farzan M, Choe H, Ohagen A, Gartner S, Busciglio J, Yang X, Hofmann W, Newman W, Mackay CR, Sodroski J, Gabuzda D. 1997. CCR3 and CCR5 are co-receptors for HIV-1 infection of microglia. Nature 385:645.
298. Derdeyn CA, Decker JM, Sfakianos JN, Wu X, Brien WA, Ratner L, Kappes JC, Shaw GM, Hunter E. 2000. Sensitivity of Human Immunodeficiency Virus Type 1 to the Fusion Inhibitor T-20 Is Modulated by Coreceptor Specificity Defined by the V3 Loop of gp120. Journal of Virology 74:8358.
299. Platt EJ, Bilska M, Kozak SL, Kabat D, Montefiori DC. 2009. Evidence that Ecotropic Murine Leukemia Virus Contamination in TZM-bl Cells Does Not Affect the Outcome of Neutralizing Antibody Assays with Human Immunodeficiency Virus Type 1. Journal of Virology 83:8289-8292.
300. Platt EJ, Wehrly K, Kuhmann SE, Chesebro B, Kabat D. 1998. Effects of CCR5 and CD4 Cell Surface Concentrations on Infections by Macrophagetropic Isolates of Human Immunodeficiency Virus Type 1. Journal of Virology 72:2855-2864.
301. Takeuchi Y, McClure MO, Pizzato M. 2008. Identification of Gammaretroviruses Constitutively Released from Cell Lines Used for Human Immunodeficiency Virus Research. Journal of Virology 82:12585-12588.
302. Morgenstern JP, Land H. 1990. Advanced mammalian gene transfer: high titre retroviral vectors with multiple drug selection markers and a complementary helper-free packaging cell line. Nucleic acids research 18:3587-3596.
303. Chen C, Okayama H. 1987. High-efficiency transformation of mammalian cells by plasmid DNA. Molecular and cellular biology 7:2745-2752.
304. Wehrly K, Chesebro B. 1997. p24 antigen capture assay for quantification of human immunodeficiency virus using readily available inexpensive reagents. Methods 12:288-93.
305. Chesebro B, Wehrly K, Nishio J, Perryman S. 1992. Macrophage-tropic human immunodeficiency virus isolates from different patients exhibit unusual V3 envelope sequence homogeneity in comparison with T-cell-tropic isolates: definition of critical amino acids involved in cell tropism. Journal of virology 66:6547-6554.

306. Varthakavi V, Browning PJ, Spearman P. 1999. Human immunodeficiency virus replication in a primary effusion lymphoma cell line stimulates lytic-phase replication of Kaposi's sarcoma-associated herpesvirus. Journal of virology 73:10329-10338.
307. Krishnan L, Li X, Naraharisetty HL, Hare S, Cherepanov P, Engelman A. 2010. Structure-based modeling of the functional HIV-1 intasome and its inhibition. Proc Natl Acad Sci U S A 107:15910-5.
308. Svarovskaia ES, Barr R, Zhang X, Pais GCG, Marchand C, Pommier Y, Burke TR, Pathak VK. 2004. Azido-Containing Diketo Acid Derivatives Inhibit Human Immunodeficiency Virus Type 1 Integrase In Vivo and Influence the Frequency of Deletions at Two-Long-Terminal-Repeat-Circle Junctions. Journal of Virology 78:3210-3222.
309. Zhang X, Pais GC, Svarovskaia ES, Marchand C, Johnson AA, Karki RG, Nicklaus MC, Pathak VK, Pommier Y, Burke TR. 2003. Azido-containing aryl beta-diketo acid HIV-1 integrase inhibitors. Bioorg Med Chem Lett 13:1215-9.
310. Butler SL, Hansen MS, Bushman FD. 2001. A quantitative assay for HIV DNA integration in vivo. Nat Med 7:631-4.
311. Li H, Durbin R. 2010. Fast and accurate long-read alignment with Burrows-Wheeler transform. Bioinformatics 26:589-95.
312. Kim D, Langmead B, Salzberg SL. 2015. HISAT: a fast spliced aligner with low memory requirements. Nat Methods 12:357-60.
313. Li H, Handsaker B, Wysoker A, Fennell T, Ruan J, Homer N, Marth G, Abecasis G, Durbin R. 2009. The Sequence Alignment/Map format and SAMtools. Bioinformatics 25:2078-9.